

POLITECNICO DI MILANO

School of Civil and Environmental Engineering

Master of Science in Civil Engineering



INVESTIGATION OF INTERLAMINAR SHEAR  
BEHAVIOR OF FABRIC REINFORCED CEMENTITIOUS  
MATRIX (FRCM) COMPOSITE SYSTEMS

SUPERVISOR: Prof. Carlo POGGI

CO-SUPERVISOR: Dr. Antonio NANNI (University of Miami)

AUTHOR: Michele MONTESI

MATR. 804674

Academic Year 2014/2015

*To my family,  
who gave me everything,  
and allowed me to realize this dream.*

---

## ACKNOWLEDGMENTS

I would like to thank the people who made this thesis possible and those who contributed to my personal growth throughout my studies. In particular, I desire to acknowledge:

- Dr. Antonio Nanni, my American advisor, for his guidance, patience and constant motivation, which pushed me to give everything to this work.
- Dr. Carlo Poggi, my Italian advisor, for allowing me to live this amazing experience, for his support and help in solving any kind of problem I encountered in these months.
- Dr. Diana Arboleda, incredible person, for her huge help, patience and contagious enthusiasm, which made me love what I was doing.
- Giulia Carozzi, who has my admiration and gratitude for her great help.
- Carmela and Marco, exemplary parents, who literally have done everything for me. Any word would be reductive for the love I feel for them.
- Matteo, much more than a brother, an extraordinary person and a life model, for his love and care throughout my life.
- Laura, the sweetest person I have ever met, for being always there for me, for her kindness, support, patience and true love.

---

## ABSTRACT

The evolution of alternative materials and techniques for structural rehabilitation is of essential importance to the preservation of existing reinforced concrete (RC) and masonry structures. Fabric Reinforced Cementitious Matrix (FRCM) composite systems represent a suitable repair methodology for structural strengthening. To this purpose, a research program is undertaken to investigate their interlaminar shear characteristics.

The current test method ASTM D2344 "*Standard Test Method for Short-Beam Strength of Polymer Matrix Composite Materials and Their Laminates*", because of the complexity of internal stresses in the specimen loaded under three-point bending, makes it difficult to relate the short-beam strength to any one material property. Although shear is the dominant applied loading at the fabric-mortar interface in this test method, a variety of failure modes can occur. To date, FRCM specimens tested demonstrate a flexural or matrix diagonal tension failure which does not exactly address interlaminar properties.

This work aims to investigate new specimen designs targeted at characterizing the interlaminar shear behavior. After an introductory section covering composite materials for structural applications and a review of the Short-Beam Shear test, the first study focuses on demonstrating why the current test method is inadequate for examining the interlaminar shear strength of FRCM systems. The second study concentrates on exploring varying specimen geometries, different number of layers, and new test configurations in order to identify a methodology which is reliable and consistent for studying FRCM interlaminar shear behavior.

The objective of these two studies is to improve AC434 "*Acceptance Criteria for Masonry and Concrete Strengthening Using Fiber-reinforced Cementitious Matrix*

---

*(FRCM) Composite Systems"* including recommendations to characterize the interlaminar shear performance of FRCM systems. The results of this modified test method can be used for quality control for material selection by manufacturers.

Moreover, to confirm that the test method developed in the previous studies is actually the most suitable way to investigate the interlaminar shear behavior of FRCM systems another test methodology is evaluated.

An additional study addresses a durability analysis for 1000-hour exposure aimed at examining the FRCM specimen behavior under the SBS test subject to aggressive environmental conditions. The goal is to evaluate the environmental durability tests presented in AC434 in order to characterize the FRCM reaction to the proposed conditions.

---

## SOMMARIO

L'evoluzione di materiali e tecniche alternative per la riabilitazione strutturale è di essenziale importanza per la preservazione di strutture esistenti in calcestruzzo armato e muratura. I sistemi compositi FRCM rappresentano un eccellente metodo di rinforzo strutturale. Il progetto di ricerca nasce con lo scopo di indagare il comportamento interlaminare a taglio di materiali compositi con matrice cementizia.

Il test proposto per tale ricerca è lo standard ASTM D2344 "*Standard Test Method for Short-Beam Strength of Polymer Matrix Composite Materials and Their Laminates*" e in molti casi, a causa della complessità delle tensioni interne nel provino, è difficile relazionare la forza delle Short-Beam ad una specifica proprietà del materiale. Sebbene il taglio è il carico dominante all'interfaccia tessuto-malta in questo tipo di test, possono avvenire una varietà di modi di rottura. Fino ad oggi, tutti i campioni FRCM testati mostrano una rottura per flessione o per tensione diagonale della matrice cementizia che non riguarda esattamente le proprietà interlaminari.

Questo lavoro ha lo scopo di indagare nuove geometrie e configurazioni di campioni volte a caratterizzare il comportamento interlaminare a taglio. Dopo una panoramica introduttiva dei materiali compositi ed una revisione dello Short-Beam Shear test, il primo studio dimostra il motivo per cui il test proposto è inadeguato per esaminare la resistenza a taglio interlaminare di sistemi FRCM. Il secondo studio indaga nuove geometrie, differenti numeri di layers e nuove configurazioni di test al fine di individuare una metodologia che sia affidabile e coerente per lo studio del comportamento interlaminare a taglio del composito FRCM.

L'obiettivo di questi due studi è quello di migliorare la norma AC434 "*Acceptance Criteria for Masonry and Concrete Strengthening Using Fiber-reinforced Cementitious Matrix (FRCM) Composite Systems*" introducendo

---

raccomandazioni per caratterizzare la resistenza interlaminare dei sistemi FRCC. I risultati di questa nuova metodologia di test possono essere utilizzati ai fini di controllo qualità per la scelta del materiale da parte dei produttori.

Inoltre, per dimostrare che il metodo sviluppato negli studi precedenti è realmente il modo più adatto per studiare il comportamento interlaminare a taglio di sistemi FRCC viene valutata un'altra tipologia di test.

Un ulteriore studio affronta un'analisi della durabilità per 1000 ore di esposizione volta ad esaminare la risposta dell'FRCC soggetto a diverse condizioni ambientali aggressive. Questo lavoro ha lo scopo di valutare i test sulla durabilità ambientale proposti nella norma AC434 al fine di caratterizzare la reazione dell'FRCC alle condizioni proposte.

---

# TABLE OF CONTENTS

ABSTRACT .....	iii
SOMMARIO .....	v
TABLE OF CONTENTS .....	vii
1 INTRODUCTION .....	1
1.1 Structural rehabilitation.....	1
1.2 Overview of composite materials for structural applications: FRP and FRCM as repair methods.....	4
1.3 Acceptance of new composite materials into IBC and applicable European standards.....	14
1.4 Research objectives .....	16
2 FABRIC REINFORCED CEMENTITIOUS MATRIX (FRCM) COMPOSITE SYSTEM.....	19
2.1 FRCM Composite System.....	19
2.1.1 FRCM Components .....	19
2.1.2 Material Preparation and Installation Procedure .....	24
2.1.3 Use and Applications .....	27
2.1.4 Acceptance and Reports .....	32
2.2 FRCM Mechanical Properties.....	35
2.2.1 Mechanical and Failure Behavior of FRCM Systems.....	35
2.2.2 Tensile Characterization.....	40
2.2.3 Bond Characterization.....	43
2.3 FRCM Effectiveness in Structural Rehabilitation.....	46
2.3.1 Flexural Strengthening .....	46
2.3.2 Shear Strengthening .....	49
2.3.3 Axial Strengthening: Column Confinement.....	51
2.3.4 Masonry Strengthening .....	52



---

3	TEST METHODOLOGIES FOR DETERMINATION OF INTERLAMINAR SHEAR BEHAVIOR OF COMPOSITES .....	55
3.1	Interlaminar Shear Test Methods for FRP Composite Systems.....	56
3.1.1	Short Beam Shear (SBS) Test.....	57
3.1.2	Four Point Shear (FPS) Test .....	63
3.1.3	Iosipescu Shear Test.....	65
3.1.4	Axial Tension of a Laminate .....	67
3.2	Applicability of Interlaminar Shear Test Methods to FRCM Composites.....	69
3.3	Addressing Section 4.2.4 of AC434.....	71
4	INTERLAMINAR SHEAR BEHAVIOR OF FRCM COMPOSITES.....	74
4.1	FRCM Materials Description.....	75
4.1.1	Fabrics .....	75
4.1.2	Mortars .....	77
4.2	Critical Analysis of Test Methodology (ASTM D2344) for FRCM Composites ..	79
4.2.1	Specimen Preparation.....	80
4.2.2	Test Setup and Procedure.....	81
4.2.3	Test Results .....	82
4.3	Investigation of Interlaminar Plane: Contact Surface Area Reduction .....	94
4.3.1	Specimen Preparation.....	96
4.3.2	Test Setup and Procedure.....	97
4.3.3	Test Results .....	98
4.4	Composite Sandwich Beam: Increasing Flexural Strength.....	103
4.4.1	Specimen Preparation.....	105
4.4.2	Test Results .....	105
4.4.3	Stress Analysis .....	112
4.5	Image Analysis of FRCM Composite Systems.....	121
4.6	Splitting Tensile Test .....	123
4.6.1	Specimen Preparation.....	125
4.6.2	Test Setup and Procedure.....	127
4.6.3	Test Results .....	129
5	FRCM PERFORMANCE AFTER ENVIRONMENTAL EXPOSURE .....	135
5.1	Exposure Environments .....	135

---

5.1.1	Environments Description.....	137
5.1.2	Specimen Preparation.....	138
5.1.3	Test Setup and Procedure.....	139
5.2	Test results .....	140
5.2.1	Control Condition.....	141
5.2.2	Freezing and Thawing Resistance.....	143
5.2.3	Alkaline Resistance.....	145
5.2.4	Water Vapor Resistance.....	147
5.2.5	Seawater Resistance.....	149
5.3	Comparison of the Results .....	151
5.4	Conclusions.....	154
6	CONCLUSIONS.....	156
	REFERENCES.....	160
	APPENDIX A: Complete test matrix .....	173
	APPENDIX B: Image analysis procedure .....	176

# 1

## INTRODUCTION

### 1.1 Structural rehabilitation

The repair of deteriorated, damaged, and substandard civil infrastructure has become one of the most important issues for civil engineering worldwide. The rehabilitation of existing structures is fast growing, especially in developed countries, in which most of their infrastructure was already established by the middle period of the last century. Furthermore, structures which were built after World War II had little attention paid to durability issues, and the USA and Japan had inadequate knowledge of seismic design (Hollaway and Teng 2008). In the European Union nearly 84,000 reinforced and prestressed concrete bridges require maintenance, repair, and strengthening with an annual budget of €215 million. In the United States, infrastructure upgrading has been estimated at \$20 trillion (National Science Foundation, NSF, 1995).

Within the scope of rehabilitation of concrete structures, it is essential to differentiate between the terms repair, strengthening, and retrofitting; these terms are often erroneously interchanged, but they do refer to three different structural

conditions. In ‘repairing’ a structure, the composite material is used to improve a structural or functional deficiency such as a crack or a severely degraded structural component. In contrast, the ‘strengthening’ of a structure is specific to those cases where the addition or application of the composite would enhance the existing designed performance level. The term ‘retrofit’ is specifically used to relate to the seismic upgrade of facilities, such as in the case of the use of composite jackets for the confinement of columns. Typical structural elements in need of reinforcement include beams, slabs, columns, and walls (Figure 1.1).

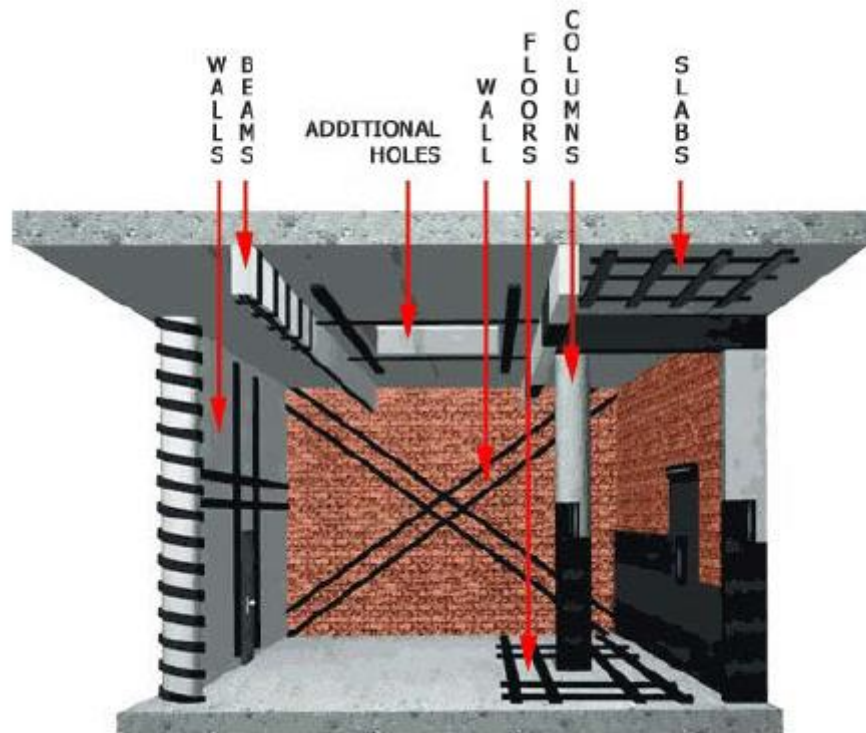


**Figure 1.1 – Typical structural elements of a building showing repairs (Arboleda 2014)**

A vast number of RC structures are in urgent need of repair and strengthening, due to either a change in use or structural degradation. Many concrete structures were built prior to the introduction of modern design codes, and hence do not meet modern design requirements.

Strengthening is often needed due to a change in loading requirements, or due to structural modifications such as the formation of openings. Structural assessment may highlight inadequate reinforcement within the concrete, when compared to today's more stringent requirements. A particular concern is the seismic performance of structures originally designed for only gravity loads. RC frames that were not designed for seismic loads can have inadequate ductility and a lack of robustness. Seismic upgrade of these structures can have profound economic and social implications. The need for economically viable seismic retrofit systems has driven research in Japan into FRP strengthening following the disastrous Hyogoken–Nanbu earthquake which occurred in 1995 (Hollaway and Teng 2008).

Moreover, reinforced concrete structures built between World War II and the 1980s were often designed with little attention to durability issues, and have thus suffered severe degradation. Material deterioration in concrete structures typically involves corrosion of the internal steel reinforcement due to long-term chloride ingress or carbonation of the concrete. This deterioration results in poor service load performance (i.e. excessive cracking, spalling of the concrete cover and increased deflections) and a reduction in the ultimate capacity of the structure (Hollaway and Teng 2008). Material deterioration is particularly likely in aggressive marine or industrial environments, and in cold regions where deicing salts are used.

Concrete structures are also susceptible to hazard events, and to design or construction errors. Prestressed concrete (PC) members are susceptible to steel strand fatigue and may require strengthening to prevent further loss of prestress (Hollaway and Teng 2008).

## **1.2 Overview of composite materials for structural applications: FRP and FRCM as repair methods**

The term composite means any system of two or more material phases combined and working together whose mechanical performance and properties are designed to be superior than those of the constituent materials. One of the phases is dispersed and stronger called the reinforcement, and another phase is continuous and weaker called the matrix (Daniel & Ishai 1994). In civil engineering, steel reinforced concrete is the most important composite material that is used for structural applications. The combination of the high compressive strength of concrete and the high tensile strength of steel reinforcement leads to an appropriate load carrying capacity for many applications in the building industry.

Classification of composites is at two levels, by matrix type and by reinforcement type which can be particulates, short distributed fibers, continuous fibers (Donaldson & Miracle 2001), or nano-sized particles or structures. The main composite categories with fibrous reinforcement include metal matrix composites (MMC), polymer matrix composites (PMC), and brittle matrix composites (BMC). In order to frame the context within which FRCM composites are studied and can be better understood, the following overview is limited to polymer and brittle matrix composites only.

A fiber reinforced composite essentially consists of two component materials: the matrix material, which is generally the low strength and low-modulus component, and the fiber, which is the relatively high-strength and high-modulus component. Under stress, the fiber utilizes the matrix to transfer the load to the fiber; this results in a high-strength and high-modulus composite. The primary phase, the fibers of high aspect ratio, must be well dispersed and bonded into the secondary phase, the matrix. The principal constituents of the composite are, therefore, the fiber, the matrix and the interface. This last component is an anisotropic transition region. The interface is required to provide adequate chemical and physical bonding

stability between the fiber and the matrix in order to maximize the coupling between the two phases and thus allow stresses to be dispersed through the matrix, and thus transferred to the reinforcement (Hollaway and Teng 2008). Consequently, the main function of the matrix is to combine and to protect the fiber against the external environment into which the composite will be placed.

Over the last two decades there has been a growing awareness among structural engineers of the importance to develop new composite materials. Under the umbrella of brittle matrix composites, a response to this need has been represented by Textile Reinforced Concrete (TRC) which is a composite system reinforced by the use of technical textiles made out of yarns/strands. The development of TRC is based on the fundamentals of Fiber Reinforced Concrete (FRC) with short filaments (Figure 1.2). Similar to ordinary reinforced concrete (RC) the filaments are aligned in the direction of the tensile stresses, which leads to an increase in their effectiveness. The load-carrying capacity increases compared to FRC with randomly distributed short fibers (Hegger et al. 2004).

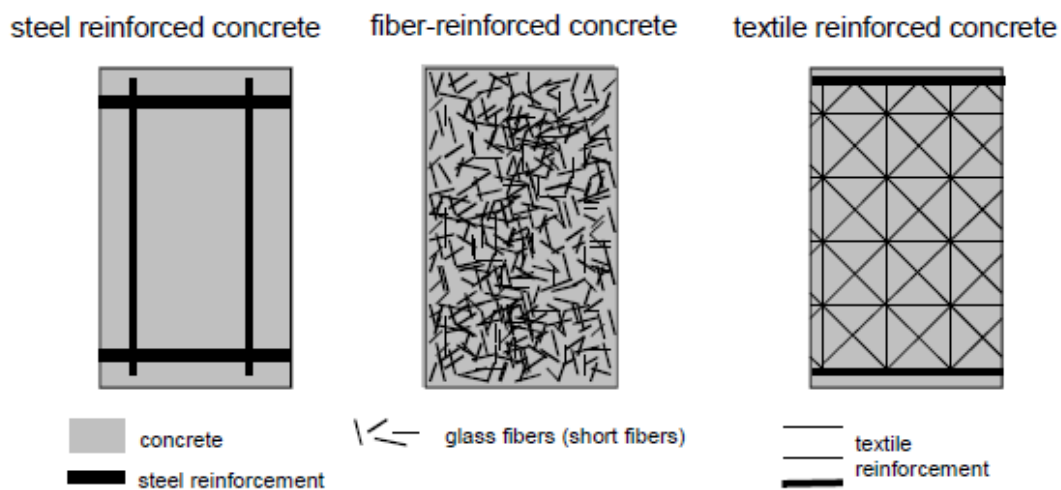


Figure 1.2 – Concrete reinforcing systems (Hegger et al. 2004)

This rather newly developed composite material, TRC, is made with a multi-axial fabric used in combination with an inorganic cementitious binder which holds in place the fabric structural reinforcement. The fabric is a manufactured planar

textile structure made of fibers and/or yarns assembled to give the structure sufficient strength and other properties required for its intended application.

The use of TRC allows the design of very thin-structured concrete elements with high strength in compression as well as in tension which provides a considerable load bearing capacity. Profile thickness can be achieved with textile reinforcement as well as high quality homogenous surfaces. These advantages lead to an entirely new potential application for concrete as a building material, especially for facade construction (Leardini 2013). In addition, environmental protection elements (water protection walls and water tanks), load-bearing structures (integrated formwork element for RC floors, diamond-shaped framework, light pedestrian bridges (Figure 1.3)) or multi-layer composite pipes are typical applications of the TRC material.



**Figure 1.3 – 17 meter bridge made of TRC in Kempten (Allgäu)**

In addition to the more appropriate use of TRC for new construction such as cladding applications or industrially-manufactured products (Nanni 2012), TRC composite systems have been widely used as an external reinforcement to be applied on existing structures where rehabilitation is needed. The need for further research in developing new methods of repairing, strengthening and retrofitting of structures may be illustrated through the example of the United States where it has been estimated that \$20 trillion investment is needed in operant civil infrastructure systems (National Science Foundation, NSF, 1995). Because of aging, overuse,



exposure, misuse, and neglect, many of these systems are deteriorating and becoming far from the more stringent design requirement recently introduced. Moreover, in seismic areas, where design was performed according to old seismic codes, structures now have to meet performance levels demanded by updated seismic design standards. Since it would be prohibitively costly and disruptive to replace these vast networks, the call for rehabilitating existing structures has been very frequent in the recent years.

Strengthening/rehabilitating/retrofitting existing structures by utilizing advanced Fiber Reinforced Polymer (FRP) composites is another powerful and viable alternative to the use of steel. Since the 1980s, the realization among civil engineers of the importance of the specific weight and stiffness, the resistance to corrosion, durability, tailorability and ease of installation has encouraged the use of FRP composites in the rehabilitation of structures throughout the world. FRP is a polymer matrix composite material reinforced with a fiber continuous cloth, mat, or strands. Although the fibers and resins used in FRP systems are relatively expensive compared with traditional strengthening materials such as concrete and steel, labor and equipment costs to install FRP systems are often lower (Nanni 1999).

The mechanical behavior of fiber-reinforced composites is governed by a complex relationship between the material properties of the constituent materials, their volume fraction, the bond interface between them, and their orientation with respect to the load applied. Polymer matrix composites (PMC) have a very strong interfacial bond with a fiber reinforcement strain limit generally lower than the strain limit for the epoxy matrix, ( $\epsilon_f < \epsilon_m$ ). In this case, the longitudinal (fiber parallel to the direction of load) and transverse (fiber perpendicular to the direction of load) elastic moduli,  $E_{1c}$  and  $E_{2c}$ , respectively, can be estimated using the rule of mixtures (Daniel & Ishai 1994).

The estimation of the longitudinal modulus can be attained by Equation 1.1, in which the fiber and matrix are assumed under the same state of strain and the composite will theoretically fail when the strain limit of the fibers is reached.

$$E_{1c} = E_f V_f + E_m V_m \quad (1.1)$$

Where  $E_f$  and  $V_f$  denote the modulus and volume fraction of the fiber; and  $E_m$  and  $V_m$  are the modulus and volume fraction of the matrix. This expression states that each constituent material contributes to the composite properties in a manner proportional to their volume fraction. In the same way, Equation 1.2 is used for estimation of the transverse modulus where the fiber and matrix are assumed to be under same state of stress.

$$E_{2c} = \frac{E_f E_m}{E_f V_m + E_m V_f} \quad (1.2)$$

Initially, the matrix and fibers deform elastically. Eventually, the matrix yields and deforms plastically but the fibers continue to stretch elastically (Callister and Rethwisch 2012). These relationships give rise to the nearly linear elastic characteristic stress-strain curve shown in Figure 1.4.

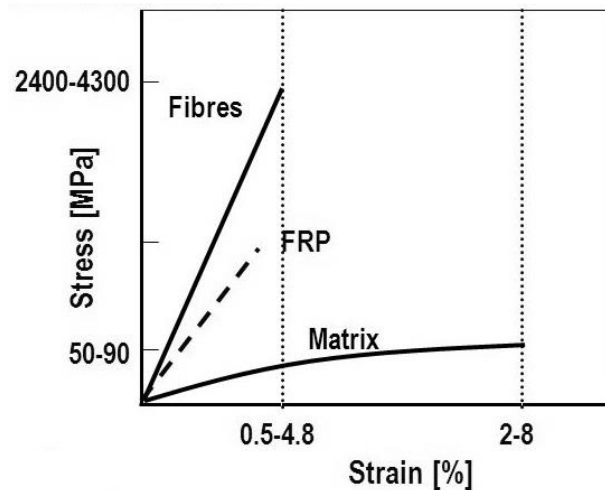


Figure 1.4 – Typical stress-strain curves for organic polymer matrix composites

In the same way, through Equation 1.3 it is possible to estimate the shear modulus  $G_{12}$ , presuming that the shearing stresses on the fiber and on the matrix are the same, which is clearly not the case.

$$G_{12} = \frac{G_m G_f}{V_m G_f + V_f G_m} \quad (1.3)$$

Where  $G_f$  and  $V_f$  denote the shear modulus and volume fraction of the fiber; and  $G_m$  and  $V_m$  are the shear modulus and volume fraction of the matrix.  $G_{12}$  is matrix dominated and is a series combination like  $E_{2c}$  (Yadama 2007).

Furthermore, although PMCs show a superior strength compared to steel, once they reach their ultimate capacity, the failure exhibited presents no yielding phase. Figure 1.5 shows a comparison of the idealized mechanical behavior of carbon (CFRP) and glass FRP (GFRP) composites, with steel.

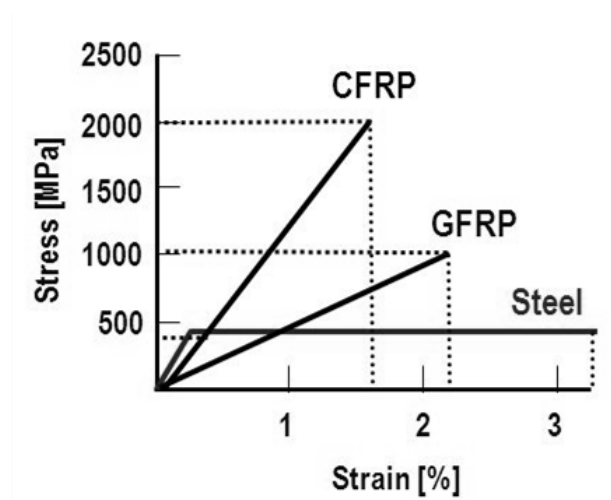


**Figure 1.5 – Comparison of idealized mechanical behavior between carbon (CFRP) and glass (GFRP) composites, and steel**

As discussed above, FRP gained its popularity in the civil engineering community due to the favorable properties possessed, specifically the high strength to weight ratio, corrosion resistance, minimal change in geometry and ease and speed of application (Fib bulletin 2001). These extraordinary properties of FRP composites

enable them to be used in areas where conventional construction materials might be restricted.

Despite of numerous advantages associated with the use of FRP for strengthening of concrete and masonry structures, some possible drawbacks attributed to the organic resins used to bind and impregnate the fiber reinforcement (Al-Salloum et al. 2012) are as follows:

- poor performance above the glass transition temperature of the polymer resin;
- fire protection measures may be required;
- inability to apply FRP on wet surfaces or at low temperatures;
- lack of vapor permeability, which may cause damage to the interface;
- incompatibility with some substrate materials;
- relevance for application on historical buildings;
- difficulty to conduct post-earthquake assessment of the damage suffered by the reinforced concrete behind (undamaged) FRP jackets;
- toxic health hazards for the installers;
- special handling equipment and special training for installation personnel.

An alternative solution to the listed drawbacks is the replacement of the organic binder with an inorganic one, i.e. use a composite made with a cement-based matrix. One possible solution is the development of Fabric Reinforced Cementitious Matrix (FRCM) composites which consist of a "dry" fabric in a cementitious matrix. The definition of "dry" fabric is generally used in literature in order to differentiate from fabrics impregnated by resin. The cementitious matrix in FRCM does not fully penetrate and impregnate the dry-fiber strands in the fabric, which is a significant factor affecting the mechanical behavior and performance of the FRCM composite.

In brittle matrix composites (BMC), the matrix is either a ceramic or a cement-based material which are typically porous and have a relative high compressive strength, but low tensile resistance. The mechanical behavior of BMC is very different from polymer or metal composites and the rule of mixtures model usually

cannot be applied because for some BMCs the interfacial bond between fiber and matrix is weaker and more complex or because the strain limit of the matrix is much lower than that of the fibers ( $\epsilon_m \ll \epsilon_f$ ). In those cases, the matrix starts to crack at its strain limit and instead, fiber debonding and slipping are the mechanisms that mitigate crack localization. This mechanism leads to a sort of pseudo-ductility for the composite which is fully recommendable in the civil-engineering field.

Figure 1.6 shows the mechanical behavior of a typical brittle matrix composite. In particular, it is possible to note that BMCs behave linear-elastically up to the tensile strength of the matrix. Then, as the load increases, multiple cracks develop in the matrix and the stress is redistributed through the fibers allowing the composite material to sustain additional strain, at this point, either strain-softening or strain-hardening behavior will develop depending on the amount of fibers and the quality of the interfacial bond (Arboleda 2014).

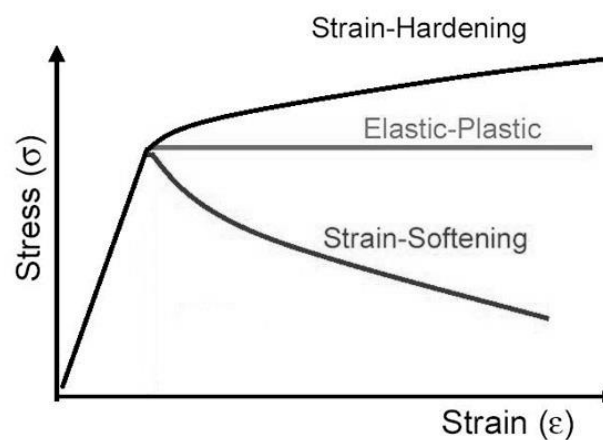


**Figure 1.6 – Idealized mechanical behavior of brittle matrix composite**

Several types of composites in which a brittle matrix is reinforced with fibers of different composition, mechanical characteristics and geometry have been developed for a variety of applications. Fibers used for reinforcement can be metal (usually steel), mineral (glass), natural (sisal, jute, hemp, or other cellulose materials), or synthetic (polypropylene, polyolefins, carbon, aramid, PBO). The fibers can be either

short dispersed fibers, as in FRC, or continuous fibers in the form of a mesh or fabric also referred to as textile, i.e. TRC. Fabric Reinforced Cementitious Matrix (FRCM) system, which is the content of the present work, has a more specific definition but it can also fall in the broad category of TRC.

In addition to TRC, FRCM has also been identified in technical literature as Textile Reinforced Concrete (TRC), Textile Reinforced Mortar (TRM), Fiber Reinforced Concrete (FRC), the Mineral Based Composites (MBC) and fiber-reinforced cement (ACI 549.4R-13).

TRC has had some traction in Europe: among the leaders are academic institutions in Germany (Dresden University of Technology and RWTH Aachen University) and Israel (Ben-Gurion University of the Negev and Technion-Israel Institute of Technology), where development work has been conducted since the late 1990. Recent experimental and theoretical works show the effectiveness of cement-based composites for strengthening of RC structures in terms of column confinement (Al-Jamous et al. 2006; Ombres 2007; Peled 2007; Triantafillou et al. 2006; Wu and Sun 2005), shear and flexural strengthening (Bisby et al. 2009; Blanksvärd et al. 2009; Brückner et al. 2006, 2008; Ombres et al. 2009; Pareek et al. 2007; Täljsten and Blanksvärd 2007; Triantafillou and Papanicolau 2006; Wiberg 2003; Wu and Sun 2005), and seismic upgrading (Bournas et al. 2009; Triantafillou and Bournas 2008).

Nevertheless, it may be used in new construction such as thin shells, cladding panels, facade construction or prefabricated components. On the other hand, FRCM systems were found to be more suitable for strengthening applications on RC beams and columns or on un-strengthened masonry. Indeed, numerous commercial projects in Europe and United States have already demonstrated the potential for FRCM composite applications (Nanni 2012) for infrastructure strengthening. The mechanical behavior of FRCM deviates from that of the other composites discussed so far and will be further examined in the next chapters.

Compared to FRP, FRCM systems present the following advantages (RILEM TC 201-TR 2006, Peled 2007, Fallis 2009, Bianchi et al. 2013, Arboleda 2014, Carozzi et al. 2014):

- good compatibility with the concrete or masonry substrate in terms of chemical, physical and mechanical properties. Thus, no need to grind the surface or round the edges;
- ease of installation as traditional plastering or trowel trades can be used;
- breathability of the system, which allows air and moisture transport through the matrix;
- good performance at elevated temperatures in addition to partial fire resistance;
- efficient in aggressive environments such as alkaline, water vapor and sea water environments;
- reversibility, essential for the conservation of historic structures.

The main difference between FRP and FRCM consists in the fact that the continuous reinforcement used for FRP is embedded and fully impregnated in an organic resin, while the cementitious matrices used for FRCM cannot fully impregnate the individual fibers. Therefore, FRCM should not be confused with the use of FRP reinforcing grids embedded in concrete or mortar. Even if a polymeric coating is used to bond together the strands of the fabric for manufacturing, installation and handling purposes and to increase the long-term durability of the fabric, the yarns of the fabric are not to be considered fully impregnated because the coat is not able to transfer stresses through the depth of the strands.

The FRCM system is suitable for RC elements or masonry strengthening: in particular, flexural, shear and torsion capacity enhancement can be provided for RC beams as well as concrete column confinement. In addition, both for RC elements and masonry a considerable work can be done in seismic zones by the increase of the fatigue resistance in flexure and shear for beams, columns and walls. Some interesting field of applications are shown in the following chapter.

An overview of composite materials for structural applications has been presented in order to frame the context within which FRCM composites are studied and can be better understood. Certainly, other composites are in use in civil engineering field and an effort with regard to standardization would allow better communication among researchers community improving the state of advancement of these innovative and exciting composite materials.

### **1.3 Acceptance of new composite materials into IBC and applicable European standards**

The present work was accomplished within the CICI teamwork of the University of Miami. The Center for the Integration of Composites into Infrastructure (CICI) is a multi-university National Science Foundation Industry/University Cooperative Research Center (I/UCRC), established in July 2009 to conduct research that would stimulate applications and cost effective rehabilitation schemes using composites in civil and military structures. CICI originates from a merger of the efforts of four American universities: West Virginia University (Virginia), the lead institution, Rutgers University (Rutgers), University of Miami (Miami), and North Carolina State University (NC State). The mission of CICI is to accelerate the adoption of polymer composites and innovative construction material into infrastructure and transportation applications through collaborative research.

Since FRCM systems are recognized as alternative strengthening methods for masonry and concrete structural elements, a specific evaluation of this material had to be performed in accordance with the relative Acceptance Criteria issued by the International Code Council Evaluation Service (ICC-ES) in order for the material to be commercially available in the United States.

ICC Evaluation Services (ICC-ES) first addressed Acceptance Criteria for cement-based matrix fabric composite systems for reinforced and unreinforced



masonry in 2003. This document was entitled: “*Acceptance Criteria for Cement-Based Matrix Fabric Composite Systems for reinforced and Unreinforced Masonry*” (AC218). In October 2011, an expanded version of this paper was released being entitled: “*Acceptance Criteria for Masonry and Concrete Strengthening Using Fabric-Reinforced Cementitious Matrix (FRCM) Composite Systems*” (AC434 2011). In February 2013, this document was superseded by AC434-13. Thus, for FRCM manufacturers, AC434-13 establishes guidelines for the necessary tests and calculations required to receive a product research report from ICC-ES.

Section 4.2.4 of AC434 requires the investigation of composite interlaminar shear strength on FRCM stating “to follow general procedures of ASTM D2344. Alternatively, test procedures of ASTM C947 can be adopted for FRCM in conjunction with provisions of ASTM D2344 for interpretation of results and reporting regarding interlaminar related issues”.

Therefore, the current test methods are ASTM D2344 “*Standard Test Method for Short-Beam Strength of Polymer Matrix Composite Materials and Their Laminates*” and ASTM C947 “*Standard Test Method for Flexural Properties of Thin-Section Glass-Fiber-Reinforced Concrete (Using Simple Beam With Third-Point Loading)*”. In particular, the present work focuses on the use of ASTM standard D2344 as main methodology to investigate the interlaminar shear behavior of FRCM composite system. In fact, the alternative ASTM standard C947 covers determination of the flexural ultimate strength in bending and the yield strength of glass-fiber reinforced concrete sections and it has not been recognized as an appropriate procedure to evaluate the interlaminar properties of brittle matrix composites.

Furthermore, although this project has been developed in the United States and concentrates on the American standards, other guidelines are in use around the world. Specifically, in addition to the ASTM procedures, in Europe the International Standard ISO 14130 “*Fibre-reinforced plastic composites - Determination of apparent interlaminar shear strength by short-beam method*” is widely used to examine the interlaminar behavior of fiber-reinforced composites. In particular, this

International Standard specifies a procedure for determining the apparent interlaminar shear strength of fiber-reinforced plastic composites. Although this method is suitable for use with plastic composites providing interlaminar shear failure is obtained, it has never been applied to FRCM systems and further studies are recommended. As the ASTM standards, this methodology is not suitable for the determination of design parameters, but it may be used for screening materials, or as a quality-control test.

## 1.4 Research objectives

Following the first experimental investigations developed in recent years on FRCM to test its effectiveness in structural applications, this work proposes a detailed study of the material properties with the aim to establish reliable criteria to evaluate the actual interlaminar shear strength capacity.

As discussed in the previous paragraph, in the United States, new materials such as FRCM can be accepted by the International Building Code (IBC), by means of supporting evidence in the form of valid reports demonstrating compliance to published acceptance criteria. The ICC Evaluation Service (ICC-ES) developed a criterion for evaluation and characterization of FRCM composites used to strengthen existing masonry and concrete structures, which is the AC434-2013 “*Acceptance Criteria for Masonry and Concrete Strengthening Using Fabric-Reinforced Cementitious Matrix (FRCM) Composite Systems*”.

The AC434 about the investigation of composite interlaminar shear strength on FRCM recommends following general procedures of ASTM D2344 “*Standard Test Method for Short-Beam Strength of Polymer Matrix Composite Materials and Their Laminates*”. Hence, the current test method is ASTM D2344 and in most cases, because of the complexity of internal stresses in the specimen loaded under three-point bending, although shear is the dominant applied loading at the fabric-mortar

interface, it is not generally possible to relate the short-beam strength to any one material property and a variety of failure modes can occur.

To date, all the FRCM specimens tested in the previous work (Arboleda 2015) demonstrate a flexural or matrix diagonal tension failure which does not exactly address interlaminar shear properties. Consequently, there is a growing awareness of the need to investigate an alternative methodology to replace the current AC434 requirement.

Therefore, the purpose of this work is to investigate new specimen designs targeted at characterizing the interlaminar shear behavior. In particular, after a critical analysis of the test methodologies encountered during literature search in order to understand the available methods to examine interlaminar shear behavior, the first study focuses on demonstrating the reason why the current test method is not appropriate for examining the interlaminar shear behavior of FRCM systems. Great attention is placed on the failure mode experienced during the test, which represents a key factor on the measured interlaminar shear strength. This part demonstrates the complexity of developing an interlaminar shear failure with the FRCM composites.

The second study concentrates on exploring varying specimen geometries, different number of layers and new test configurations in order to define a procedure which is reliable and consistent for studying the interlaminar shear behavior of FRCM composites. In other words, this part of the project aims to develop a methodology which is more intelligent in addressing a parameter which is critical for this composite system, but that until now, is not possible to be measured.

To this end, the proposed method is to consistently reduce by means of a bond breaker the sectional area at the shear plane until obtaining an interlaminar failure. In this way, reducing the amount of contact surface area, there is less continuity between the two layers of mortar and it is possible to give a limiting value between the interlaminar and the flexural failures. This method represents a matrix characterization, which is one crucial constituent of FRCM system, and gives the

chance of comparing different types of brittle matrixes related to the fabric under consideration.

Based on these findings, a further variation of the original specimen configuration is proposed with the ultimate goal of making interlaminar shear the control failure mode. In this phase, a composite sandwich beam made by FRCM and steel is analyzed to increase the flexural strength of the samples and generate interlaminar shear failures. Also in this study, several parameters are varied in order to find the proper configuration to compute the actual interlaminar shear strength.

The ultimate goal of these two studies is to provide evidence that can be used to improve AC434 providing recommendations and a general method to characterize the interlaminar shear performance of FRCM composites. The results determined by this test method can be used for quality control and as screening tool for material selection.

An additional study concerns a durability analysis for 1000-hour exposure aimed at examining the response of FRCM composites under the short-beam shear test subject to aggressive environmental conditions. In particular, this part of the work has the goal to characterize the FRCM reaction to the conditions proposed in AC434.

Moreover, other tests have been performed within the FRCM material characterization. These include the performing of pull-off FRCM adherence test, and some material characterization tests on the fibers and the mortar separately taken.

# 2

## **FABRIC REINFORCED CEMENTITIOUS MATRIX (FRCM) COMPOSITE SYSTEM**

In this chapter, the FRCM composite system is presented. The Chapter is divided into three main sections: the first is an overview of the composite material, the second deals with the FRCM mechanical properties, whereas the third demonstrates the FRCM effectiveness in its structural applications.

### **2.1 FRCM Composite System**

#### **2.1.1 FRCM Components**

Three commercially available FRCM systems were selected for this research project in order to validate the test methodology used in the determination of design parameters. A PBO-FRCM system and two Carbon-FRCM systems, from two

different suppliers, which have found application in several projects in Europe and in the United States.

Each FRCM system consists of two main elements, a cementitious matrix which is usually a grout system based on Portland cement and a low dosage of dry polymers (less than 5% by weight), and a dry fiber network (fabric) or mesh. The cementitious matrix is studied and produced specifically to optimize its performance with the relative fabric with which it forms a composite system.

- **Carbon 1-FRCM System**

The Carbon 1-system is a combination of cementitious mortar and a coated carbon fabric (Figure 2.1). The system is used for static retrofitting (flexural, axial, shear) of RC structures. In this composite system, carbon mesh is rolled out on site, laid out and grouted using a reactive spray mortar.



**Figure 2.1 – Carbon 1 fabric roll and inorganic cementitious material**

In Table 2.1 the technical specifications provided by the manufacturer of the Carbon 1-FRCM system are shown, where the component properties can be divided into Carbon fiber properties, fabric properties and mortar properties.

<b>Carbon Fiber Properties</b>	<b>Units</b>	<b>Value</b>
Density	g/cm <sup>3</sup>	1.79
Tensile strength	GPa	4.00
Modulus of elasticity	GPa	160
Ultimate deformation	%	1.50
Breakdown temperature	°C	-
Coefficient of thermal dilation	10 <sup>-6</sup> °C <sup>-1</sup>	-
<b>Unidirectional Fabric Properties</b>	<b>Units</b>	<b>Value</b>
Weight of the fabric	g/m <sup>2</sup>	280.8
Weight of Carbon fibers in the fabric	g/m <sup>2</sup>	-
Equivalent dry fabric thickness in the direction of the warp	mm <sup>2</sup> /mm	0.157
Ultimate tensile strength of the warp by width unit	kN/m	628
Ultimate tensile strain of the warp by width unit	-	0.015
Axial Stiffness of the warp by width unit	kN/m	-
<b>Mortar Properties</b>	<b>Units</b>	<b>Value</b>
Consistency (UNI EN 13395-1)		-
Specific weight of fresh mortar	g/cm <sup>3</sup>	2.05 ± 0.05
Liters of water per 100 kg of mortar		15 - 17
Yield (dry product)	kg/m <sup>2</sup> /mm	2.0 – 2.2
Compressive strength (28 days)	MPa	> 45.0
Bending strength (28 days)	MPa	> -
Secant modulus of elasticity (28 days)	MPa	-

**Table 2.1 – Carbon 1-FRCM component properties according to the technical sheet provided by the manufacturer**

- **Carbon 2-FRCM System**

Carbon 2-FRCM system, engineered for masonry structural reinforcement, is a composite material consisting of a carbon fabric, which acts as continuous reinforcement, and a stabilized inorganic matrix, which binds the fabric to the masonry support. Carbon 2-FRCM is a Fabric Reinforced Cementitious Matrix, which, different from FRP systems with epoxy resin, utilizes an inorganic matrix consisting of a pozzolanic hydraulic binder that is chemically, physically, and mechanically compatible with masonry support.



Figure 2.2 – Carbon 2 fabric roll and the inorganic cementitious mortar

In Table 2.2 the technical specifications provided by the manufacturer of the Carbon 2-FRCM are shown, where the material properties can be divided into Carbon fiber properties, fabric properties and mortar properties.

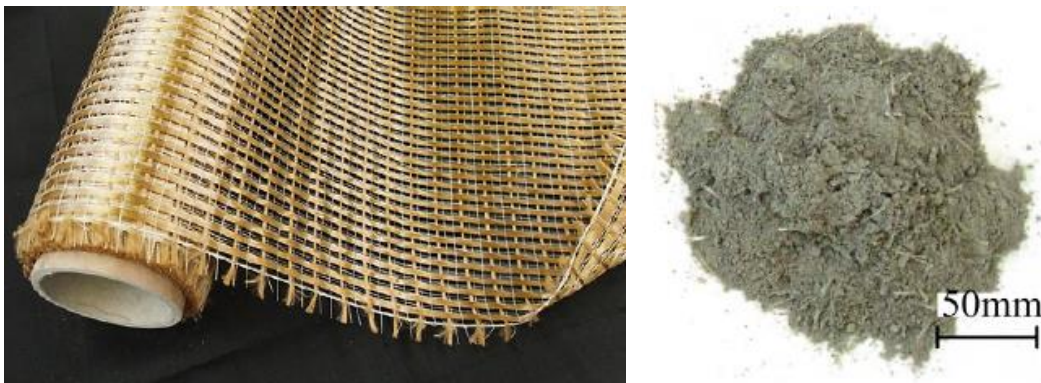
Carbon Fiber Properties	Units	Value
Density	g/cm <sup>3</sup>	1.78
Tensile strength	GPa	4.80
Modulus of elasticity	GPa	240
Ultimate deformation	%	1.80
Breakdown temperature	°C	650
Coefficient of thermal dilation	10 <sup>-6</sup> °C <sup>-1</sup>	0.50
Fabric Properties	Units	Value
Weight of the fabric	g/m <sup>2</sup>	202
Weight of Carbon fibers in the fabric	g/m <sup>2</sup>	168
Equivalent dry fabric thickness in the direction of the warp	mm <sup>2</sup> /mm	0.0475
Equivalent dry fabric thickness in the direction of the weft	mm <sup>2</sup> /mm	0.0475
Ultimate tensile strength of the warp by width unit	kN/m	252
Ultimate tensile strength of the weft by width unit	kN/m	252
Ultimate tensile strain of the warp by width unit	-	0.0192
Ultimate tensile strain of the weft by width unit	-	0.0192
Axial Stiffness of the warp by width unit	kN/m	13.1
Axial Stiffness of the weft by width unit	kN/m	13.1
Mortar Properties	Units	Value
Consistency (UNI EN 13395-1)		165
Specific weight of fresh mortar	g/cm <sup>3</sup>	1.50 ± 0.05
Liters of water per 100 kg of mortar		25 - 27
Yield (dry product)	kg/m <sup>2</sup> /mm	1.160 – 1.220
Compressive strength (28 days)	MPa	>20.0
Bending strength (28 days)	MPa	> 3.5
Secant modulus of elasticity (28 days)	MPa	-

Table 2.2 – Carbon 2-FRCM component properties according to the technical sheet



- **PBO-FRCM System**

PBO-FRCM, typically used for concrete flexural and shear reinforcement, is a composite material consisting of a PBO (Polyparaphenylene benzobisoxazole) fabric, which acts as continuous reinforcement, and a stabilized inorganic matrix, which binds the fabric to the concrete support.



**Figure 2.3 – PBO fabric roll and the inorganic cementitious mortar**

PBO-FRCM mortar is an inorganic matrix consisting of a pozzolanic hydraulic binder that is chemically, physically, and mechanically compatible with the concrete support. In Table 2.3 the technical specifications provided by the manufacturer of PBO-FRCM are shown, where the material properties can be divided into PBO fiber properties, fabric properties and mortar properties.

<b>PBO Fiber Properties</b>	<b>Units</b>	<b>Value</b>
Density	g/cm <sup>3</sup>	1.56
Tensile strength	GPa	5.80
Modulus of elasticity	GPa	270
Ultimate deformation	%	2.15
Breakdown temperature	°C	650
Coefficient of thermal dilation	10 <sup>-6</sup> °C <sup>-1</sup>	-6

<b>Fabric Properties</b>	<b>Units</b>	<b>Value</b>
Weight of the fabric	g/m <sup>2</sup>	110-126
Weight of PBO fibers in the fabric	g/m <sup>2</sup>	88
Equivalent dry fabric thickness in the direction of the warp	mm <sup>2</sup> /mm	0.0455
Equivalent dry fabric thickness in the direction of the weft	mm <sup>2</sup> /mm	0.0115
Ultimate tensile strength of the warp by width unit	kN/m	264
Ultimate tensile strength of the weft by width unit	kN/m	66.5

Ultimate tensile strain of the warp by width unit	-	0.0215
Ultimate tensile strain of the weft by width unit	-	0.0215
Axial Stiffness of the warp by width unit	kN/m	12.830
Axial Stiffness of the weft by width unit	kN/m	3.497
<b>Mortar 750 Properties</b>		
	<b>Units</b>	<b>Value</b>
Consistency (UNI EN 13395-1)		175
Specific weight of fresh mortar	g/cm <sup>3</sup>	1.80 ± 0.05
Liters of water per 100 kg of mortar		25 - 27
Yield (dry product)	kg/m <sup>2</sup> /mm	1.400 – 1.450
Compressive strength (28 days)	MPa	>30
Bending strength (28 days)	MPa	> 4
Secant modulus of elasticity (28 days)	MPa	7000

**Table 2.3 – PBO-FRCM component properties according to the technical sheet provided by the manufacturer**

## 2.1.2 Material Preparation and Installation Procedure

Following the work instructions provided by the commercially available FRCM manufacturers, the preparation of the composite material starts with the mixture of the inorganic matrix product. In particular, the cementitious grout has to be prepared by mechanical mixing, since hand mixing is not recommended. The dry powder cementitious matrix is added to 90% of the water needed for the mix. Mixing continues for at least three minutes until creating a homogeneous matrix paste. If necessary, the remaining water is mixed for an additional two minutes. Upon completion, the mortar rests for two minutes before applying on the substrate surface.

The matrix to water ratio for the inorganic matrix used for the preparation of the product depends on the type of inorganic matrix considered and is a value suggested by the manufacturer. Since for the present work different FRCM systems were used, the matrix to water ratio are provided in the previous section. The product was applied at an environmental temperature range between 20 °C to 35 °C.

Moreover, the installation procedure of the material requires the preparation of the concrete or masonry substrate of the element on which the FRCM has to be installed. The substrate is pressure cleaned to make it completely saturated with

water and after that, making sure to remove excess water. After this process, the surface must be kept in a saturated-surface-dry (SSD) condition. No sandblasting of the surface is needed.

Once the surface is ready, the cementitious mortar can be applied with a smooth metal trowel in a layer about 3-4 mm thick; then the pre-cut fabric has to be embedded in it with the appropriate fiber orientation making sure that all the fibers are completely placed into the matrix. Finally, a second layer of mortar about 3-4 mm thick has to be applied in order to cover completely the fabric. The same procedure can be repeated to install the designed number of plies. Figure 2.4 shows the installation procedure for a two-ply reinforcement of PBO and Carbon FRCM systems.

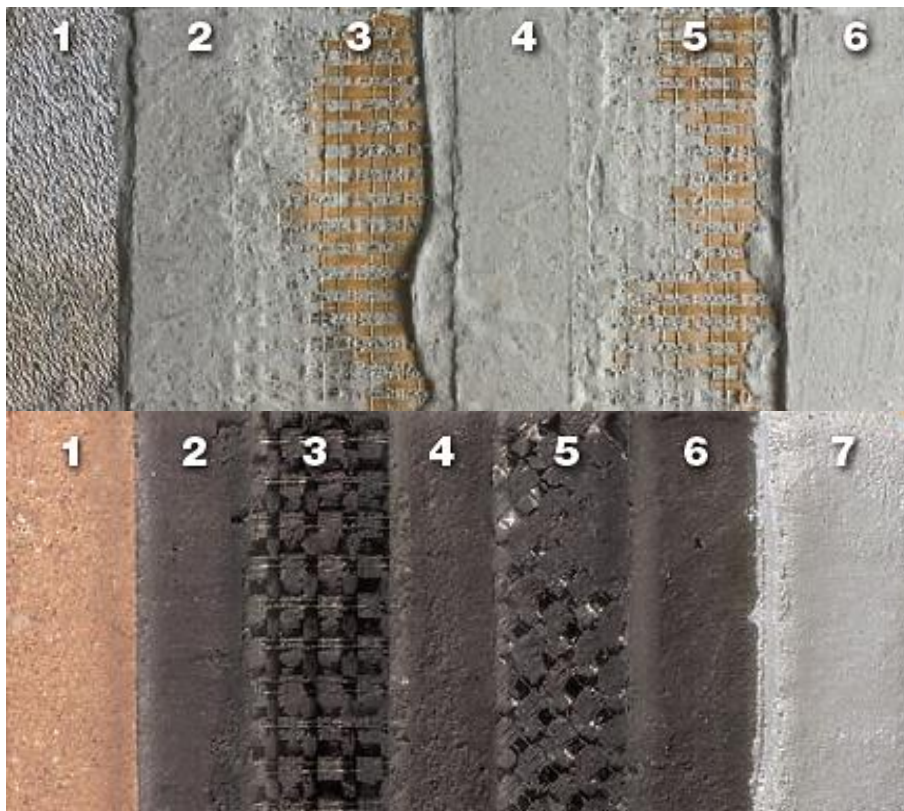


Figure 2.4 – Application sequence for a two-ply reinforcement of PBO and Carbon FRCM

Figure 2.5 shows a practical demonstration of the installation procedure of FRCM strengthening system on a reinforced concrete slab. Trained personnel performs the installation of the product.



**Figure 2.5 – Demonstration of installation procedure of FRCM strengthening**

Throughout the processes of product preparation and installation of FRCM systems application, quality control evaluations are performed. Quality control evaluations consist of verification checks of the mass prior mixing the matrix with the water; visual checks on the consistency of the matrix before, during, and after installation; matrix thickness layer verification with a Vernier caliper (Figure 2.5); and environmental temperature check before, during, and after installation.

### 2.1.3 Use and Applications

In this paragraph, an overview of some external reinforcement applications is presented. In addition, some FRCM examples currently available in literature (Nanni 2012, Nanni 2013) are provided.

- *Strengthening unreinforced concrete vaults*

This FRCM application comprised strengthening a bridge along the Rome-Formia- Naples railway in Italy (Nanni 2012).



**Figure 2.6 – Bridge structure with scaffolding (Nanni 2013)**

The 10.5 m bridge deck is supported by six semicircular arches made of unreinforced concrete having approximately the same span and supported by masonry abutments made of blocks of tuff.

This intrados strengthening prevents the formation of extrados hinges, modifying the ultimate behavior of the vault without affecting its behavior under service loads. The final design called for strengthening of the soffit of each vault by

an application of two plies of PBO-FRCM. The technical choice to work on the intrados rather than the extrados was driven by the need to not interrupt the use of the bridge, which would have been necessary if strengthening of the extrados had been applied. A thorough cleaning of the concrete surface and the removal and reconstruction of portions of deteriorated concrete occurred first. Then the standard FRCM installation procedure was carried out until the installation of two plies was done (Figure 2.7).

Since it was not necessary to stop train traffic on the viaduct the project execution was fast and relatively easy. Furthermore, because the cementitious matrix is compatible with the concrete substrate, it was not necessary to wait until it was dry in the regions where concrete was replaced in order to proceed with the strengthening, as it would be required with the use of an epoxy-based matrix.



**Figure 2.7 – Left: Workers install the first layer of PBO-FRCM on the soffit of concrete vault.  
Right: Application of the second ply of PBO fabric (Nanni 2012)**

- *Retrofitting the Aachen cathedral*

Considering the preservation of historic structures, the retrofitting of the Aachen cathedral represents another appropriate example. The following work was developed by Buttner et al. (2011). In collaboration with a structural engineer and the building authority of the cathedral a concept of minimizing the crack movement in combination with sealing the crack was developed (Figure 2.8).



Figure 2.8 – Photograph of the crack through the roof above the octagon (Buttner et al. 2011)

The boundary conditions of the problem (cultural heritage, crack origin and crack movement) led to the following requirements:

- following the guidelines for preserving cultural heritage during the whole process of retrofitting
- minimizing the crack movement and sealing the cracked area
- strengthening the whole structure allowing the load transfer over the crack
- use of extremely durable materials

Besides the already mentioned conditions, the design of the crack bandage had to be done considering if possible the use of “traditional” materials, minimizing intrusions into the existing structure and taking into account a maximum height of 30mm.

Due to the restrictions of the building authority the crack bandage could not be made out of FRP because the polymeric matrix does not satisfy the “traditional” material requirement. Therefore, the matrix material used was cement-based. In order to ensure a highly durable system with a maximum thickness of 30 mm, and to have a feasible system to be adjusted to the irregular shape of the cathedral, a combination of a cementitious matrix with fabric reinforcement (FRCM) was used.

- *Repair of trestle pedestals*

In this installation, FRCM was used to provide confinement and protection to concrete pedestals supporting a Metro North Railway trestle over a valley in northern New York. The pedestal shown in Figure 2.9 has a truncated pyramid shape that measured about 2.4 x 2.4 m at the base and was 2.4 m in height.

Over the years, weathering had led to significant cracking and spalling (Figure 2.9). A repair was deemed necessary, to restore some of the initial strength and to ensure long-term performance. Hence, FRCM was installed: the first part of the project was to remove and replace the deteriorated concrete, the FRCM matrix was then applied to the substrate and the fabric was pressed into it. Then, the crew installed the top mortar layer and a curing compound to provide proper curing.

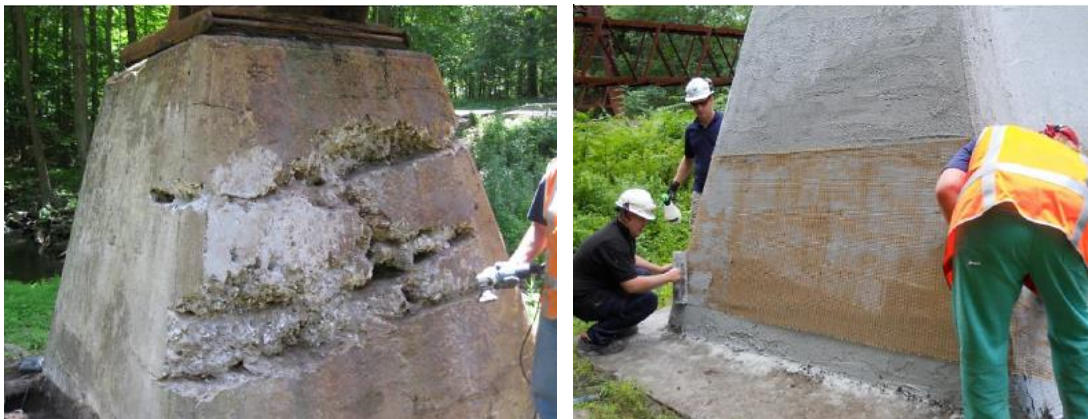


**Figure 2.9 – Left: Deteriorated pedestal base support. Right: Application of PBO network over a layer of mortar (Nanni 2012)**

- *Strengthening a masonry chimney*

This project consisted of strengthening an unreinforced masonry chimney of a historic sawmill in the municipality of Gerardmer, France. This chimney, a symbol of industrial heritage, was to be preserved and restored. The chimney has a height of about 38 m with a diameter ranging from 3.60 m at the base to 1.70 m at the top



(Figure 2.10). From a design perspective, the chimney was analyzed as a cantilever beam with wind as a primary load condition.

The analysis indicated that strengthening of the structure with FRCM was needed, using a single carbon fiber network (Figure 2.10). The resulting FRCM thickness was only 10 mm and was equivalent to using a mat of D4 reinforcing steel bars (6 mm in diameter) with spacing of 0.56 m in both directions.



**Figure 2.10 – Left: Chimney surrounded by scaffolding during repair. Right: Chimney masonry surface before and during strengthening (Nanni 2012)**

- *Strengthening of cooling towers*

One last interesting application of the FRCM composite is related to the strengthening of cooling towers in a thermal power plant in Germany. In particular, what is fascinating about this example is the heat resistance of the FRCM system and at the same time the capability of modelling nontraditional shapes and dimensions.



Figure 2.11 – Strengthening of cooling towers (Germany)

## 2.1.4 Acceptance and Reports

FRCM systems have been only recently inserted in North American building codes and the International Building Code (IBC). The first document on FRCM was released by the International Code Council Evaluation Services (ICC-ES) and approved in 2003. The document was entitled “*Acceptance Criteria for Cement-Based Matrix Fabric Composite Systems for Reinforced and Unreinforced Masonry*”

(AC218). In October 2011, this document was superseded by another document issued by ICC-ES titled Acceptance Criteria 434: “*Acceptance Criteria for Masonry and Concrete Strengthening Using Fabric-Reinforced Cementitious Matrix (FRCM) Composite Systems*” (AC434 2011). This document provides the appropriate guidance for characterization and design of FRCM systems and establishes requirements for recognition of FRCM in an “Evaluation Report” under the 2009 and 2012 IBC.

As any other Acceptance Criteria, AC434 was developed by ICC-ES technical staff in consultation with industry and academia. For manufacturers, AC434 establishes the guidelines for tests and calculations in order to receive a product Evaluation Report from ICC-ES. Once obtained, the “evaluated” FRCM system/s is/are recognized by any building official as an approved repair method.

Within the research team of the University of Miami, a set of suggestions was proposed to the ICC-ES technical staff with some considerations and rational developments on the October 2011 version. All the improvements on the document were collected in a proposed document edition issued in December 2012 (AC434 2012). In February 2013, the proposed changes were formally approved by the ICC commission and included in the February 2013 version release of the document (AC434 2013).

In addition, FRCM is covered by ACI Committee 549 (“*Thin Reinforced Cementitious Products and Ferrocement*”) that deals with thin cementitious products and ferrocement. ACI 549 committee has recently released a document entitled ACI 549.4R-13: “*Guide to Design and Construction of Externally Bonded Fabric-Reinforced Cementitious Matrix (FRCM) Systems for Repair and Strengthening Concrete and Masonry Structures*” which is now the first released FRCM repairing guide.

In July 2002, RILEM (International Union of Laboratories and Experts in Construction Materials, Systems and Structures) formed the Technical Committee

201-Textile Reinforced Concrete and, four years later, this committee published a state-of-the-art report (RILEM TC 201-TR 2006).

This report includes information on applications of textile reinforced concrete and strengthening systems for unreinforced masonry. Also the Italian “Consiglio Nazionale delle Ricerche” (CNR) is developing a new document intended to provide guidelines and information in compliance with the European standards. As for now, the currently available documents in Europe are only referred to FRP composite system: CNR document entitled “*Guide for the Design and Construction of Externally Bonded FRP Systems for Strengthening Existing Structures*” (CNR-DT 200/2004).

The relevance of this composite system is also highlighted by the efforts of several US and European companies which, with high priority, are in the process of FRCM certification and acceptance, making the investigation of its characteristics of central importance to this purpose.

## 2.2 FRCM Mechanical Properties

Defining and performing the mechanical testing necessary to determine the material parameters to be used for design is of primary importance to the acceptance of new materials into the building codes. To this end, in this section the mechanical properties of FRCM composites are presented.

### 2.2.1 Mechanical and Failure Behavior of FRCM Systems

#### *General behavior of a fabric reinforced composite*

The behavior of an FRCM-RC beam is described in literature (Ombres 2012) as follows: as soon as a crack is formed in the concrete because of its low tensile capacity, the tensile stresses released by the concrete are transferred to the strengthening fabric, thanks to the capacity of the interfacial bond to carry shear stresses. As the applied load increases together with the required tensile strength of the fabric, the cementitious-based bond between the fabric and the concrete becomes more critical. Finally, when the shear stress applied on the fabric reaches its maximum capacity the system fails.

The bond at the interface between the constituents of a composite system is essential for the composite behavior because it determines the strength and ductility of the material (RILEM TC 201-TRC 2006). Therefore, great relevance has to be given to the quality of the bond within the fabric and concrete provided by the matrix. The capacity of an FRCM system to transfer shear stresses from the concrete element surface to the fibers is a very complex phenomenon involving: the bond between the fibers and the matrix; the capacity of the mortar to fully embed the fiber strands; the non-uniformity of tensile stress of a strand and the fibers telescopic failure; the cracking of the cement based matrix; the bond between the new cement based matrix and the old concrete surface (D'Ambrisi et al. 2012).

Debonding failure modes, both in the matrix-fabric and matrix-concrete interface, as well-known, reduce drastically the strength enhancement provided by external reinforcement systems whether applied on existing concrete structures (Ombres et al. 2012). Also shown by Ombres (2009), from the results of the flexural tests it appears that the failure modes of the strengthened beams consistently depend on the amount of FRCM plies installed on the concrete element. Indeed, one-ply strengthened specimens failed due to the debonding between the fabric and the cementitious matrix (slippage), whereas those strengthened with four-ply failed due to the intermediate crack-induced debonding within the inner fabric ply (delamination). Figure 2.12 shows the possible failure modes of external reinforcement presently documented in literature.

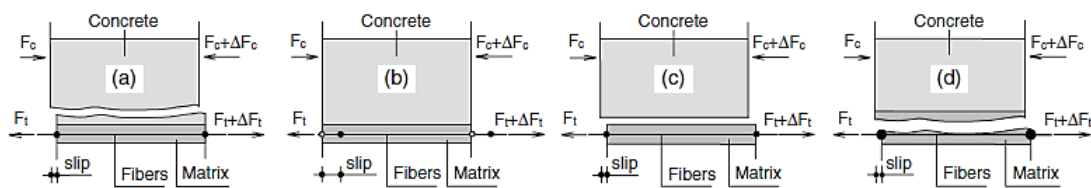


**Figure 2.12 – Observed failure modes: (a) fracture surface within the concrete, (b) slippage of the fibers from the matrix, (c) debonding at the matrix/concrete interface, (d) delamination in the net's layer (D'Ambrisi et al. 2011)**

Among all the failure modes, only slippage, case (b), and delamination, case (d), are expected to occur in cementitious-based external reinforcements. In particular, with FRCM, failure mode (a) is not expected to occur because the mortar applied on the concrete surface has the same tensile capacity of the concrete itself. Thus, failure mode (a) can occur only for FRP composite systems where the bond is provided by inorganic binders such as epoxy, which has a tensile capacity up to ten times greater than that of the concrete. Also, as observed by Brückner et al. (2006) and Ortlepp et al. (2004, 2006), failure mode (a) can be caused by the low tensile capacity of the concrete substrate that in most of the cases is not well preserved, common when FRCM repair is necessary.

Furthermore, due to the good compatibility properties between the mortar and the surface of the existing concrete member and to the effectiveness of the material installing procedure, failure mode (c) it is not likely to be observed. Instead, failure mode (c) is usually observed in FRP systems, where the organic binder material may not perfectly attach the reinforcement system to the concrete surface even if it is perfectly smooth. In this case, the strengthening completely peels off. The same failure may occur between different layers belonging to the same FRP system.

Slippage and delamination failure modes are experienced consistently by one- and four-ply strengthened beams (Figure 2.13). Consequently, a detailed description of the failure mechanisms is presented in the next two subsections.

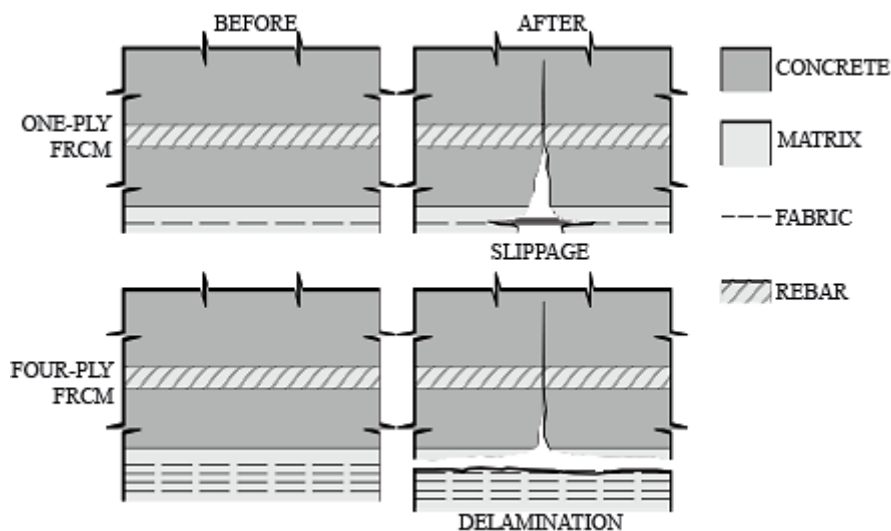


Figure 2.13 – Failure modes observed with the FRCM (Loreto et al. 2013)

- *Slippage*

As described in literature (D’Ambrisi and Focacci 2011), slippage failure mode is caused by the debonding of the fabric from the matrix in the maximum bending moment regions in the case of flexural reinforcement where the concrete tensile crack propagates immediately through the mortar exposing the fabric to the external environment.

As a consequence of this failure mode, the tensile stress transferred from the concrete is carried only by the adhesion capacity between the fabric and the mortar, which is the capability of the entire fabric to avoid any relative displacement between the fabric itself and the mortar. The effectiveness of the adhesion depends mostly on the chemical bond that the fibers are able to establish with the respective matrix, the presence of fibers in the orthogonal direction, and the friction itself between the fabric and the mortar.

Friction, in particular, is created by the irregularity of the PBO fiber strand cross section (Figure 2.14a) because it is characterized by the presence of numerous sleeve filaments outside the core filaments. The external filaments are the ones that contribute to the “roughness” of the fiber strands since they are impregnated by the mortar, whereas the inner filaments are the ones that actually carry the load. Carbon fiber strands, instead, have a regular cross section that avoids any shear stress transferring between the strands and the mortar in which they are impregnated, inducing more likely a slippage failure mode.

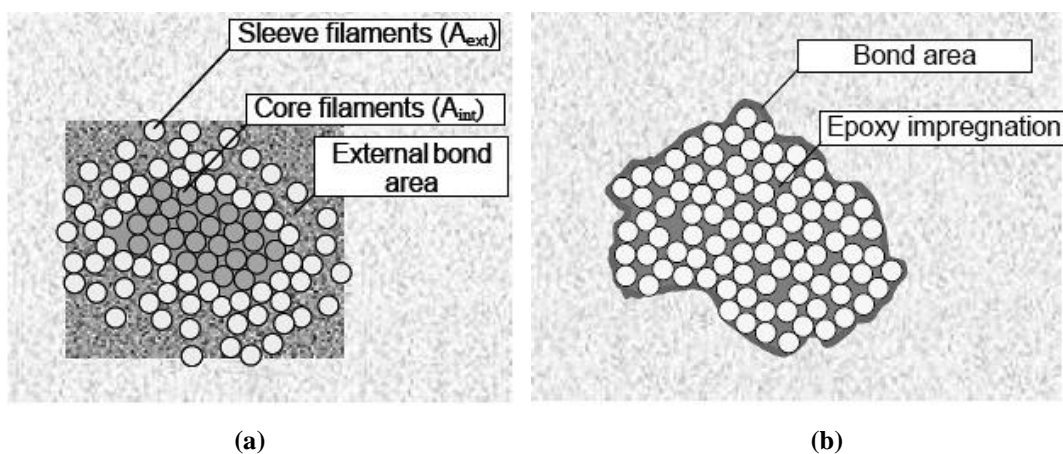


**Figure 2.14 – (a) Strand with inner bond < outer bond (e.g. FRCM strand not fully embedded with cementitious matrix); (b) Strand with inner bond > outer bond (e.g. FRP epoxy impregnated strand) (Krüger et al. 2002)**

Because of the uncontrolled penetration of the cement-based binder, outer filaments in direct contact with the concrete matrix have better bond performance than the inner filaments. This phenomena leads to a different formation of the inner



and outer bond characteristics. Among all the currently available models in literature, the failure mechanism that occurs after the tensile failure of the outer filament layers is described as a so-called “telescopic failure” i.e. the pull-out of the core of inner filaments of the strand. In accordance with the telescopic failure, the capacity of the fiber strands to carry tensile stresses is related only to the friction between the inner filaments that are not reached by the hydrated cement, thus free to slip (Leardini 2013).

However, for the FRP systems the internal bond may be influenced by the use of a resin for the strand impregnation. Then the strand is more or less a rigid composite material made up of the filaments and the resin (Figure 2.14b). Instead, FRCM is defined as a *dry system* because even if for manufacturing, installation or handling purpose a resin has to be applied on the exterior fiber strands, no redistribution of the stress along the fiber strand occurs.

If someone were to argue that with further developments fabric slippage phenomena can be avoided by developing a new material able to establish a perfect bonding between the mortar and the fabric, as the fiber-matrix interaction becomes tighter, the failure mode would change from the loss of adherence to the failure of the mortar in tension, being not able to carry the significant tensile stress that the fibers can transfer. Therefore, fiber slippage has not to be considered a weakness of the external reinforcement material, rather an actually acceptable failure mode. Indeed, as observed in literature (Ombres 2011), the bond slippage leads to a pseudo ductile overall failure of the composite system.

- *Delamination*

Delamination failure mode (or intermediate crack failure) is defined in literature (D’Ambrisi et al. 2011) as the matrix intermediate-crack grown within the FRCM mesh layer, with the formation of a fracture surface within the matrix, preceded by

relevant fabric/matrix slip. It generally occurs due to the excess of the adhesive tensile strength required by the strengthening within the fabric layer and the mortar.

In most cases, a thin layer of the matrix remains perfectly attached to the concrete surface. This is why the layer where the fabric is installed can be considered a defect that breaks the continuity among the matrix. This happens mostly because the fine graded mortar cannot fully impregnate the fiber strands (Banholzer 2004; Hartig et al. 2008; Hegger et al. 2006; Soranakom and Mobasher 2009; Wiberg 2003; Zastrau et al. 2008) and also penetrate into the openings of the fabric. Indeed, the density of the fabric net (i.e. quantity and spacing between the strands in each direction) is of great importance when a cement-based matrix is used, as also observed by several authors (Curbach et al. 2006; Ortlepp et al. 2004, 2006). The surface of the matrix/strand interface should be maximized, e.g., by reducing the strands dimension and at the same time increasing the number of strands (Badanoiu and Holmgren 2003). Moreover, the presence of the mesh reduces the capacity of the matrix to transfer shear and tensile stresses because of surface reduction (Ortlepp et al. 2004, 2006).

### **2.2.2 Tensile Characterization**

Tensile testing is performed to understand the behavior of FRCM composites in tension and determine the values necessary for analysis and design of structural elements. This type of test is currently the most common test in literature in order to provide representative values on the FRCM mechanical behavior. Results are then used to develop models able to predict the load capacity of a given concrete element strengthened with external reinforcement.

Since tensile testing procedures for continuous fabric reinforced cementitious matrix composites are not yet standardized, FRCM tensile properties are determined according to the test procedure specified in Annex A of AC434 (2013). Figure 2.15 shows a typical tensile test setup with clevis grips and a typical stress-strain curve.

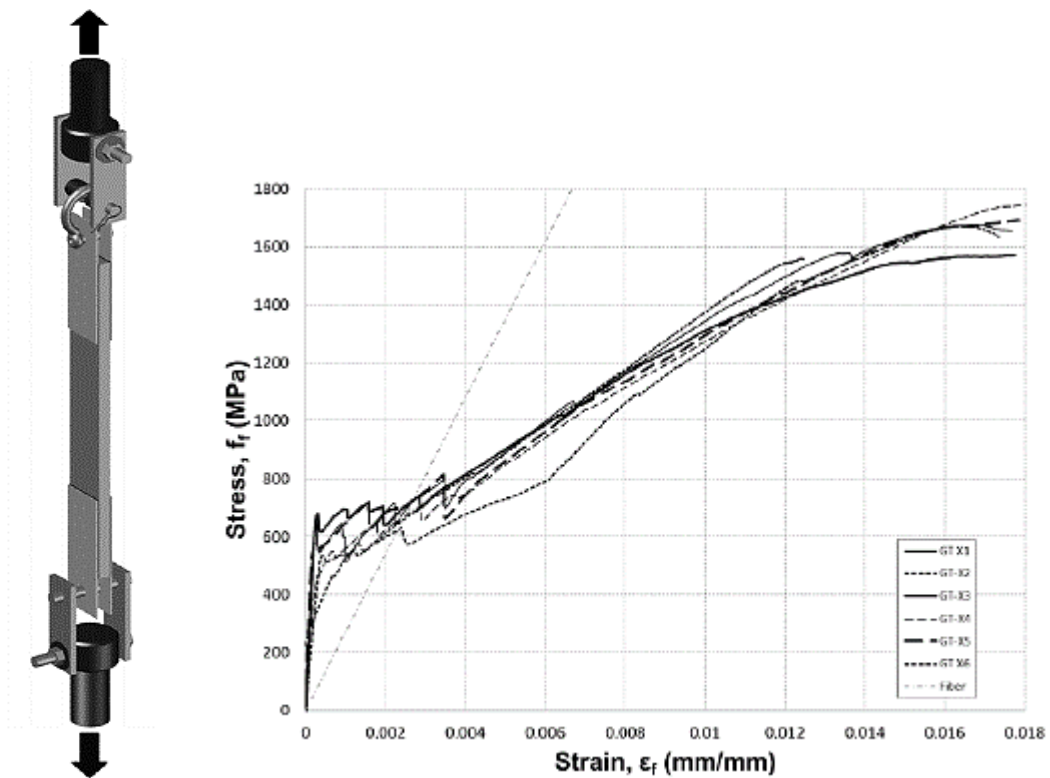
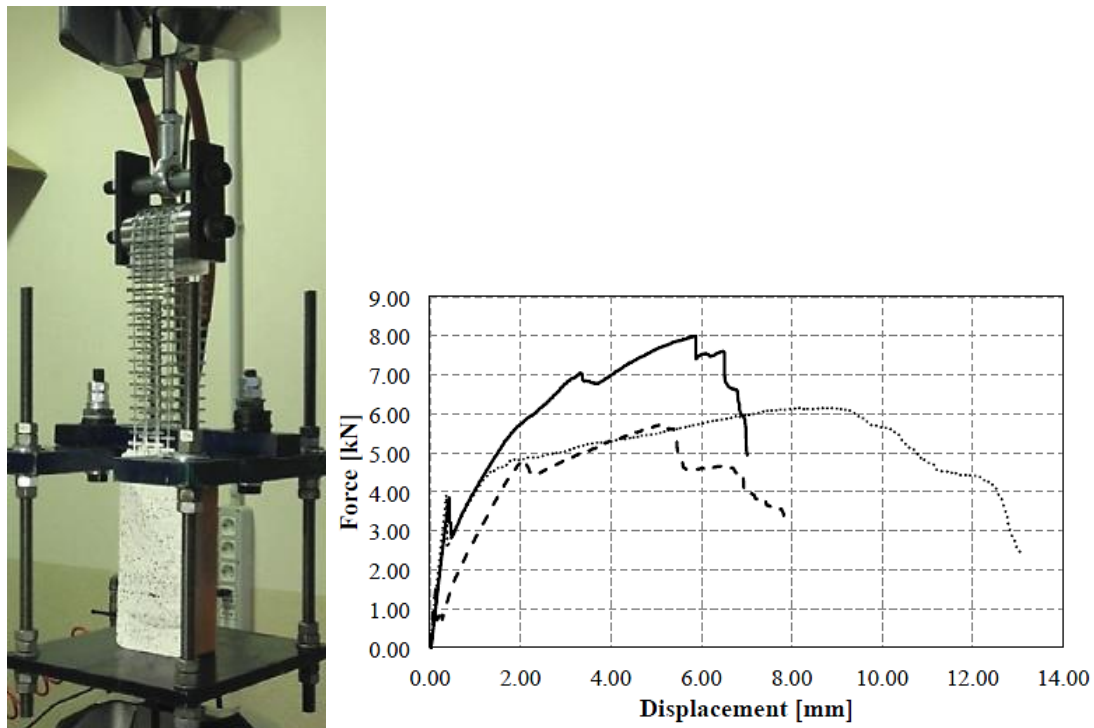


Figure 2.15 – Typical tensile test setup and stress-strain curve (modified from Arboleda 2014)

As far as the stress-strain behavior is concerned, the tensile strength of the fabric is never reached because the main failure mode of the FRCM in tension occurs due to the slippage of the fibers when the adherence between the fabric and the mortar gradually decreases (Leardini 2013). Therefore, the idealized tensile stress-strain curve of an FRCM coupon specimen is a simple bilinear curve initially linear until cracking of the cementitious matrix occurs, then, deviates from linearity and becomes linear again until the tensile failure happens.

Further developments including different testing procedures may lead to a better characterization of the material properties. A new test configuration was recently introduced (Carozzi et al. 2014) in order to examine the behavior of the FRCM once applied on a concrete or masonry element, this test is called “double shear fabric loop test” (DSFL).

The double shear fabric loop test consists of a simple traction test performed on an FRCM composite applied to both sides of a concrete or masonry element and with the fabric extending in a U shape to connect the two sides (Figure 2.16). To date, only one-ply strengthened configurations have been tested.



**Figure 2.16 – Experimental setup for a double shear fabric loop test and the typical force-displacement curve (Carozzi et al. 2014)**

The double shear fabric loop test has been carried out by Carozzi et al. (2014) in the *Laboratorio Prove Materiali* at Politecnico di Milano and the typical force-displacement curve is shown in Figure 2.16.

According to Carozzi et al 2014, compared with the standard tensile test, the DSFL test presents two main advantages: (1) the FRCM configuration is more representative of the in-situ installation configuration. The presence of the substrate reduces the mortar cracking as it actually happens in in-situ FRCM applications. On the other hand, standard tensile tests experienced an evenly and widely distributed

crack pattern that affects the strain measurements and the slippage phenomenon. (2) More representative FRCM failure modes can be reproduced during the test.

### **2.2.3 Bond Characterization**

The effectiveness of an FRCM external reinforcement strongly depends on the bond between the strengthening material and the concrete and on the concrete mechanical properties. It is therefore crucial to accurately characterize the bond between these strengthening materials and the concrete. In particular, an FRCM system has to be stronger than the material it is reinforcing, and at the same time, it must be able to work together with that material (Bianchi 2013). For this reason, adhesion properties for the strengthening system have to be studied.

The bond between the FRCM materials and the concrete have different peculiarities with respect to the bond between FRP materials and the substrate. In fact, in the case of FRP the debonding surface is generally within the substrate or at the FRP/substrate interface, while in the case of FRCM materials different debonding mechanisms, including the fabric/matrix interface, are observed (D'Ambrisi et al. 2012).

The shear stress transfer between the fabric net of the FRCM material and the supporting concrete is influenced by the bond between the fabric net and the cement-based matrix and by the bond between the matrix and the concrete surface. The bond between the fabric and the matrix has been experimentally studied in several papers (Peled et al. 1998, 2000, 2008; Badanoiu 2003). These works demonstrate that the fabric/matrix bond is influenced by the bond between single fibers and matrix, the matrix penetration into rovings and the capacity of wetting single filaments, the bond between the external fibers directly in contact with the matrix and the internal fibers, the non-uniformity of tensile stress in fibers of a roving and the fibers telescopic failure, and the influence of the fibers arrangement in the net.

In the case of an FRCM material used to strengthen a concrete surface, the shear stress must be transferred to the concrete. Therefore, in addition to the mentioned phenomena characterizing the fabric/matrix bond, also the bond between the cement matrix and the concrete, the cracking of the matrix and the failure of the supporting concrete play an important role. These features were studied and several tests were performed in order to define the bond properties of the system. Both Europeans (Ortlepp et al. 2006; D’Ambrisi et al. 2012) and Americans (Verbovszky and al.; ASTM International) researchers proposed several kinds of tests, usually based on the shear resistance of the surface bond between mortar and support and seldom between mortar and fabric, despite this interface being the most critical one (Bianchi 2013). Indeed, often the weakest link of the system is the debonding on the fabric discontinuity surface.

The Pull-Off test is a common way to analyze the bond strength of an applied material on a support, performed according to ASTM C1583: “*Tensile Strength of Concrete Surfaces and the Bond Strength or Tensile Strength of Concrete Repair and Overlay Materials by Direct Tension*”. It consists of a normal force applied on an established area, which is a 50 mm (2.0 in) diameter disk cored from a specimen. Figure 2.17 shows the possible failure modes in the Pull-Off test.

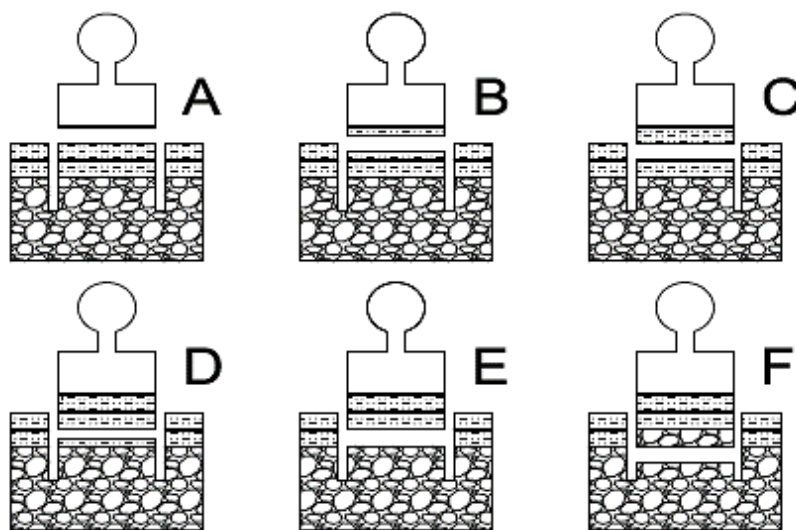


Figure 2.17 – Failure modes in accordance to AC434

The failure mode (A) corresponds to the bond failure at the epoxy/overlay interface; the failure modes (B), (C), and (D) correspond to the failure in overlay or repair material; the failure mode (E) corresponds to the bond failure at the concrete/overlay interface; the failure mode (F) corresponds to the failure in the substrate.

After a Pull-Off test, the critical stress reached when the failure occurred is computed dividing the peak load by the area on which the load itself was applied. Since an FRP system can be considered a continuum, the failure phenomenon always involves the entire loaded area. In contrast, an FRCM system is actually a composite material where the two constituents are only applied together but they do not represent a continuum. Therefore, when the failure occurs on the interface between the first and the second layer of mortar, where the fabric is embedded, the failure itself occurs because the mortar that connects the two layers of matrix (through the fabric) breaks. In this unique case, the loaded surface is not the entire area but only the net area, which is the entire area minus the area covered by the fabric. Therefore, the net area has to be used for the stress computation.



**Figure 2.18 – Failure on the interface between the first and the second layer of mortar**

A new and more accurate way to compute the net area necessary for the stress calculation will be presented in Chapter 4 (Section 4.5).

## **2.3 FRCM Effectiveness in Structural Rehabilitation**

In addition to tests to determine material parameters, tests on structural members are performed to examine the effectiveness of FRCM on strengthening application. FRCM bonded to surfaces of RC members can be used to enhance beam flexure and shear strength by acting as external reinforcement.

### **2.3.1 Flexural Strengthening**

When used as a flexural strengthening system, FRCM behaves like an external tensile reinforcement for RC elements. When a flexural crack occurs inside the concrete due to its low tensile capacity, the tensile stresses released by the concrete are transferred to the strengthening material by interfacial bond. As the applied load increases together with the tensile stress in FRCM, the bond between the fabric and its matrix becomes critical. When the shear stress applied on the FRCM reaches its maximum capacity, the strengthening system fails (Ombres 2012).

Overall, three possible failure modes are observed: fracture surface within the concrete, slippage of the fabric within the matrix, and delamination of the FRCM from the substrate (D'Ambrisi and Focacci 2011). Moreover, it was observed that specimens with low level of strengthening fail due to fabric slippage, whereas specimens with higher level of strengthening fail due to delamination between FRCM and the concrete substrate. Both the slippage and delamination failure modes make it impossible to attain fiber rupture (Ombres 2011; Loreto et al. 2013).

In particular, slippage is the predominant failure mode that initiates at the location of the concrete cracks reflecting through the FRCM matrix (Loreto et al. 2014). This bond slippage leads to a pseudo-ductile behavior of the flexural member (Ombres 2011) and, as observed by Triantafillou and Papanicolaou (2006), offers the possibility of inspection of damaged regions before catastrophic failure occurs. Because the cementitious matrix cannot fully impregnate the fiber strands, the presence of the fabric itself reduces the capacity of the matrix to transfer shear



stresses (Ortlepp et al. 2004, 2006). Consequently, as observed by many authors (Curbach et al. 2006; Ortlepp et al. 2004, 2006), a major role in slippage-type failure is played by the density of the fabric defined as the width and spacing of the strands in each direction.

According to the studies, the main parameters affecting the response of concrete beam elements under bending actions are: beam geometric properties (section size and span), beam internal reinforcement (longitudinal and transversal reinforcement ratio), external reinforcement properties (number of plies and orientation), fabric properties (density and net area), binder properties (cement and aggregates type), test set-up (three- and four-point-bending) and load application path (cyclic and monotonic). Because of the high number of the parameters affecting the reinforced element response, it becomes difficult to compare results obtained by different research studies. Moreover, since this reinforcement technique is a recent development, few papers are found in literature on this topic.

Relevant studies were found that use two of the FRCM systems used for this research. Specifically, experimental results of RC beams strengthened in flexure have been reported and discussed in D'Ambrisi and Focacci (2011), Leardini et al. (2014) and Loreto et al. (2014). Both carbon and PBO FRCM were considered. Beams strengthened with PBO-FRCM materials showed a load-carrying capacity increase of the same order of magnitude as that observed for beams strengthened with FRP. PBO-FRCM performed better than carbon-FRCM.

The work conducted by Leardini et al. (2014) represents an appropriate example of the FRCM effectiveness in flexural strengthening. Figure 2.19 shows the layout of a beam strengthened with the FRCM system, including fabric arrangement for a representative one-ply reinforcement. The three-point bending test was performed on simply-supported specimens.

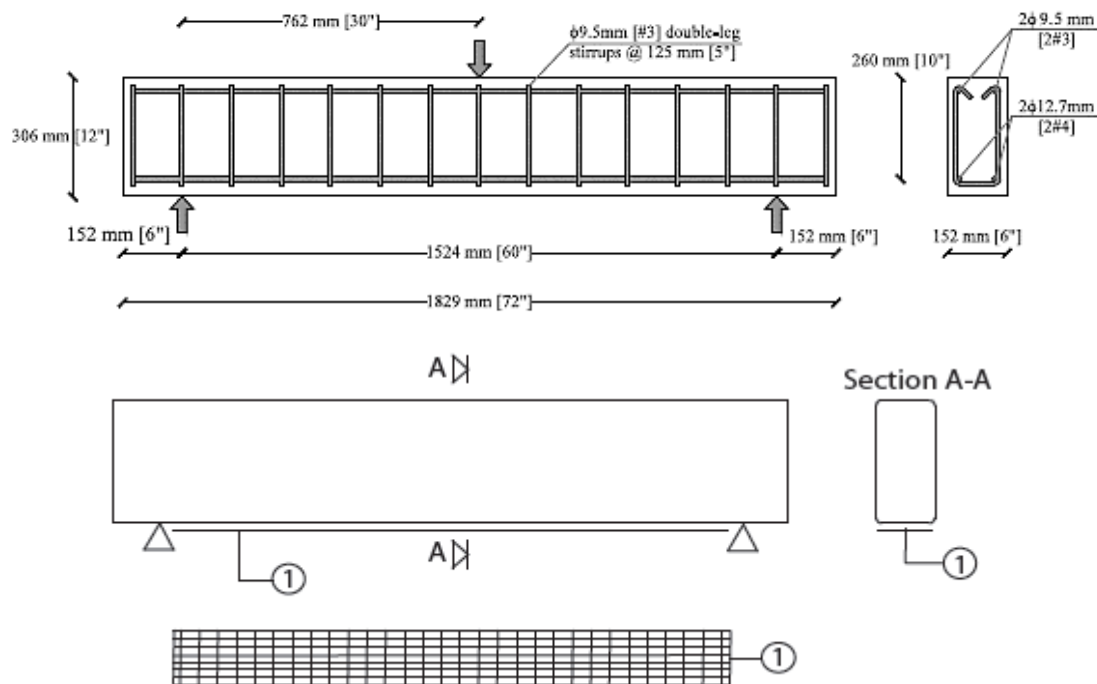


**Figure 2.19 – Structural specimen layout and fabric arrangement for a one-ply strengthened beam (modified from Leardini 2014)**

According to Leardini et al. (2014), the flexural strength enhancement, defined as the ratio of the maximum capacity of the strengthened specimen to the capacity of the respective unstrengthened one (control specimen), was found to be 132 and 192% for beam-type elements with low strength concrete and 113 and 173% for beam-type elements with high-strength concrete, using one-ply and four-ply PBO-FRCM, respectively. The effects of FRCM were evident resulting in an increase in strength, proportional to the fabric amount, but also in a corresponding decrease in ductility.

Moreover, this work provides a detailed description of the failure modes experienced during the tests. In particular, slippage phenomenon was observed with a high consistency in the case of flexural strengthening provided with one-ply of FRCM, while delamination failure mode was observed in the case of flexural strengthening provided with four-ply of reinforcing material.

### 2.3.2 Shear Strengthening

Compared to FRCM strengthening for bending, less experimental studies have been conducted so far on the application of FRCM systems for shear strengthening of reinforced concrete beams. In addition to the parameters considered for the bending response of externally reinforced concrete beams, the beam response under shear actions is strongly affected by the shear span to effective depth ratio ( $s/d$ ). This ratio affects the beam failure mode and therefore its overall behavior. This is the reason why results obtained with different  $s/d$  ratios may not be consistent.

Brückner et al. (2006) demonstrated how thin layers of concrete with fabric reinforcement could be used for strengthening of RC members improving serviceability and shear capacity with reduction of deflection and crack width. Problems related to the force transfer mechanisms between the external strengthening system and the concrete substrate were also investigated. Tests were performed to describe the relationship between shear loading and deformation, as well as the necessary bond length and the transferable bond forces. Investigations proved that relatively short bond lengths were sufficient for the anchorage of the strengthening.

Triantafillou and Papanicolaou (2006) experimentally and analytically investigated the use of FRCM to increase the shear resistance of RC members under monotonic or cyclic loading. They concluded that FRCM jacketing provides substantial gain in shear resistance. This gain was higher as the number of layers increased and sufficient to transform shear-type failure to flexural-type failure.

Al-Salloum et al. (2012) investigated the use of basalt-FRCM as a means of increasing the shear resistance of RC beams. The studied parameters included: two different mortar types (cementitious and polymer-modified cementitious mortars), the number of reinforcement plies and their orientation. It was concluded that FRCM provides substantial gain in shear resistance. This gain was directly dependent upon the number of fabric plies installed.

Loreto et al. (2014) examined the effectiveness of shear reinforcement offered by the addition of FRCM, analyzed the failure modes experienced by FRCM strengthened elements, and investigated the FRCM load transfer mechanism. This experimental program was carried out by casting, strengthening and testing under three-point bending several beams heavily reinforced in flexure to ensure shear deficiency. Figure 2.20 shows the layout of a beam strengthened with the FRCM system, including fabric arrangement for a representative one-ply and four-ply reinforcement.

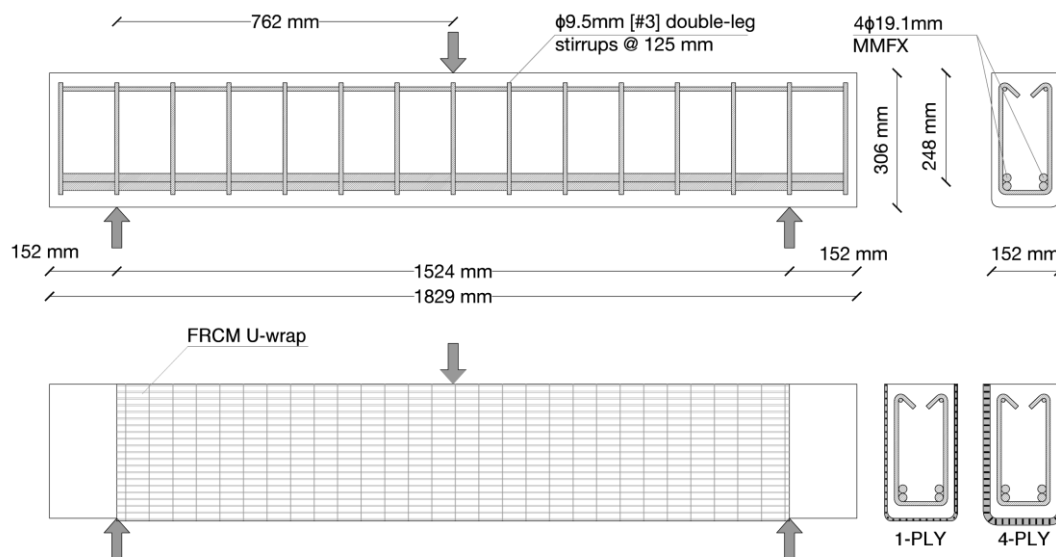


**Figure 2.20 – Structural specimen layout (Loreto et al. 2014)**

The results demonstrate the technical viability of FRCM for shear strengthening of RC beams. Based on the experimental and analytical results, FRCM increases shear strength but not proportionally to the number of plies installed. The strength enhancement was found to be 121 and 151% for beams with low-strength concrete and 126 and 161% for beams with high-strength concrete with one-ply and four-ply FRCM, respectively. The effects of FRCM resulted in an increase in strength, not proportional to the fabric amount. Contrarily to what was expected from the flexural tests, beams experienced increase in ductility, proportional to the fabric amount.

Moreover, FRCM failure modes were found to be related with a high consistency to the amount of external reinforcement applied. In particular, slippage failure mode occurred for one-ply strengthened specimens while delamination from the substrate characterized the ones with four plies.

### **2.3.3 Axial Strengthening: Column Confinement**

Axial strengthening represents another relevant application of FRCM composites. Confinement with FRCM systems has been investigated for damaged and undamaged RC members.

Triantafillou et al. (2006) used cylindrical and prismatic plain concrete specimens. The investigation with cylindrical specimens studied the effects and strength of two inorganic mortars and a number of reinforcement layers (two and three). Jacketing of all cylinders was accomplished with the use of a single mesh in a spiral configuration until the desired number of layers was achieved. Testing on rectangular prisms aimed at investigating the number of reinforcement layers (two and four) and effectiveness of bonded versus unbonded confinement. This work concluded that: a) FRCM-confining jackets provide a gain in compressive strength and deformation capacity, which for example in the case of ultimate load, represents an increase over the unconfined specimen between 25 and 75 percent based on mortar type, number of reinforcement layers, and specimen cross section type. b) This gain increases as the number of fabric layers increases and depends on the tensile strength of the mortar. c) Failure of FRCM jackets is due to the slow progressing fracture of individual fiber strands.

De Caso y Basalo et al. (2009, 2012) studied the feasibility of developing a reversible and potentially fire-resistant FRCM system for concrete confinement applications. A prospective system was chosen from different fiber and cementitious matrix combinations. The selected FRCM system was further evaluated using different reinforcement ratios and by introducing a bond breaker between concrete and jacket to facilitate reversibility. Substantial increases in strength and

deformability with respect to unconfined cylinders were observed. In the case of bonded jackets, for example, the increase in ultimate capacity over the unconfined specimen varied between 21 and 121 percent when the number of reinforcement layers varied from one to four. The predominant failure mode was fabric-matrix separation, which emphasized the need of improving fabric impregnation.

Abegaz et al. (2012) tested several RC columns wrapped with FRCM to examine the enhancement in strength and ductility for different cross-sectional shapes. Rectangular, square, and circular specimens with equal cross-sectional area and slenderness ratio were analyzed to properly identify the effect of shape on the confinement effectiveness. In addition, columns with one and four layers of FRCM wrapping were tested to investigate the effect of the number of plies. Results demonstrated that FRCM wrapping can significantly enhance the load-bearing capacity (up to 71 percent) and ductility (exceeding 200 percent) of RC columns subjected to a monotonic axial compressive load, with the highest improvement obtained for circular cross sections.

### **2.3.4 Masonry Strengthening**

Masonry structures constitute the major portion of most urban aggregates. This Section presents some literature references regarding the behavior of masonry structures reinforced with FRCM composite system.

Seismic events induce out of plane loads on the walls between restraining floors. Most existing unreinforced masonry walls often cannot bear this type of load. The failure of this kind of walls occurs in a sudden and brittle way, causing huge damages. Indeed, even though the whole structure does not fail, the walls collapse, crumbling on the people inside and provoking deaths.

Experimental results indicate that FRCM systems represent a viable solution for structural strengthening of masonry structures. Results in literature are available for FRCM systems to strengthen walls made of concrete masonry units (CMUs), fired

clay bricks, tuff blocks, and stone blocks. Some examples from ACI.549.4R-13 are reported.

Marshall (2002), Mobasher et al. (2007), and Aldea et al. (2007) reported in-plane shear concrete masonry full-scale pier (lightly reinforced single-wythe masonry walls) tests to simulate seismic action. The FRCM system was compared with a number of commercially available FRP systems as part of a broad experimental program. Results demonstrated that the FRCM system added 38 to 57 percent to the shear strength and 29 to 44 percent to horizontal displacement for the wall specimens tested in in-plane shear. In the FRCM strengthened walls, failures were due to shear between the front and rear faces of the blocks, with no delamination of the inorganic system.

Papanicolaou et al. (2007, 2008) studied the effectiveness of carbon FRCM for out-of-plane and in-plane strengthening of unreinforced masonry (URM) walls made of fired clay bricks. Medium-scale masonry walls were subjected to out-of-plane bending (Papanicolaou et al. 2008) and in-plane cyclic loading. In addition, the effect of matrix type, number of reinforcement layers, and the compressive stress level applied to the shear walls and beam columns were investigated (Papanicolaou et al. 2008). In conclusion, it was found that FRCM jacketing provides substantial increase and effectiveness in terms of strength and deformation capacities for both out-of-plane and in-plane cyclic loads.

As far as tuff masonry structures are concerned, in the past decade, the interest in strengthening historical tuff masonry buildings has led to the development of specific and noninvasive architectural and engineering strategies. Faella et al. (2004) and Prota et al. (2006) tested walls in diagonal compression to measure their in-plane deformation and strength properties, and to evaluate performance in a seismic event. The increase in shear strength provided by FRCM was between 20 percent up to 250 percent depending on the number of plies and the orientation of the fibers.

The FRCM system assessed by Prota et al. (2006) by means of diagonal compression tests on tuff panels was also validated on a two-story building subjected to dynamic tests on a shake table (Langone et al. 2006).

Augenti et al. (2011) studied the application of the FRCM strengthening to a full-scale tuff masonry wall with an opening, which was tested under cyclic in-plane lateral loading up to near collapse. The unstrengthened wall was first tested under monotonically increasing lateral displacements until diagonal shear cracking occurred in the masonry panel above the opening connecting the piers (spandrel panel). The pre-damaged wall was then cyclically tested up to approximately the same lateral drift reached during monotonic loading, and diagonal cracking was again observed in the spandrel. Cracks were filled with mortar and the specimen was upgraded by applying FRCM to both sides of the spandrel. Finally, the FRCM-upgraded wall was cyclically tested to evaluate the increase in the energy dissipation capacity of the spandrel, which is a critical design parameter for strengthening existing masonry buildings. The failure mode of the FRCM-upgraded spandrel panel changed from brittle diagonal shear cracking to ductile horizontal uniform cracking, producing a 17 percent increase in the lateral load-bearing capacity of the wall.

Parisi et al. (2011) have validated this result through a nonlinear finite element analysis and a simplified analytical model showing that the increase in the load-bearing capacity of the wall were due to the FRCM-strengthening system.

Papanicolaou et al. (2011) investigated the effectiveness of externally bonded FRCM as a means of increasing the load-carrying and deformation capacity of unreinforced stone masonry walls subjected to cyclic loading. In particular, beam-type specimens were subjected to out-of-plane flexure according to different configurations and shear walls were exposed to in-plane shear under compressive loading. The results demonstrated that even the weakest FRCM configuration, when adequately anchored, results in more than a 400 percent increase in strength and a 130 percent increase in deformation capacity.



# 3

## **TEST METHODOLOGIES FOR DETERMINATION OF INTERLAMINAR SHEAR BEHAVIOR OF COMPOSITES**

In order to understand the available methods for investigation of interlaminar shear behavior, this Chapter explores the test methodologies encountered during the literature search. Although the present work focuses on FRCM composites, most of the material in literature is for FRP and, therefore, needs to be modified for FRCM systems.

The Chapter is divided into three sections: the first gives an overview of test methods for determination of shear behavior of FRP composites, the second discusses the applicability of these test methodologies to FRCM systems, whereas the third examines the requirements for interlaminar shear strength of FRCM suggested by section 4.2.4 of AC434.

### **3.1 Interlaminar Shear Test Methods for FRP Composite Systems**

Several test methods have been introduced for characterizing the shear properties of FRP composite materials. Descriptions of the principal characteristics of the commonly used shear test methods are presented, followed by a general discussion of their relative advantages and drawbacks.

The determination of composite shear properties is a difficult task, due to the anisotropic nature of these materials and their nonlinear response in shear. According to Adams and Lewis (1994), the ideal shear test method should provide a region of pure and uniform shear, be reproducible, require no special test equipment, and provide the entire stress-strain response to failure from a single specimen. Although many shear test methods have been developed for use with composite materials, none completely satisfies all of these criteria (Cui et al. 1994) suggesting that the state of shear testing for composites is still unresolved.

The majority of problems in shear testing of composites arise from the anisotropic nature of the material. Anisotropy increases stress concentrations and the distance required for these stresses to transition to a uniform state, compared to isotropic materials (Adams and Lewis, 1994). This adds to the already complex problem of defining a suitable specimen and fixture geometry for reliable shear testing.

Four shear test methods were selected for review and reported in detail here, viz., short beam (three-point) shear, four-point shear, Iosipescu shear, and axial tension of a laminate. These tests appear to be among the most commonly used, as highlighted by the number of studies reported in literature, and represent the starting point for investigation of shear behavior of FRCM composite systems.

### 3.1.1 Short Beam Shear (SBS) Test

What is commonly referred to as the short beam shear test method, defined by ASTM Standard D2344 "Standard Test Method for Short-Beam Strength of Polymer Matrix Composite Materials and Their Laminates" and ISO Standard 14130 "Fibre-reinforced plastic composites - Determination of apparent interlaminar shear strength by short-beam method", utilizes three-point bending to induce transverse shear in specimens with low support span to specimen thickness (s/h) ratios. This test method determines the apparent interlaminar shear strength of high-modulus fiber-reinforced composite materials.

- *ASTM D2344*

ASTM D2344 is the standard most commonly used to determine the short beam strength of FRP composites. In this test method, the specimen is a short beam machined from a curved or a flat laminate up to 6.00 mm thick. The beam is loaded in three-point bending. Figure 3.1 shows the test configuration and specimen geometry defined by the ASTM Standard.

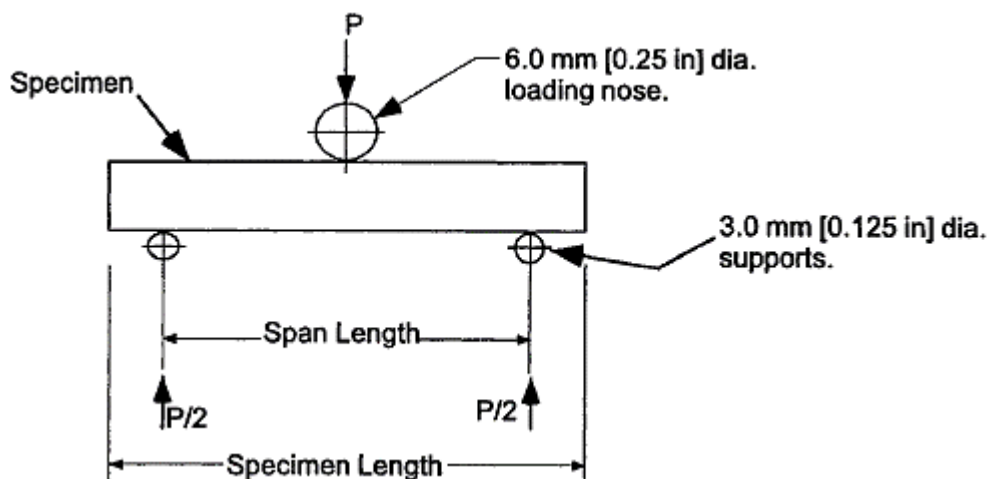
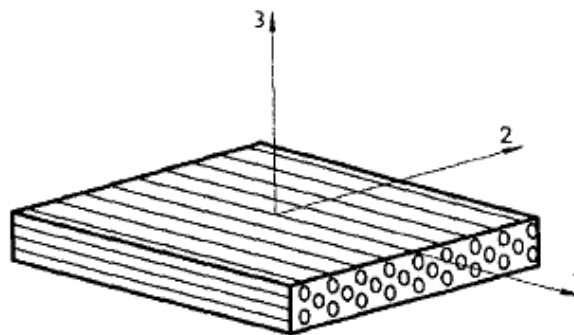


Figure 3.1 – Short beam shear test configuration (ASTM D2344)

The upper cylinder, defined as the loading nose, is 6.00 mm in diameter, and the two lower cylinders, defined as the supports, are 3.00 mm in diameter. ASTM D2344

recommends a span to thickness ( $s/h$ ) ratio of 5 for glass fiber composite materials and an  $s/h$  ratio of 4 for carbon fiber composite materials. Moreover, the standard recommends that the specimen overhang the support cylinders by at least one specimen thickness. Therefore, the specimen configuration presents a specimen length equal to 6 times the thickness while the specimen width is recommended to be 2 times the thickness. Analysis reported by Lewis and Adams (1991) has shown that a width-to-thickness ratio greater than 2.0 can result in a significant shear-stress variation.

For orthotropic materials, the one-direction typically is defined to correspond to the primary material orientation, i.e., the fiber direction in a unidirectional composite (Figure 3.2), and the two-direction is taken to be perpendicular to the one-direction in the plane of the specimen. The three-direction is thus the through-the-thickness direction. Both the short beam and four-point shear test methods apply a  $\tau_{13}$  shear stress, i.e., a through thickness shear stress, referred to as interlaminar shear stress.



**Figure 3.2 – Unidirectional reinforced composite showing principal axes**

Although shear is the dominant applied loading in this test method, the internal stresses are complex and a variety of failure modes can occur. In particular, the stress state local to the loading nose in which the severe shear-stress concentration combined with transverse and in-plane compressive stresses has been shown to initiate failure (D2344 2006). However, for the more ductile matrices, plastic yielding may alleviate the situation and allow other failure modes to occur (Berg et al. 1972). Consequently, unless mid-plane interlaminar failure can be clearly

observed, the short-beam strength determined from this test method cannot be attributed to a shear property.

Nevertheless, for FRP system failures are dominated by resin and interlaminar properties (Whitney et al. 1985), and ASTM D2344 test results have been found to be repeatable for a given specimen geometry and material system.

Figure 3.3 shows typical failure modes that are visually identified. However, these may be preceded by less obvious, local damage modes such as trans-ply cracking (D2344 2006).

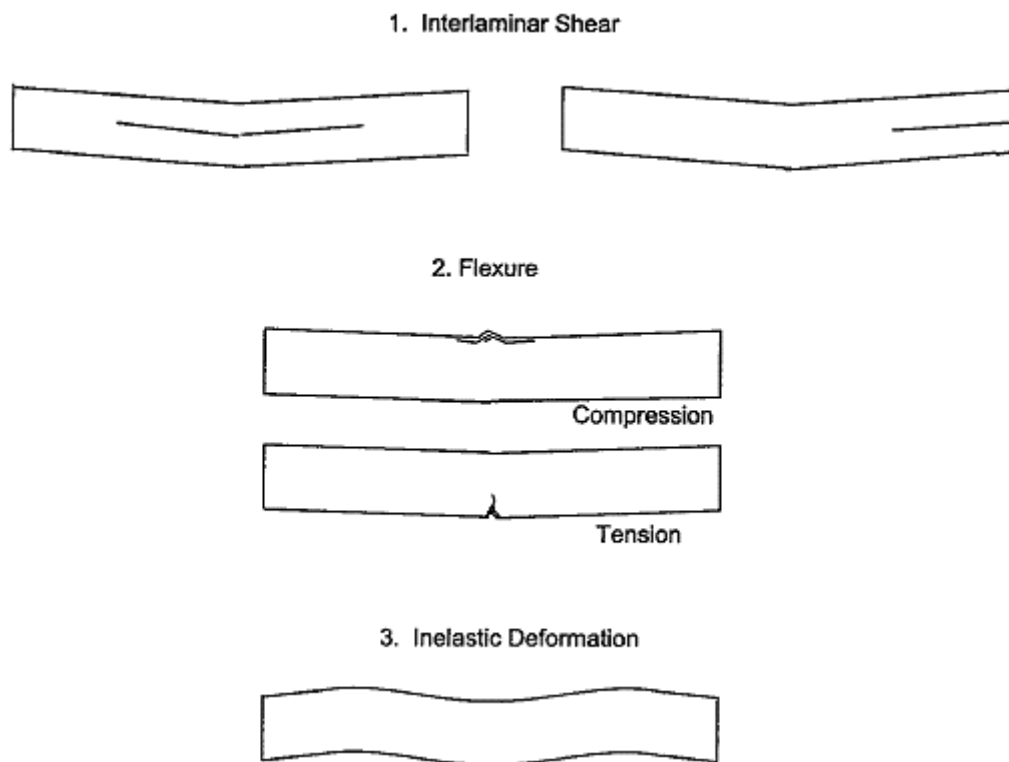


**Figure 3.3 – Typical failure modes in the Short Beam Test for FRP composites (ASTM D2344)**

For FRP composites, several studies (Whitney and Browning 1985, Cui et al. 1992, Cui et al. 1994) concluded that the failure mode has a significant effect on the measured interlaminar shear strength. In order to measure the interlaminar shear strength correctly, a valid shear failure mode must be obtained. For other failure modes, the values of interlaminar shear strength could be significantly in error.

Therefore, the failure mode becomes a fundamental precondition for measuring interlaminar shear strength and for consistency of the results.

Short-Beam strength is computed according to elementary beam theory through Equation 3.1:

$$\tau_{13} = \frac{3}{4} \frac{P}{bh} \quad (3.1)$$

where:

P = failure or maximum load observed during the test, N;

b = measured specimen width, mm;

h = measured specimen thickness, in mm.

The short-beam strength is measured in MPa. It will be noted from Equation 3.1 that the shear stress is independent of span length, while bending moment is directly proportional to span length. Thus, a short support span minimizes bending stresses, allowing the transverse shear stresses to dominate. Nevertheless, in the next chapter, it will be shown that the span length is a relevant factor for the shear stress distribution and will be further discussed.

Moreover, Adams and Lewis (1994) demonstrated that this test method is influenced by the span to thickness (s/h) ratio and by the width to thickness (b/h) ratio. These effects are examined in Chapter 4 in which it will be shown how these factors have been considered for the study of interlaminar properties of FRCM systems.

The results determined by this test method can be used for quality control and process specification purposes. They can also be used for comparative testing of composite materials, if failures occur consistently in the same mode (Cui et al. 1994).

- *ISO 14130*

ISO 14130 represents another standard commonly used to determine the interlaminar shear strength of FRP composites. It is a test method in some aspects similar to the ASTM D2344, which is widely adopted.

This standard specifies a procedure for determining the apparent interlaminar shear strength by the short-beam method and is suitable for use with fiber-reinforced plastic composites with a thermoset or a thermoplastic matrix, providing interlaminar shear failure is obtained. Figure 3.4 shows the test configuration defined by the ISO Standard.

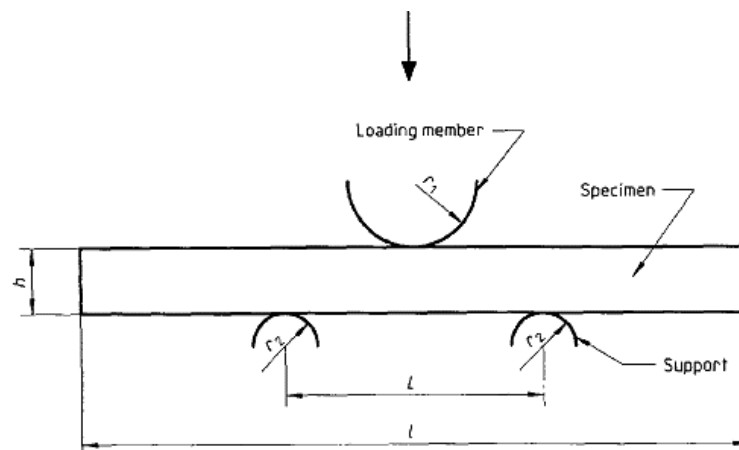


**Figure 3.4 – Short beam shear test configuration (ISO 14130)**

The principle is quite simple, a bar of rectangular cross-section is loaded as a simple beam in flexure so that interlaminar shear failure occurs. The bar rests on two supports and the load is applied by means of a loading member midway between the supports. The test is similar in nature to the three-point loading method used to determine the flexural properties of plastics. However, a smaller test span to specimen thickness ratio is adopted to increase the level of shear stress relative to the flexural stress in the test specimen to encourage interlaminar shear failure. It is emphasized that the result obtained is not an absolute value. For this reason, the term “apparent interlaminar shear strength” is used to define the quantity measured.

The upper cylinder, defined as the loading nose, shall be 5.00 mm in diameter, and the two lower cylinders, defined as the supports, are 2.00 mm in diameter. The width of the loading member and the supports shall be greater than the test specimen width. ISO Standard 14130 recommends that an s/h ratio of 5 be used for all types of FRP composite materials. In addition, the standard recommends that the specimen configuration presents a specimen length equal to 10 times the thickness while the specimen width is recommended to be 5 times the thickness.

Figure 3.5 shows the typical failure modes that can be identified with this methodology. However, these may be preceded by less obvious, local damage modes such as trans-ply cracking.

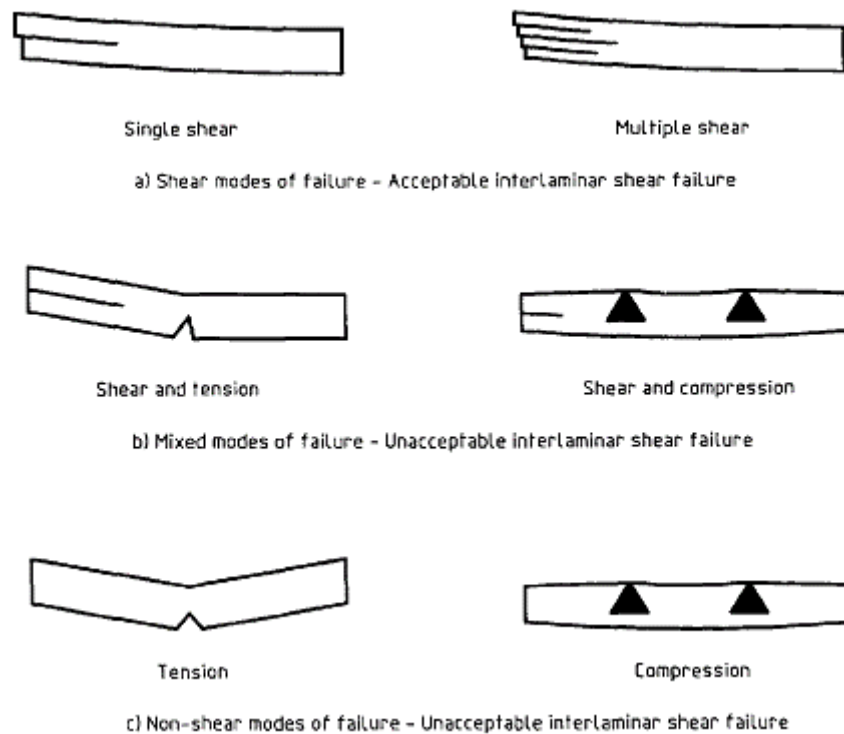


**Figure 3.5 – Modes of failure (ISO 14130)**

Although this method presents a different specimen geometry, with a longer overhang and a greater width, the concentration of the stresses in the specimen



loaded under three-point bending and the complexity of relating the short beam strength to a material property remain two key factors with this standard.

In addition, in order to measure the interlaminar shear strength correctly, a valid shear failure mode must be obtained. Therefore, the failure mode is an important precondition for measuring interlaminar shear strength and for consistency of the test results. The apparent interlaminar shear strength, expressed in MPa, can be computed using Equation 3.1, considering the different section configuration.

As the ASTM D2344 standard, this method is not suitable for the determination of design parameters, but may be used for screening materials, or as a quality-control test. Test results from different-sized specimens, or from specimens tested under different conditions, are not directly comparable.

### **3.1.2 Four Point Shear (FPS) Test**

As reported by Browning et al. (1983), some unidirectional composites, i.e. 16-ply carbon/epoxy, short beam shear (SBS) tests typically do not yield an interlaminar shear failure. An available alternative to a SBS test includes a thicker SBS specimen or the use of a four-point shear (FPS) test method. The thicker SBS specimen was claimed by Browning et al. (1983) to be less affected by the stress concentrations caused by the cylinders than a thin specimen. However, the results of Whitney (1985) and Lewis (1991) suggest that this assumption is not correct and that in fact the reverse is true. Therefore, for this type of composite the FPS test appears to be the better solution.

The four-point shear test method is similar to the short beam shear method, but the load is applied through two cylinders rather than one. Figure 3.6 shows the test geometry. Since this test methodology is not standardized, provisions for the loading and support cylinder diameters are not available. Moreover, the data used for the mentioned diameters by Browning et al. (1983) was not given. The loading points are

located at a distance one-fourth the support length from the support cylinders, which is usually defined as quarter-point loading.

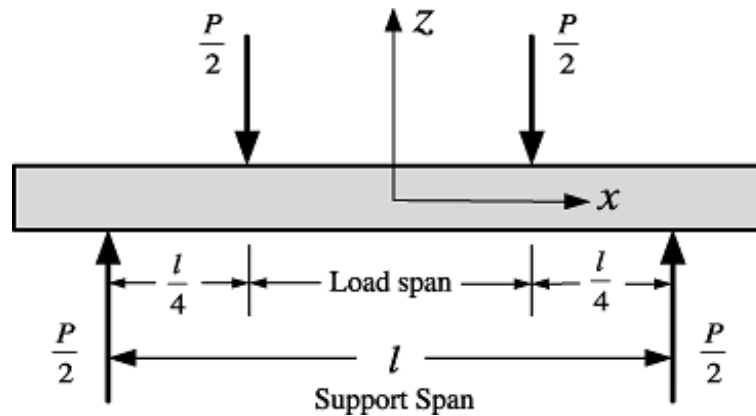


Figure 3.6 – Four-point shear test configuration

Browning et al. (1983) used an  $s/h$  ratio of 16 in the FPS testing considered in their work. It was stated that this high  $s/h$  ratio was used to minimize the stress concentration effects at the loading and support cylinders. The elasticity solution elaborated by Whitney (1985) showed that the shear stress distribution in a 16-ply SBS specimen at an  $s/h$  ratio of four is similar to that in a FPS specimen at an  $s/h$  ratio of 16.

Adams and Lewis (1994) concluded that a comparison using a FPS specimen at an  $s/h$  ratio of eight would be more appropriate because the flexural stresses would then be comparable. Indeed, the flexural stresses for the FPS specimen were not presented by Whitney (1991), but they must have been much larger in the FPS specimen than in the SBS specimen. The reduction in contact stress was claimed by Browning et al. (1983) to be the major advantage of the FPS test, since the compression buckling under the SBS loading cylinder was stated to be a common failure mode when testing SBS specimens. It is definitely true that the contact stresses induced by the two FPS loading cylinders will be one-half those induced by the single SBS loading cylinder.

### 3.1.3 Iosipescu Shear Test

This test method was originally developed for isotropic materials such as metals or ceramics by Nicolai Iosipescu of Bucharest, Romania in the early 1960's. Adams and Walrath (1987) extensively studied the method for use with composite materials in the early 1980's. In 1993, this test method was adopted as ASTM Standard D5379 “*Standard Test Method for Shear Properties of Composite Materials by the V-Notched Beam Method*”.

This test method covers the shear properties of composite materials reinforced by high-modulus fibers. The composite materials are limited to continuous-fiber or discontinuous fiber-reinforced composites in the form of unidirectional fibrous laminae, with the fiber direction oriented either parallel or perpendicular to the loading axis, unidirectional fibrous laminae, containing equal numbers of plies oriented at 0 and 90° in a balanced and symmetric stacking sequence, and short-fiber-reinforced composites with a majority of the fibers being randomly distributed.

Both in-plane or interlaminar shear properties may be evaluated, depending on the orientation of the material coordinate system relative to the loading axis. In order to better understand these different shear properties, the material coordinate system is presented in Figure 3.7.

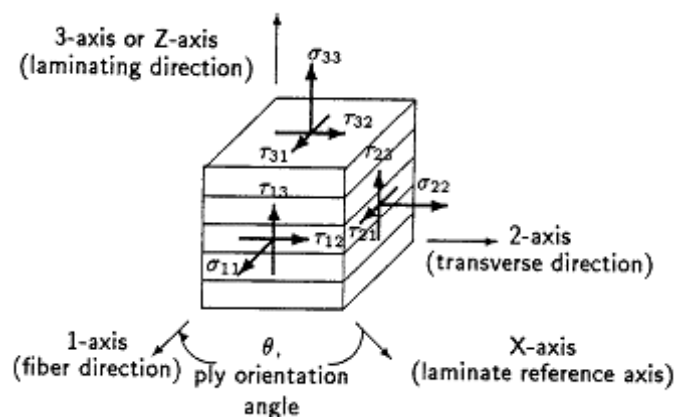


Figure 3.7 – Material coordinate system ASTM D5379

The in-plane shear is any of the shear properties describing the response resulting from a shear force or deformation applied to the 1-2 material plane, while the interlaminar shear is the response resulting from a shear force or deformation applied to the 1-3 or 2-3 material planes. Idealized loading, shear, and moment diagrams are shown for the Iosipescu specimen in Figure 3.8.

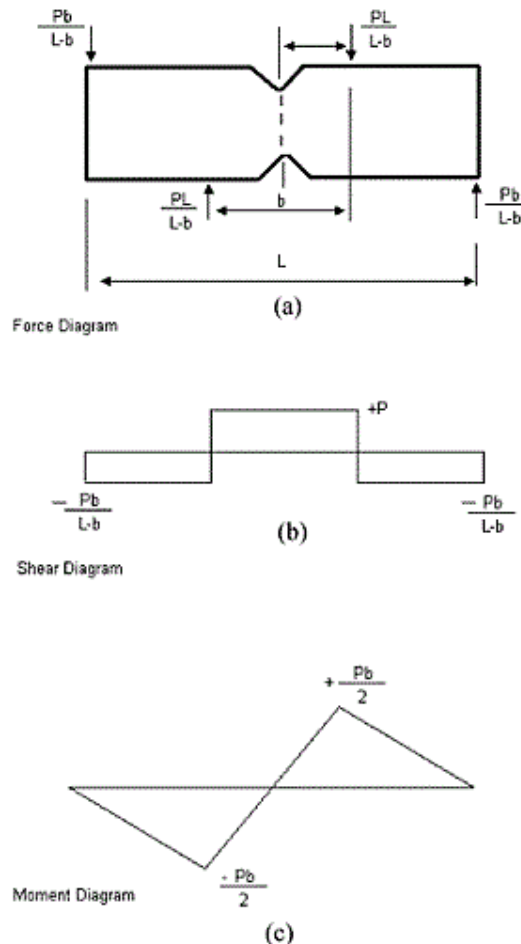


Figure 3.8 – Idealized Force, Shear, and Moment diagrams (D5379)

It will be noted that, in the center of the specimen, a constant shear force and a zero moment exist. There has been extensive research concerning the stress-strain state in the Iosipescu shear test specimen (Adams and Walrath 1983, 1987, Barnes et al. 1987, Sullivan 1988, Pindera et. al. 1990). The three main areas of concern appear to be the presence of normal stresses in the gage section, the shear stress distribution in the gage section, and the notch tip cracking that occurs in unidirectional materials

that are oriented with the fibers along the length of the specimen. Factors that may influence the shear response and should therefore be reported include the following: material, methods of material preparation and layup, specimen preparation, environment of testing, specimen alignment and gripping, speed of testing, time at temperature, void content, and volume percent reinforcement (ASTM D5379).

As mentioned before, two main types of Iosipescu specimens can be analyzed,  $0^\circ$  and  $90^\circ$  oriented unidirectional specimens. In the  $0^\circ$  oriented Iosipescu specimen the fibers are parallel to the long axis of the specimen, while in the  $90^\circ$  specimen the fibers are perpendicular to the long axis. Therefore, in the  $0^\circ$  orientation the in-plane properties are analyzed, while in  $90^\circ$  orientation the interlaminar shear behavior is examined.

According to Adams and Lewis (1994), the Iosipescu shear test method appears as the best overall choice for characterizing the shear properties of composite materials. It does induce a pure shear stress state, and shear strains can be measured using strain gages. Thus, both shear stress and shear modulus can be obtained. The specimen is simple to prepare and the test easy to perform. By varying the orientation of the material within the specimen, any one of the three independent shear stresses can be analyzed.

This test methodology is designed to produce shear property data for material specifications, research and development, and structural design and analysis (ASTM D5379).

### **3.1.4 Axial Tension of a Laminate**

Another methodology for investigation of the interlaminar shear stresses of FRP composites is represented by the axial tension of a  $\pm 45^\circ$  laminate. This test method determines the in-plane shear response of polymer matrix composite materials reinforced by high-modulus fibers. The composite material form is limited to a continuous-fiber-reinforced composite  $\pm 45^\circ$  laminate capable of being tension tested

in the laminate  $x$  direction. ASTM D3518 “*In-Plane Shear Response of Polymer Matrix Composite Materials by Tensile Test of a  $\pm 45^\circ$  Laminate*” specifies that the test specimen has to be 25 mm wide and between 200 and 300 mm long. Figure 3.9 shows the material coordinate system to help in understanding the orientation of the specimen.

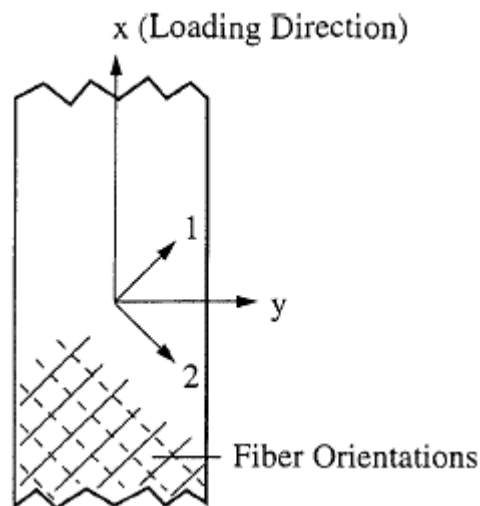


Figure 3.9 – Definition of specimen and material axes (ATM D3518)

The laminae are not in a state of pure shear. In-plane normal stresses exist that are a function of the applied axial stress  $\sigma_x$  and the shear stress  $\tau_{xy}$  induced in each ply. All angle-ply laminates also have interlaminar stresses near the free edges of the laminate (Pipes and Pagano 1970, Herakovic 1989). These typically become negligible beyond about one laminate thickness in from each edge.

According to Pipes and Pagano (1970), the maximum interlaminar stress  $\tau_{xz}$ , are at reinforcement angles between 30 and 45 degrees. In addition, there is a reversal in the sign of the interlaminar shear stress at angles higher than  $60^\circ$ . The effect of specimen width is much less important than stacking sequence and specimen thickness effects.

## **3.2 Applicability of Interlaminar Shear Test Methods to FRCM Composites**

Since the current work represents the first complete study on interlaminar shear behavior of FRCM system, part of the research focused on finding the most appropriate methodology to investigate this property. As noted in the previous section, most of the available material in literature is for FRP and, therefore, understanding the applicability of FRP test methodologies to FRCM composite becomes fundamental to examine its interlaminar shear properties.

The primary virtues of the short beam shear (SBS) test method are its simplicity of use and small specimen size. The amount of material required per test specimen is minimal, and because the test is so simple to perform, many replicates can be tested in relatively little time, thus permitting the generation of a statistically meaningful data set. The SBS test method is also attractive as a materials screening test.

Complexity in the internal stresses is more significant for FRP because the thickness of this type of composite is smaller and, therefore, the loading nose and the supports cylinders are closer. However, for FRP, analytical (Whitney 1985) and experimental (Lewis and Adams 1991) work has provided a much better understanding of the test method, permitting it to be used with confidence. Nevertheless, the span length to specimen thickness ratio ( $s/h$ ) remains a key factor of this test methodology and must be controlled. To this end, several tests were performed to understand the effects of this ratio on FRCM composites (Chapter 4).

A limitation of the SBS test method is that only shear strength is determined. Measurement of shear strain is not practical, and thus shear modulus or a shear stress-shear strain curve is not obtained. This can be an unacceptable limitation if design data are to be generated. However, since the short beam shear test method is limited to material screening and quality control, the fact that shear strains cannot be reliably measured does not represent a drawback for this method.

The short beam shear test method is defined for FRP laminates by standards ASTM D2344 and ISO 14130 (Section 3.1.1). Although they are intended to measure the same property, the two methodologies present some differences, especially for the specimen geometry. Not only the span to thickness ratio ( $s/h$ ) varies between 4 and 5 for the two standards, but the width to thickness ratio ( $b/h$ ) is recommended to be 2 for ASTM D2344 and 5 for ISO 14130. Analysis reported by Lewis and Adams (1994) has shown that a width-to-thickness ratio greater than 2.0 can result in a significant shear-stress variation and thus has to be avoided. Therefore, for the current work the standard ASTM D2344 was selected in order to examine the interlaminar shear behavior of FRCM composites.

The four-point shear (FPS) test method has been proposed as an improvement over the short beam shear test method, which utilizes three-point loading. Elementary beam theory would suggest advantages. However, more rigorous analyses and experimental data suggest this not to be the case. In fact, because of the unfavorable local stress states induced in the specimen by the loading points, the FPS test method typically produces lower shear strengths (Adams, 1994) and is rather recommended for the investigation of flexural properties. Moreover, the application of the forces generates a configuration where in the central span of the specimen a constant moment and a zero shear force exist. Therefore, the four-point shear test method was not selected for interlaminar shear investigation of FRCM system.

The Iosipescu shear test method has been thoroughly evaluated for use with FRP composite materials and there is considerable confidence regarding its use. For Adams and Lewis (1994) this test method is the best overall choice for characterizing the shear properties of all types of composite materials. For FRP systems the rationale behind this statement is that it does induce a pure shear stress state, and shear strains are easily measured using strain gauges. Thus, both shear stress and shear modulus can be obtained. The specimen is simple to prepare and the test easy to perform. One major disadvantage is that, for orthotropic materials, it does not produce a uniform elastic shear stress distribution across the gauge section.



Although it has not been performed for FRCM, the Iosipescu shear test method could represent an available alternative to the SBS test to evaluate the interlaminar strength of this type of composite. In particular, the specimen would be laid inside the fixture with the interlaminar plane (plane 1-2) parallel to the direction of the load (Figure 3.8). If the failure occurs in the mid-plane where the fabric is located, it is possible to compute the interlaminar strength of the system. However, for practical reasons, the present work does not focus on this methodology and further studies are recommended.

Axial tension of a  $\pm 45^\circ$  laminate is also a relatively simple shear test, although perhaps not as simple as short beam shear. It requires the same facility as a normal tensile test, i.e., a load frame with tensile grips, and the ability to measure both axial and transverse strains if shear strain and shear modulus have to be determined. In this test method, a very complex stress state is induced in the specimen. Thus, while interlaminar shear is present along with axial and transverse tensile stresses in each ply, the intent is to determine the in-plane shear properties. Furthermore, for cementitious composites, casting such specimens is impractical. Consequently, this test is not selected for FRCM shear investigation.

### **3.3 Addressing Section 4.2.4 of AC434**

Section 4.2.4 of AC434 requires the investigation of composite interlaminar shear strength on FRCM stating “following general procedures of ASTM D2344. Alternatively, test procedures of ASTM C947 can be adopted for FRCM in conjunction with provisions of ASTM D2344 for interpretation of results and reporting regarding interlaminar related issues”.

The proposed test methods are ASTM D2344 "*Standard Test Method for Short-Beam Strength of Polymer Matrix Composite Materials and Their Laminates*" and

ASTM C947 “Standard Test Method for Flexural Properties of Thin-Section Glass-Fiber-Reinforced Concrete”.

As already discussed, the present work focuses on the use of ASTM D2344 for investigating the interlaminar shear behavior of FRCM composites. However, the alternative standard ASTM C947 covers determination of the flexural ultimate strength in bending and the yield strength of glass-fiber reinforced concrete sections and it is not a method intended to evaluate the interlaminar properties of brittle matrix composites. Although this standard is not suitable to study the interlaminar shear behavior, it is addressed here because it is suggested by AC434. An explanation of the test is summarized to conclude that it should be removed or moved to another section of AC434.

This test method investigates the flexural strength in bending of glass-fiber reinforced concrete sections by the use of a simple beam of 25 mm (1.0 in) or less in depth using third-point loading. Figure 3.10 shows the test configuration.

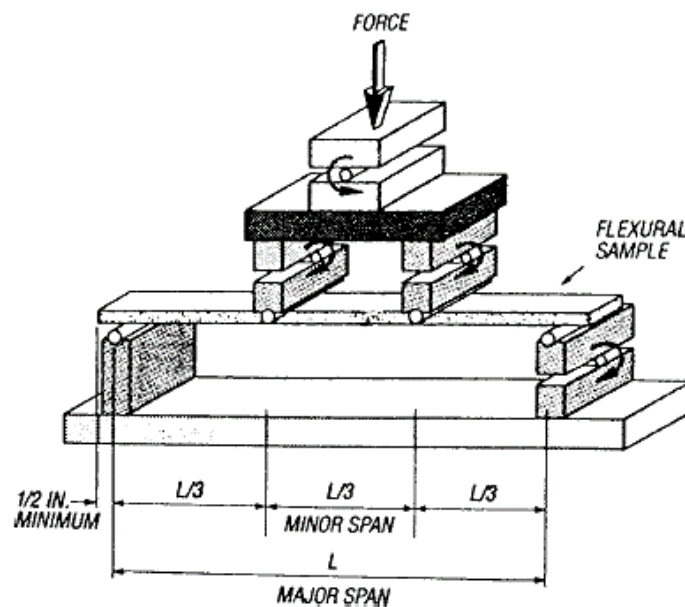


Figure 3.10 – Loading configuration for flexural testing (ASTM C947)

The loading noses and supports shall have cylindrical surfaces and in order to avoid indentation of failure shall be at least 6 mm (0.25 in) in diameter. The test

specimen shall have a ratio of major span length to depth between 16 and 30 to 1. The total specimen length shall be a minimum of 25 mm (1.0 in) longer than the specimen's major span, while the specimen width shall be 50 mm (2.0 in).

Flexural properties determined by this test method are useful for quality control of glass-fiber reinforced concrete products, research and development, and generating data for use in product design.

Based on the requirements of Section 4.2.4 of AC434, ASTM C947 standard is not applicable because it specifically covers determination of flexural strength and not any parameters related to interlaminar shear behavior. Moreover, the application of the forces generates a four-point bending where in the center of the specimen a constant moment and a zero shear force exist.

While the investigation of this standard is not part of this study, Section 4.2.4 of AC434 must be addressed and it can be concluded that this test method is in the wrong section. There could be a test for the flexural capacity of the FRCM systems, which is not present in the current version of the document. Therefore, a new section testing the flexural strength in bending of FRCM composite may be recommended.

# 4

## **INTERLAMINAR SHEAR BEHAVIOR OF FRCM COMPOSITES**

This Chapter deals with the determination of the parameters to investigate the interlaminar shear behavior of FRCM composites. Few studies have been performed in order to determine the appropriate methodology to analyze the interlaminar shear behavior and compute the interlaminar shear strength of FRCM systems. An extensive experimental campaign is presented followed by the analysis of the results.

The Chapter is divided into different sections: after a detailed description of the FRCM systems used for the research, the first study represents a critical analysis of the ASTM D2344 in order to examine if this test method is appropriate to generate an interlaminar failure in the FRCM systems, in this section specimens with different geometries and number of plies are presented. The second study presents an investigation of interlaminar plane through a new test method in order to find the limit value of contact surface to produce an interlaminar shear failure with FRCM. Based on the findings of these two studies, the third work examines sandwich composite specimens showing through an elastic analysis the reasons of this choice.

Finally, split tensile tests were performed in order to examine a different test methodology to confirm that the test method developed in the previous studies is really the most appropriate way to investigate the interlaminar shear behavior of FRCM systems.

## 4.1 FRCM Materials Description

As presented in Paragraph 2.1.1, three FRCM systems from two different manufacturers have been used for this research. Each FRCM system consists of two main elements, a cementitious matrix and a dry fiber network (fabric) or mesh. This section presents the characteristics of the constitutive materials.

### 4.1.1 Fabrics

Figure 4.1 shows the Carbon 1 type of fabric and its geometry. This fabric is an unbalanced net with 12 mm and 28 mm spaced rovings. The free space between rovings is 7 mm in the longitudinal direction and 25 mm in the orthogonal one, the nominal width is 5 mm and 3 mm respectively. Specific details can be found in the technical specifications of the material (Section 2.1.1).

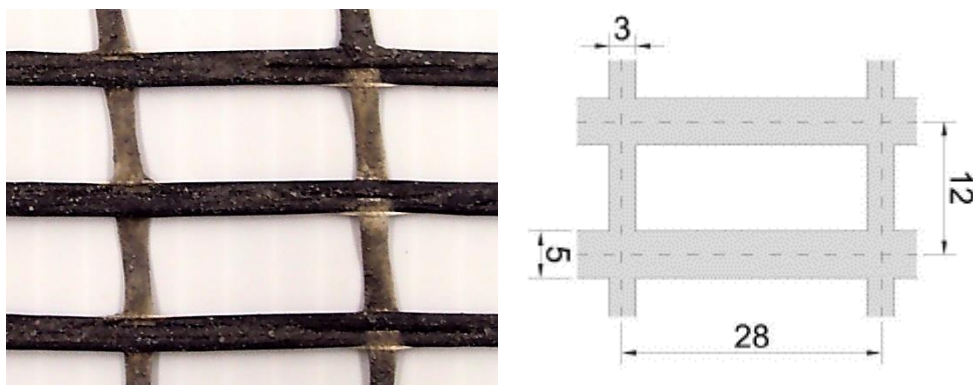


Figure 4.1 – Carbon 1 fabric

The Carbon 2 fabric is a balanced network with fiber rovings disposed along two orthogonal directions at a nominal spacing of 10 mm (6 mm clear opening between rovings) and equivalent nominal fiber thickness is 0.047 mm in both directions.

Figure 4.2 shows the Carbon 2 type of fabric and its geometry. Specific details can be found in the technical specifications of the material (Section 2.1.1).

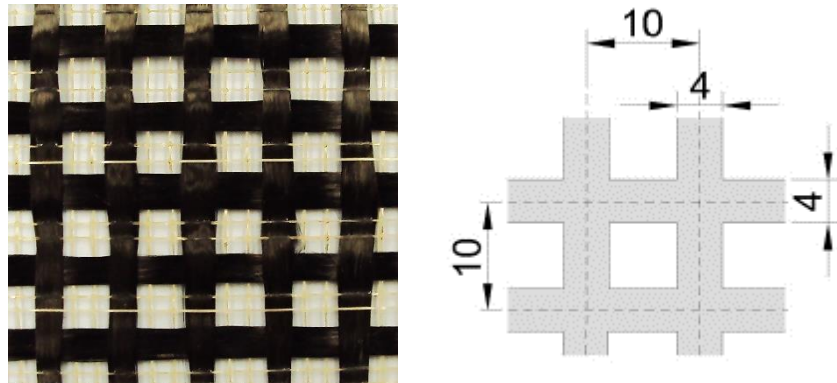


Figure 4.2 – Carbon 2 fabric

Polyparaphenylene benzobisoxazole (PBO) is the constituent of the third fabric. The unbalanced net consists of 10 mm and 20 mm spaced rovings. The free space between rovings is roughly 5 mm and 15 mm, respectively, and the nominal thickness in the two fibers directions is 0.046 mm and 0.0115 mm, respectively. Figure 4.3 shows the PBO fabric and its geometry. Specific details can be found in the technical specifications of the material (Section 2.1.1).

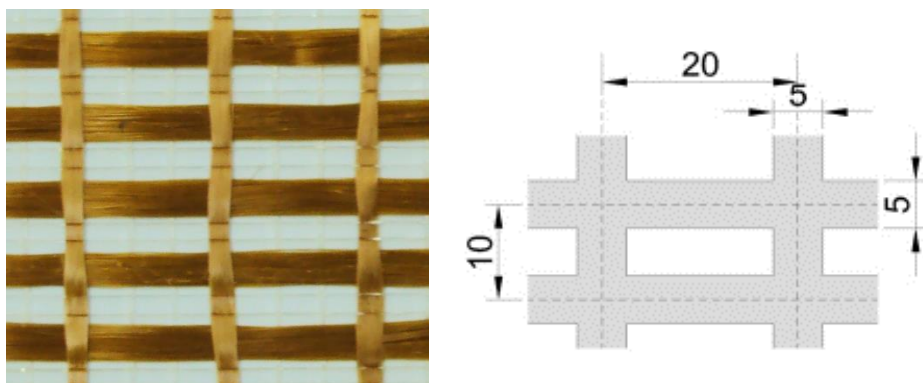


Figure 4.3 – PBO fabric

## **4.1.2 Mortars**

The cementitious matrix is a mortar system based on Portland cement and a low dosage of dry polymers (less than 5% in weight). This is engineered specifically to optimize its performance with the fabric that it forms a system with.

The compressive strength of Mortar 1 (Carbon 1-FRCM system) was defined performing simple uniaxial compressive tests. The mortar was mixed mechanically following the manufacturer's specifications and ten cube specimens were prepared tamping the fresh material in two layers. The cubes were left 48 hours in the molds before they were taken out and cured in laboratory environment (19-21 °C and 65-70% of humidity).

Uniaxial compression load was applied to the cube specimens using a screw type universal test frame. Load was applied to the cube faces that were in contact with the mold surfaces. The test was performed under displacement control at a rate of 0.5 mm/minute.

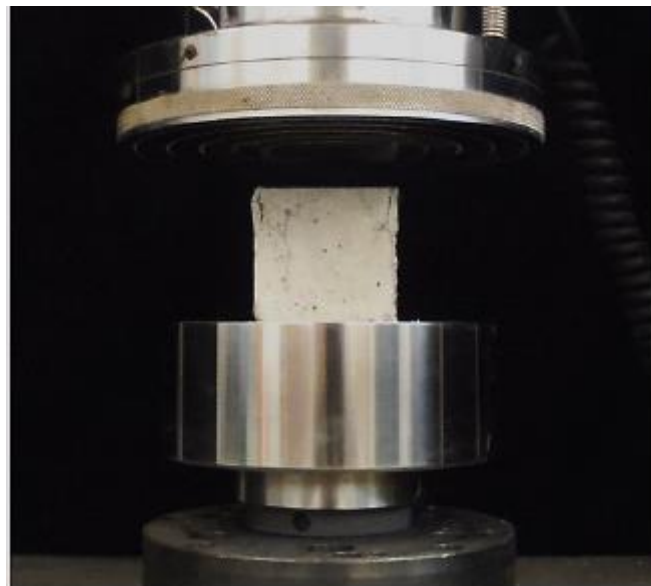


**Figure 4.4 – Compression test on cubes of Mortar 1**

The tests were performed after 7 and 28 days of curing. The cube compressive strength was determined by dividing the maximum load by the face area of the cube where the load was applied. In the following Table 4.1 and Table 4.2, the results are shown.

	Area [mm <sup>2</sup> ]	Max Load [kN]	Comp. Strength [MPa]
M1-7-1	2580	55,09	21,35
M1-7-2	2580	50,37	19,52
M1-7-3	2580	53,22	20,63
M1-7-4	2580	68,31	26,48
M1-7-5	2580	56,03	21,72
Average		56,60	21,94
Std. Dev.		6,89	2,67
C.O.V. (%)		12,17	12,17

**Table 4.1 – Compression tests results on M1 after 7 days of curing**

	Area [mm <sup>2</sup> ]	Max Load [kN]	Comp. Strength [MPa]
M1-28-1	2580	84,95	32,93
M1-28-2	2580	85,53	33,15
M1-28-3	2580	84,91	32,91
M1-28-4	2580	88,64	34,36
M1-28-5	2580	89,45	34,67
Average		86,70	33,60
Std. Dev.		2,18	0,84
C.O.V. (%)		2,51	2,51

**Table 4.2 – Compression tests results on M1 after 28 days of curing**

Bianchi (2013) defined the compressive strength of Mortar 2 (Carbon 2-FRCM system) and Mortar PBO (PBO-FRCM system). These will be used subsequently.



## **4.2 Critical Analysis of Test Methodology (ASTM D2344) for FRCM Composites**

The experimental campaign was designed as an investigation of the standard ASTM D2344. The purpose of these tests was to examine how the standard developed for FRP laminates works for the FRCM systems. In particular, this study shows that ASTM D2344 does not work for FRCM composites. This is because of: the variability on FRCM during casting, the position of the fabric relative to the tension or compression flange, the cementitious nature of the composite system.

During the study, different parameters were varied:

- dimensions of the specimens;
- number of reinforcing plies;
- span length, thickness, position of the fabric;
- diameter of loading nose and supports cylinders;
- application of the load.

Their influence is determined by comparing results of similar specimens differing only in one of the mentioned parameters. The focus was placed on the failure modes experienced during the tests in order to have a better understanding of the behavior of the FRCM specimens subjected to a test method that for FRP generates in most of the cases interlaminar shear failures. The failure mode has a significant effect on the measured interlaminar shear strength, since in order to measure the interlaminar shear strength correctly, a valid shear failure mode must be obtained. For other failure modes, the values of interlaminar shear strength could be significantly in error. The complete matrix of tested specimens can be found in Appendix A.

## 4.2.1 Specimen Preparation

Mortar mixing was made per manufacturer's instructions as previously explained in Section 2.1.2. The water to mortar ratio for each composite system is provided in the technical specifications (Section 2.1.1). Little amount of water could be added if needed to ensure the workability of mortar. Moreover, the manufacturer suggests mixing a complete bag at once because the bag contents may shift during shipping, storage, and handling which can cause variation in mortar properties when only a portion of the bag is used for mixing. Interlaminar shear coupon dimensions are function of the thickness according to the standard ASTM D2344. The specimens were cut from larger panels which were 430x560 mm (Figure 4.5) and presented a variable thickness.

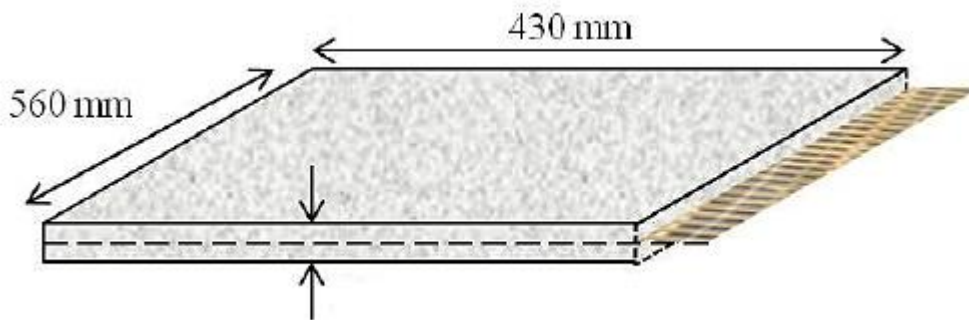
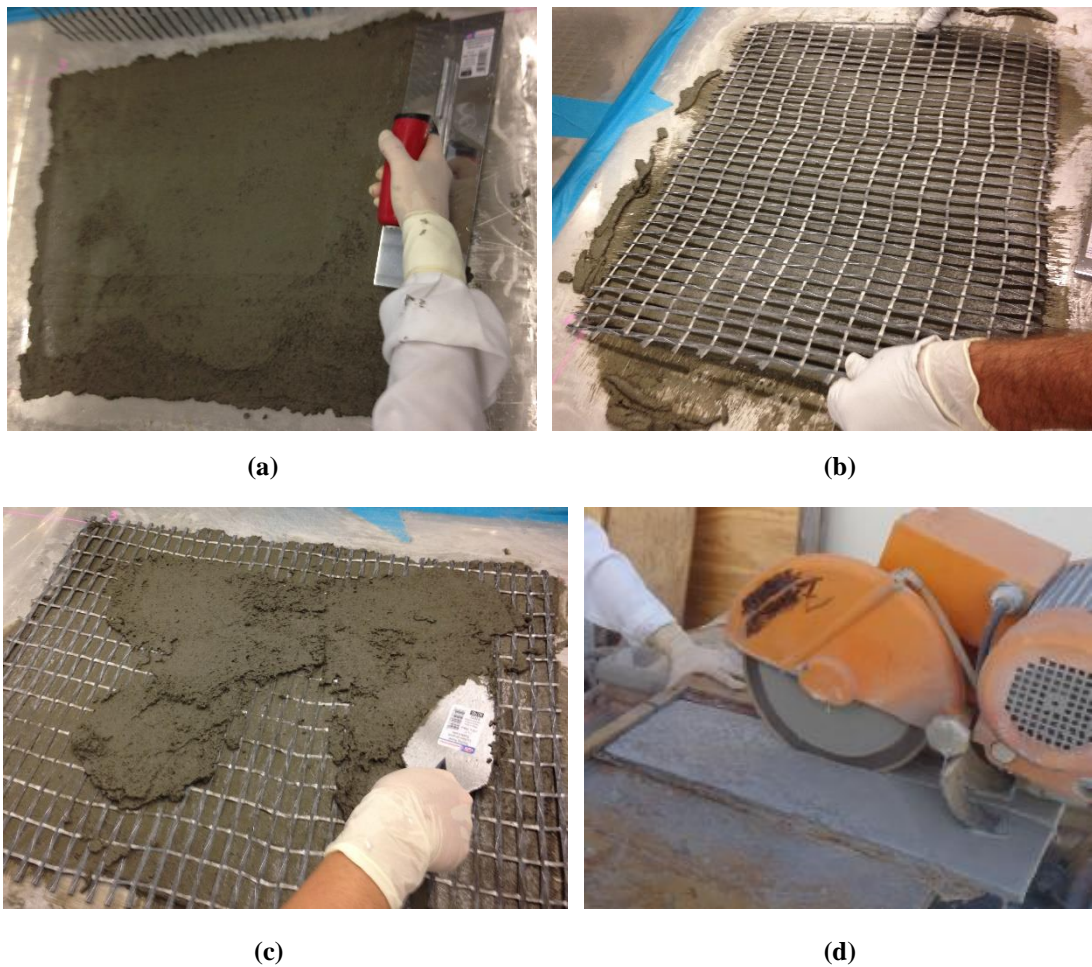


Figure 4.5 – FRCM panel configuration (Arboleda 2014)

The panels were manufactured using a manual impregnation technique by first applying a thin layer (4 mm) of cementitious matrix (Figure 4.6a), followed by a layer of fabric, pre-cut to panel size, which was purposely and evenly wetted with the fresh cementitious material (Figure 4.6b). The top layer of matrix was then applied as flat as possible with a finishing trowel (Figure 4.6c). No device was installed to control the panel thickness. The panels were cured for 28 days at laboratory conditions of 20°C and 70% relative humidity before cutting and conditioning was performed. Individual coupons were cut (Figure 4.6d) using a diamond-tipped wet saw with a rigid fixture to ensure consistent specimen widths.



**Figure 4.6 - Specimen preparation: (a) First layer of mortar in the panel form, (b) Placing of fabric mesh, (c) Second layer of mortar, (d) Cutting coupons after 28 days**

## 4.2.2 Test Setup and Procedure

The three-point bending test was performed using a screw driven Universal Test Frame (Figure 4.7) with a maximum capacity of 130kN. The load was applied in displacement control at a rate of 1 mm/min in a quasi-static configuration in order to avoid dynamic loads. The velocity of the test was determined from the standard ASTM D2344. The vertical displacement of the specimen was measured from the cross-head displacement. No device was used to measure the deformations.

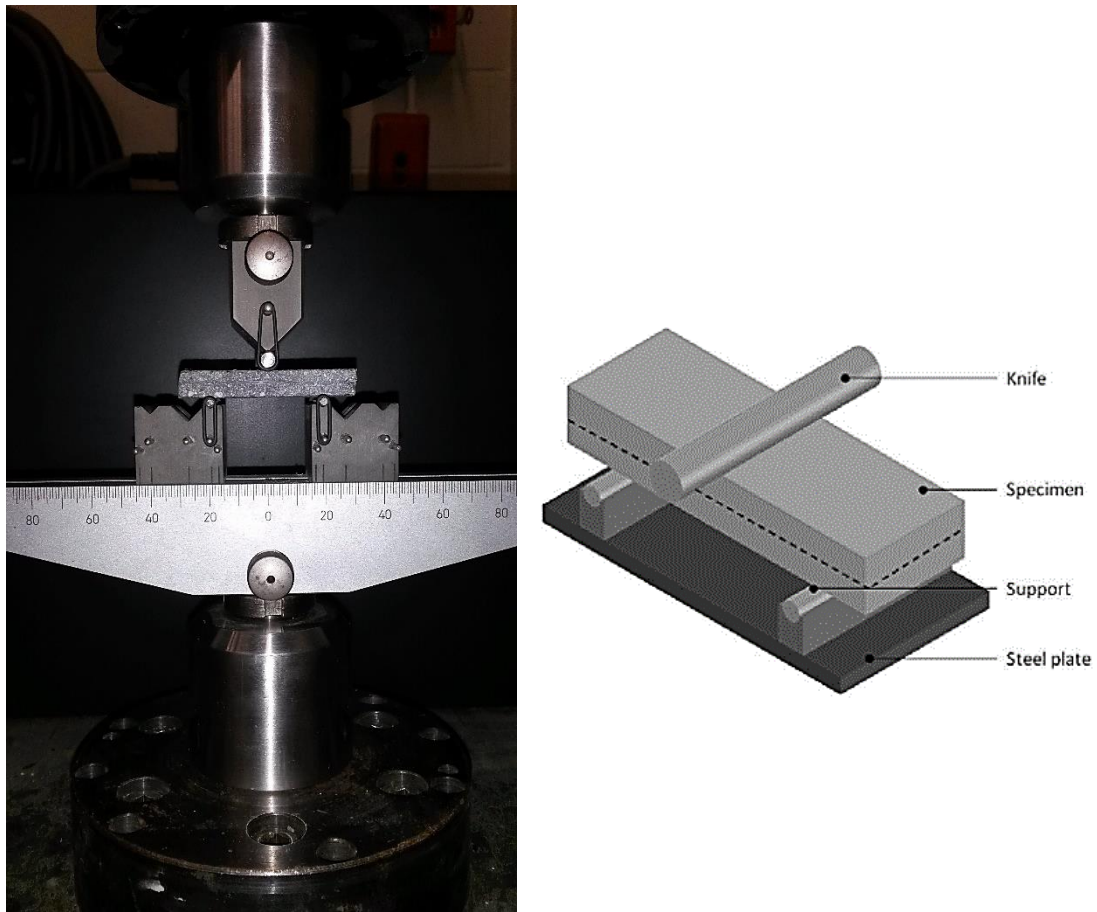


Figure 4.7 – Interlaminar Shear test setup

### 4.2.3 Test Results

First, specimens with different number of reinforcing plies were tested with the current test method (ASTM D2344). Table 4.3 shows a summary of the tests performed on plain samples and the relative failure modes experienced. The number of specimens and the specimen nominal dimensions are also shown in Table 4.3. According to AC434, at least five specimens for each FRCM configuration should be tested. However, in this study three specimens were considered sufficient if they presented the same behavior, thus if they showed flexural or matrix diagonal failures.

The thickness of the specimen, key factor for determining its geometry, was measured in three different points of the coupon: two measurements close to the ends and one in the middle of the sample. Then, an average value was computed to determine the span length and width. Since the maximum width of the loading nose was 40mm, the width of the specimen was assumed equal to two times the thickness until a maximum value of 34mm. This limit value was taken smaller than the total width of the loading cylinder to ensure proper distribution of the load.

Specimen ID	Number of reinforcing plies	Repetitions	Average thickness (mm)	Span to thickness ratio	Span length (mm)	Width (mm)	Failure mode*
Carbon1_1P_Plain	1	5	11,7	4	46,7	23,3	FL
Carbon1_2P_Plain	2	3	12,1	4	48,4	24,2	FL - DF
Carbon1_3P_Plain	3	3	15,0	4	60,1	30,1	FL - DF
Carbon1_4P_Plain	4	3	19,8	4	79,3	34,0	DF
Carbon2_1P_Plain	1	3	9,1	4	36,6	18,3	FL
PBO_2P_Plain	2	5	8,56	4	34,2	17,1	FL - DF
PBO_4P_Plain	4	3	14,5	4	58,0	29,0	DF

\*FL = flexural failure; DF = matrix diagonal shear failure

**Table 4.3 – Summary of tests performed on plain specimens and relative failure modes**

As can be observed by Table 4.3, all the tested specimens presented a flexural or matrix diagonal tension failure. No interlaminar shear failure was observed. In particular, failure modes were found to be related with a high consistency to the amount of plies. Indeed, flexural failure mode occurred for one-ply specimens while diagonal shear failure characterized the ones with four plies. The two and three-ply specimens demonstrated both the failure modes. Figure 4.8, Figure 4.9 and Figure 4.10 show the typical failure modes for the different kind of specimens.



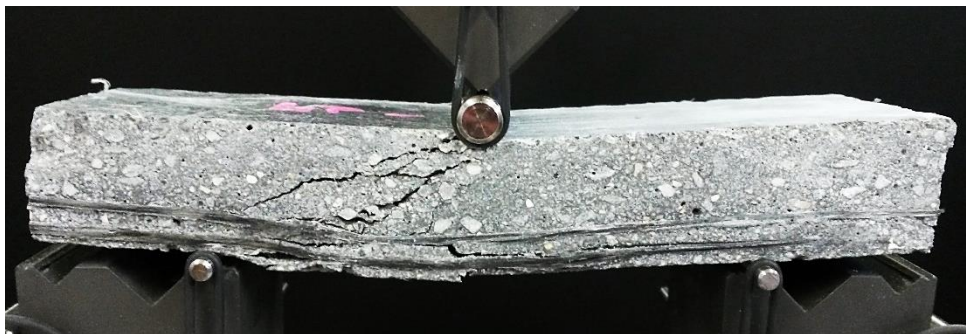
(a)



(b)



(c)

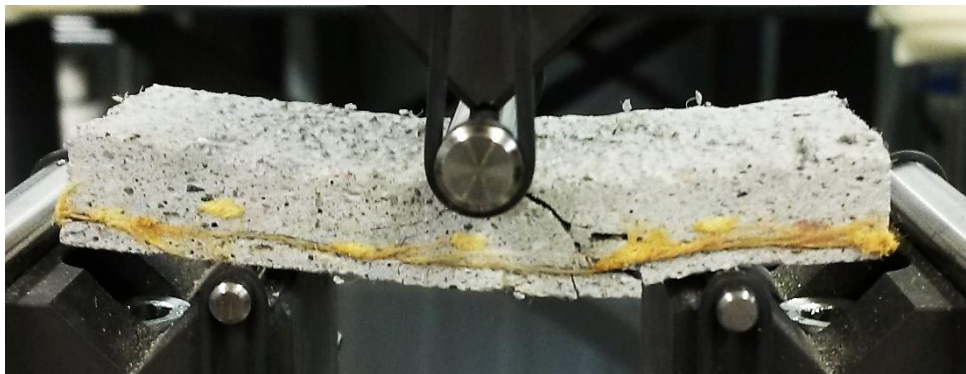


(d)

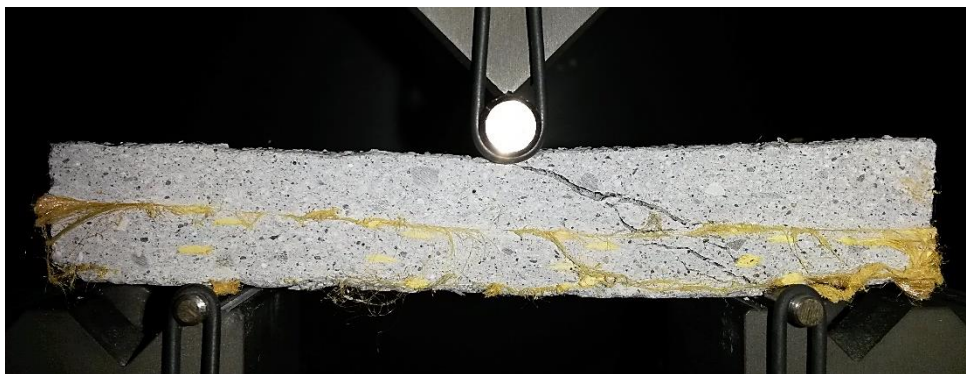
Figure 4.8 – Typical failure modes for Carbon 1-FRCM from one-ply (a) to four-ply (d)



Figure 4.9 - Typical failure mode for one-ply Carbon 2-FRCM



(a)



(b)

Figure 4.10 - Typical failure modes for two-ply (a) and four-ply (b) PBO-FRCM

The first cracks occurred in the maximum bending moment zone at the bottom side of the beam. From that region, for flexural failure, cracks grew in the vertical direction up to the loading cylinder, while for diagonal shear failure, the cracks started from the regions closer to the supports. Those cracks, which were affected

both by shear and tension stresses, followed an inclined path toward the load application point.

*Effect of varying the span to thickness (s/h) ratio*

The term “short beam” indicates that the support span length,  $s$ , is a low multiple of the specimen thickness,  $h$ . The goal is to force the beam specimen to fail in shear. This can be achieved because the shear stress is independent of the support length, whereas the flexural (bending) stresses are a linear function of the support length. Thus, the shorter the beam, the greater the shear stress relative to the bending stresses.

For FRP the standard ASTM D2344 suggests using a support span length-to-specimen thickness ratio,  $s/h$ , of 4 for all types of fiber-reinforced polymers. Before arriving to this standard value, the short-beam shear (SBS) ratio was varied from three to 14 (Adams and Lewis 1994). Flexural failures were found to be common at  $s/h$  ratios higher than five. The highest SBS strength was recorded at an  $s/h$  of three, the lowest ratio tested, but it was suggested that at this small  $s/h$  ratio the compressive normal stress under the loading point was too severe.

For FRCM experiments on one-ply plain specimens were performed to investigate varying  $s/h$  ratios. In particular,  $s/h$  ratios equal to 3 and 6 were tested. Figure 4.11 shows the typical failure modes of the specimens with the varying  $s/h$  ratio. The tested coupons presented both flexural failures, although the reasons of these failures are different. As  $s/h$  decreases from the value of 4, the support cylinders get closer to being directly under the loading cylinder, and there is more of a through-the-thickness crushing of the specimen, rather than bending, thus altering the failure mode away from shear. Moreover, the stress concentration becomes too high producing surface compressive damage under the loading roller. When considering an  $s/h$  ratio of six the supports are farther from the loading cylinder, the specimen is no longer a short beam and the bending of the sample combined with the



low capacity of the mortar in tension generate flexural failures rather than a shear failure.



(a)



(b)

**Figure 4.11 – Typical failure modes for one-ply Carbon 1-FRCM with  $s/h=3$  (a) and  $s/h=6$  (b)**

These results show that varying the span to thickness ratio does not change the failure mode. Furthermore, changing the  $s/h$  ratio did not produce any shear failures. Therefore, it is recommended that an  $s/h$  ratio of four be adopted as standard value to investigate the interlaminar shear behavior of FRCM systems.

#### *Selection of best parameters*

For FRP several studies (Cui et al. 1994, Shivakumar et al. 2002, Adams 2004) were conducted to investigate the selection of the best parameters to get an interlaminar shear failure. These studies demonstrated that two main parameters which may affect the behavior of the short-beam specimen are the diameter of the loading and support cylinders and the addition of an isotropic material element under

the loading nose. One important issue in the short beam specimens is the complexity of the stresses, using larger cylinder diameters and wood or steel elements under the loading roller may alleviate the situation.

The mentioned studies have demonstrated experimentally and numerically that larger cylinder diameters spread the applied load over a wider specimen surface area, resulting in a lower stress concentration. To this end, a diameter of 6.00 mm for the support cylinders, instead of 3.00 mm as recommended by the ASTM D2344, was used to test Carbon 1-FRCM specimens with varying number of plies. Figure 4.12 shows some typical failure modes of the specimens with the varying support cylinder diameters.

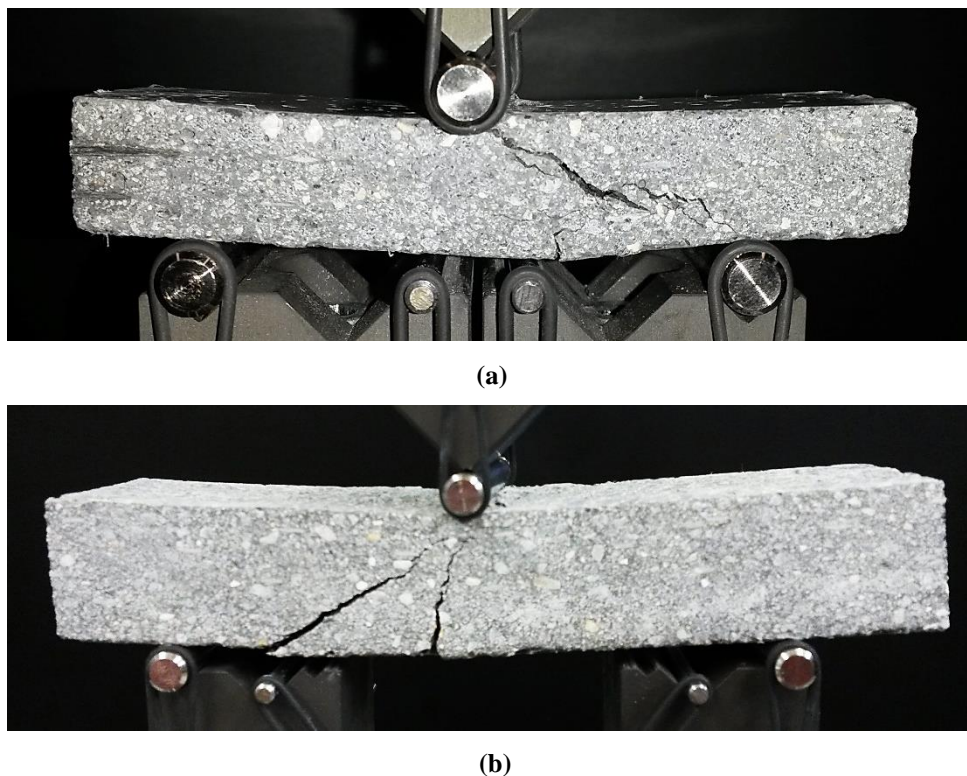
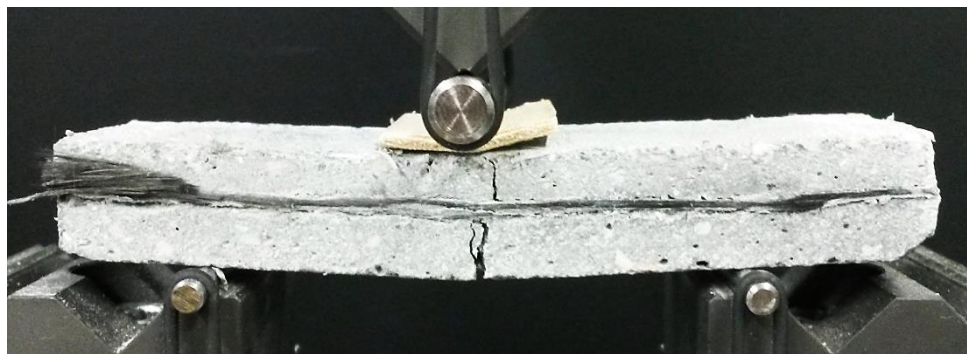


**Figure 4.12 – Typical failure modes for two-ply (a) and four-ply (b) Carbon 1-FRCM with support cylinder diameters of 6.0mm**

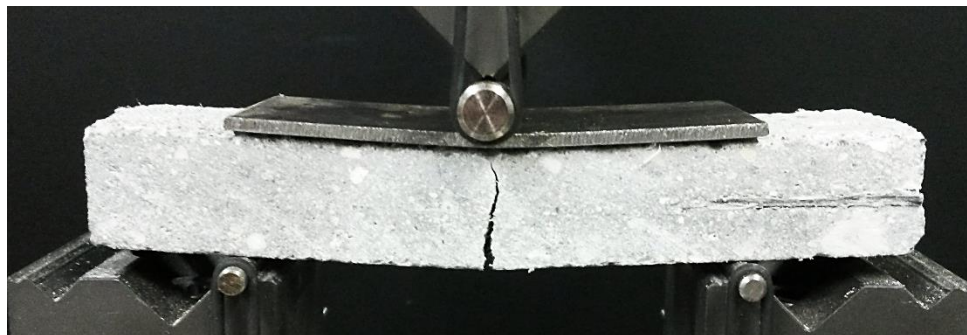
These small changes in cylinder diameters made little difference in the test results and a valid interlaminar shear failure mode could not be obtained. Also with larger cylinder diameters, the failure mode was still diagonal shear and micro-cracks

occurred in proximity of the supports. Therefore, the cylinder diameters recommended by the standard ASTM D2344 have been used for the remainder of the tests.

Other experiments were conducted on one-ply Carbon 1-FRCM, putting wood and steel under the loading roller, to understand if the commonly observed surface damage in the three point bending test could be avoided. Figure 4.13 shows the typical failure mode obtained during the tests.



(a)



(b)

**Figure 4.13 – Typical failure modes for one-ply Carbon 1-FRCM with wood (a) and steel (b) under the loading roller**

Also in this case the failure mode was flexural and local damages occurred in proximity of the loading roller. No interlaminar shear failure could be obtained and thus this solution has not been used as a reliable means for investigating the interlaminar shear behavior of FRCM composites.

*Load-Deflection diagrams*

This Section presents the three-point-bending behavior of some typical plain specimens by plotting the load versus deflection results. In particular, one-ply and four-ply Carbon 1-FRCM and two-ply and four-ply PBO-FRCM are presented in order to see the behavior of different FRCM systems with varying number of plies.

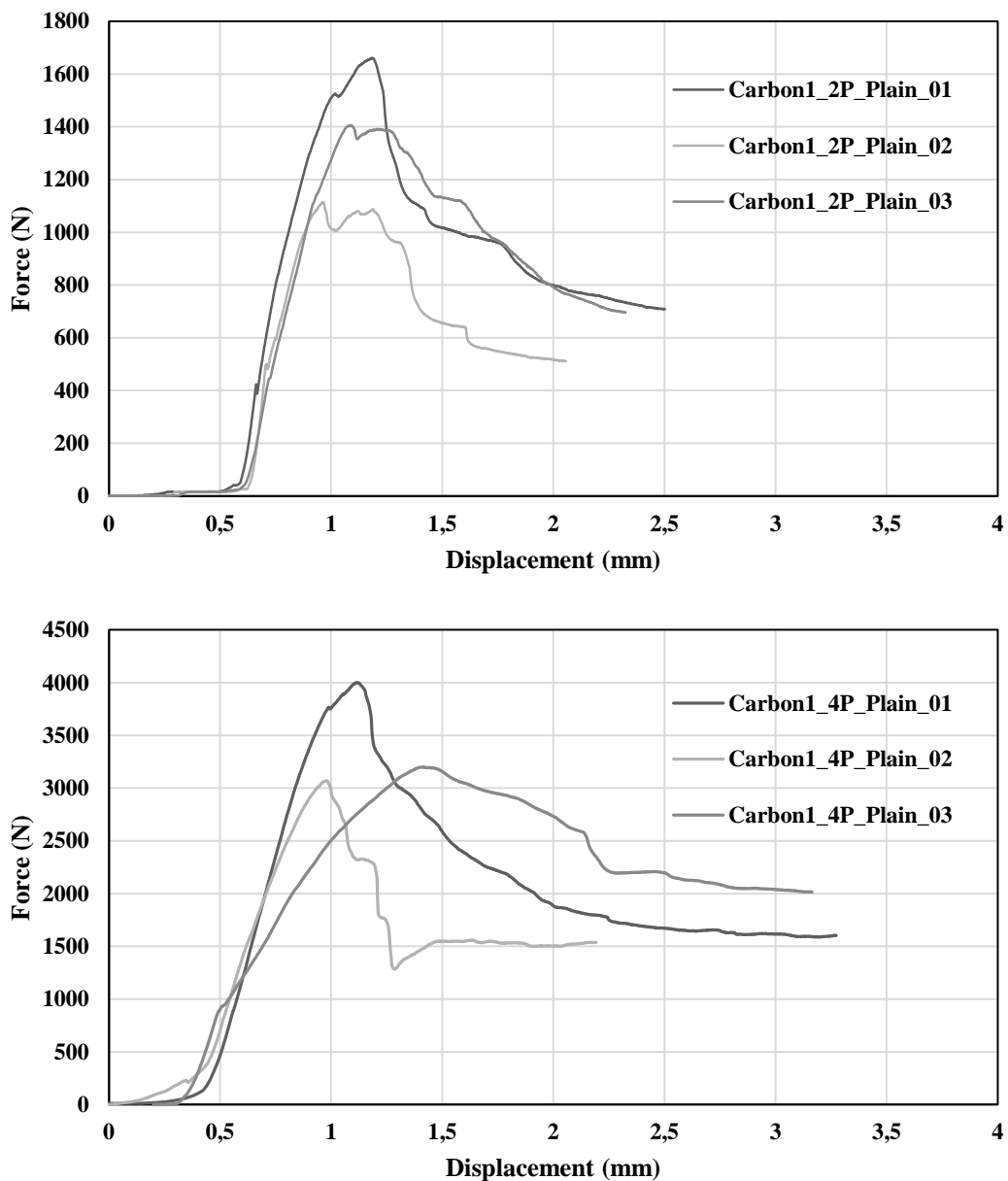


Figure 4.14 – Load-deflection curves of Carbon 1-FRCM, two and four plies respectively

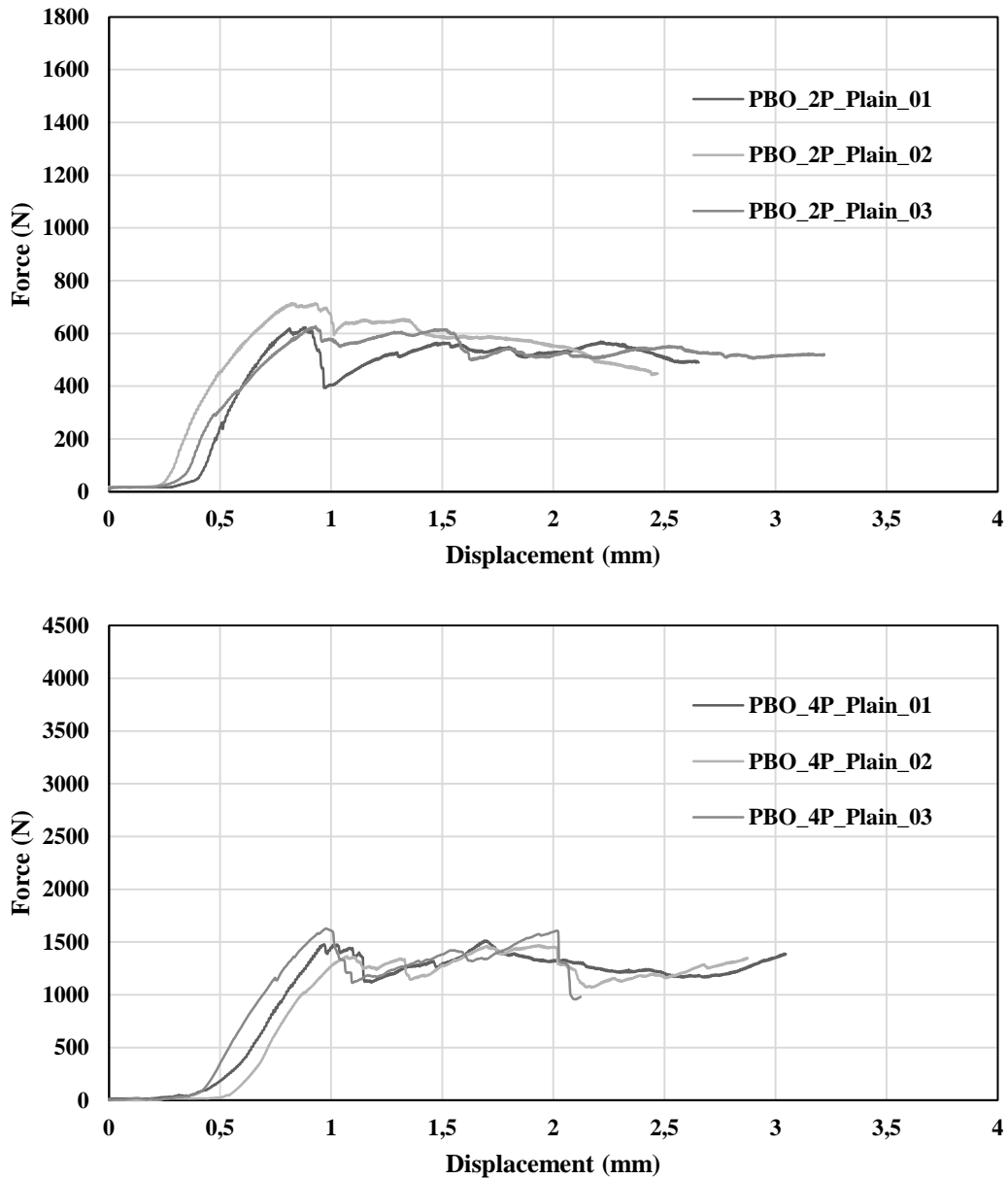


Figure 4.15 – Load-deflection curves of PBO-FRCM, two and four plies respectively

The two FRCM systems present a very different behavior. As expected, the maximum load increases with the amount of reinforcing plies. However, comparing the two composite systems, the Carbon 1-FRCM, for the same number of plies, presents a much higher maximum load with respect to PBO-FRCM. This difference in the maximum load is due to the compressive strength of the mortar and to the geometry of the specimen. Therefore, since this value is related to the dimensions of

the short beam, it becomes important comparing the apparent interlaminar shear stress. Indeed, this parameter takes into account the cross-sectional geometry.

#### *Test interpretation*

The most common way to interpret the short-beam shear test is to use classical beam theory. In this theory, it is assumed that the shear stress,  $\tau_{13}$  is parabolically distributed through the cross-section of the specimen with a maximum at the neutral axis location given by Equation 3.1:

$$\tau_{13} = \frac{3}{4} \frac{P}{bh} \quad (3.1)$$

where P is the load applied at the center of the beam, b is the width of the beam, and h is the thickness of the specimen. When the ultimate load,  $P_C$ , is substituted into equation (3.1), the shear stress thus obtained is regarded as the apparent interlaminar shear strength of the composite.

Detailed finite element stress analysis on FRP three-point short-beam specimens has shown that for linear elastic material, the above equation is valid for a large part of the region between the loading roller and the support rollers (Cui and Wisnom, 1992). However, the shear response of composites is typically very nonlinear (Ditcher et al., 1981). When this nonlinear shear response is taken into account, the interpretation by classical beam theory is significantly in error even for the region away from the rollers. The shear stress distribution will not be parabolic, but much more uniform over a large part of the section. The maximum shear stress is lower than that given by beam theory (Cui et al., 1994).

The apparent interlaminar shear strength given by equation (3.1) was used in the present study for FRCM composites. Although the actual strength can be expected to be lower, use of the apparent value is still valid for comparing different specimens. Table 4.4 shows the apparent Interlaminar Shear Strength (ISS) for plain specimens with the different FRCM systems.

Specimen ID	Number of reinforcing plies	Average thickness (mm)	Span length (mm)	Width (mm)	Average maximum Load (N)	Apparent ISS (MPa)
Carbon1_1P_Plain	1	11,7	46,7	23,3	625,9	1,722
Carbon1_2P_Plain	2	12,1	48,4	24,2	1393,9	3,570
Carbon1_3P_Plain	3	15,0	60,1	30,1	2259,7	3,749
Carbon1_4P_Plain	4	19,8	79,3	34,0	3424,5	3,809
Carbon2_1P_Plain	1	9,1	36,6	18,3	397,8	1,784
PBO_2P_Plain	2	8,56	34,2	17,1	655,0	3,352
PBO_4P_Plain	4	14,5	58,0	29,0	1536,9	2,741

**Table 4.4 – Apparent Interlaminar Shear Strength (ISS) for different FRCM systems**

The apparent ISS values are much more consistent than the load ones and allow comparing the different FRCM systems. The apparent ISS appears to be governed by the quality of the cementitious matrix; in particular, it could be related to the compressive strength of the mortar. Therefore, the ISS should be independent of the number of reinforcing plies. Disregarding the one-ply specimens in which the single layer of fabric cannot act as crack breaker, the experimental data confirm this result showing approximately constant values of ISS for the different number of plies. Based on these findings, the short-beam shear test is not recommended to be used with one-ply FRCM systems.

Nevertheless, the apparent ISS of multi-ply samples does not represent the actual strength of the material in the interlaminar plane cause all the tested specimens failed in flexure or diagonal shear, which demonstrate a higher resistance of the material in the interlaminar plane. To this purpose, in the following section an investigation of interlaminar surface will be presented in order to better understand the interlaminar strength of FRCM composites.

### 4.3 Investigation of Interlaminar Plane: Contact Surface Area Reduction

The first study demonstrated the complexity of developing an interlaminar shear failure with FRCM composites. Flexural or matrix diagonal shear failures denote that the interlaminar strength of the FRCM systems is higher than the flexural and tensional resistance. An investigation of interlaminar plane was then conducted in order to understand the actual mid-plane strength of these composites. In particular, since the continuity and the bond of the cementitious matrix ensure the strength of the FRCM samples, the proposed method is to consistently reduce the contact surface area at the shear plane until obtaining an interlaminar failure. By reducing the amount of interlaminar contact surface there is less continuity between the two layers of mortar and the interlaminar plane becomes the weaker part of the system.

#### *Percentages of investigation and procedure*

The percentages of contact area to be examined varied from 0%, where no contact between the two layers of mortar exists, to 25% with an increment of 5% each iteration. The tests were performed with a polyethylene sheet replacing the fabric inside the cementitious matrix.

The thickness of the specimens was fixed at 10 mm. In this way, the interlaminar plane presented an area of 60 mm x 20 mm (remembering that the total length is equal to 6 times the thickness, while the width is equal to 2 times the thickness). Figure 4.16 shows the mid-plane surface.

Once the interlaminar area was defined, it was possible to compute the relative percentages of contact. For practical reasons, these percentages were realized by creating stripes along the whole length of the specimen. Figure 4.17 shows the layout of the specimens with the different percentages of contact surface, the gray stripes represent the contact area of the two layers of mortar.



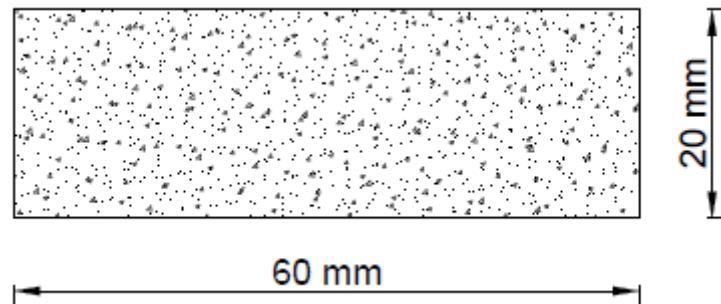


Figure 4.16 – Interlaminar plane surface

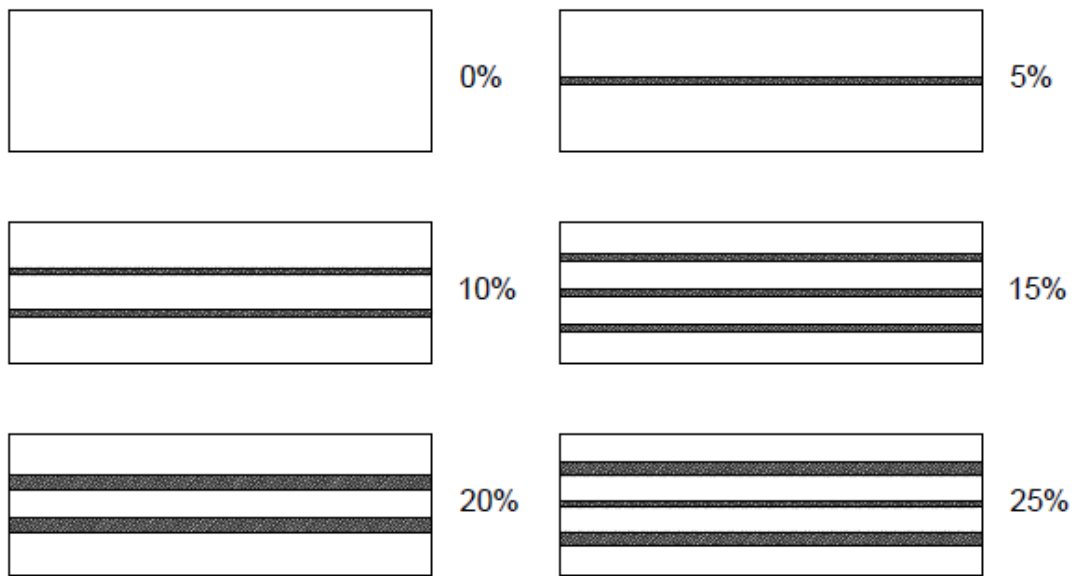


Figure 4.17 – Plane view of the layout of surface area reduction

*Test matrix*

In order to address a wide range of material characteristic behavior, the three types of mortar (Mortar 1, Mortar 2 and Mortar PBO) of the FRCM systems under investigation were used for this study in order to validate the test methodology and compare the behavior of the different cementitious matrices. In particular, five specimens for each percentage of contact and for each type of mortar were tested for a total of 90 samples. The complete matrix of tested specimens can be found in Appendix A.

### 4.3.1 Specimen Preparation

The specimens were cut from small panels which were 330x155 mm. The panel molds were made by attaching a Plexiglas surface to a particle board and installing aluminum edges (10 mm thick) to control panel thickness.

The panels were manufactured using a manual impregnation technique by first applying a thin layer (5 mm) of cementitious matrix, followed by the polyethylene sheet, pre-cut to panel size according to Figure 4.18, which was embedded in the first layer of fresh mortar (Figure 4.19). A 10 mm frame at the external board of the panel and 3 mm spacing among the specimens was considered to cut the samples without reducing their actual dimension. The top layer of matrix was then applied as flat as possible with a finishing trowel. The panels were cured for 28 days at laboratory conditions before cutting was performed. Individual coupons were cut using a 3 mm diamond-tipped wet saw with a rigid fixture to ensure consistent specimen widths.

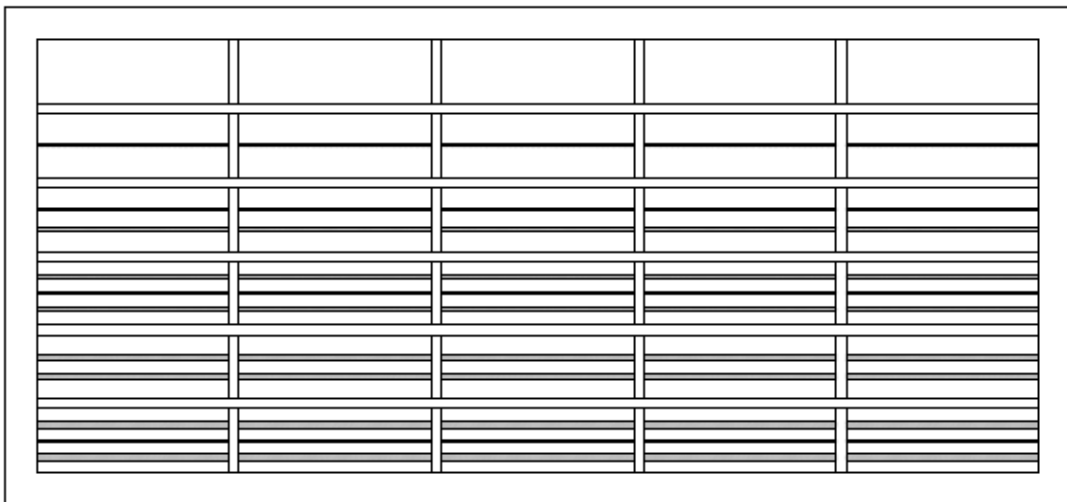


Figure 4.18 – Pre-cut polyethylene sheet

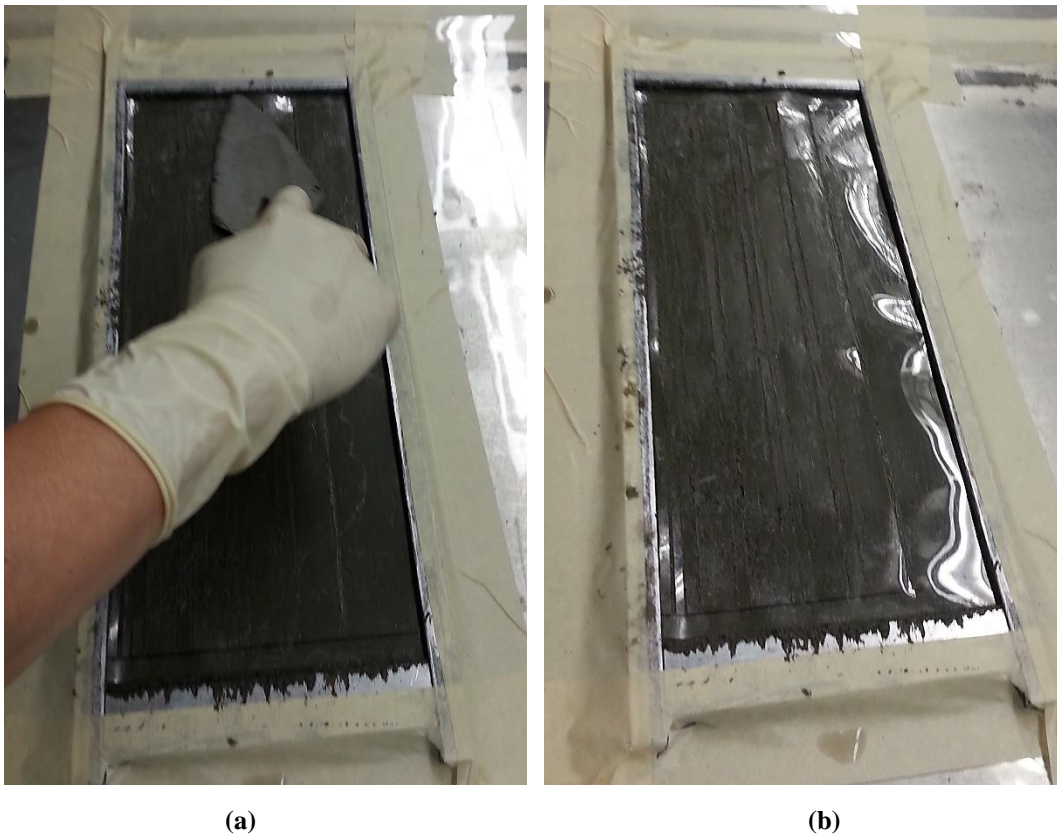


Figure 4.19 – Application of pre-cut polyethylene sheet on the first layer of mortar

### 4.3.2 Test Setup and Procedure

The test setup and procedure is the same of the plain specimens tested in the previous section. A three point bending test was performed using a screw driven Universal Test Frame with the load applied in displacement control at a rate of 1 mm/min in a quasi-static configuration. The vertical displacement of the specimen was measured according to the cross-head displacement. No device was used to measure the deformations.

### 4.3.3 Test Results

Table 4.5 shows a summary of the tests performed and the relative failure modes experienced with the cross-sectional area reduction method.

Specimen ID	Repetitions	Average thickness (mm)	Span to thickness ratio	Span length (mm)	Width (mm)	Average maximum Load (N)	Failure mode*
Mortar 1_0%	5	10,0	4	40,0	20,0	191,9	IS
Mortar 1_5%						336,1	IS
Mortar 1_10%						360,2	FL
Mortar 1_15%						376,8	FL
Mortar 1_20%						405,3	FL
Mortar 1_25%						429,9	FL
Mortar 2_0%	5	10,0	4	40,0	20,0	141,0	IS
Mortar 2_5%						208,4	IS
Mortar 2_10%						234,0	IS - FL
Mortar 2_15%						241,1	FL
Mortar 2_20%						271,3	FL
Mortar 2_25%						296,3	FL
Mortar PBO_0%	5	10,0	4	40,0	20,0	169,1	IS
Mortar PBO_5%						205,8	IS
Mortar PBO_10%						262,2	IS - FL
Mortar PBO_15%						275,1	FL
Mortar PBO_20%						327,0	FL
Mortar PBO_25%						347,6	FL

\*FL = flexural failure; DF = matrix diagonal shear failure; IS = interlaminar shear failure

**Table 4.5 - Summary of tests performed and relative failure modes**

As can be observed by Table 4.5, the cross-sectional area reduction generated interlaminar shear failures (IS) with all the three types of mortar. With this method, it is possible to give a limiting value between interlaminar shear and flexural failures, which at the same time represents an indicator of the limiting ratio between voids and open cross section. This value varies depending on the type of cementitious matrix according to their different properties. The characteristics of the different mortars were given in Section 2.1.1. In particular, for Mortar 1 the limiting value

between interlaminar shear and flexural failure was found to be between 5% and 10% of contact surface with no interlaminar failure experienced over 5%. Also for Mortar 2, this value was found to be between 5% and 10% of contact surface but some of the tested specimens with 10% and 15% of contact area presented interlaminar shear failures denoting a higher limiting value. Finally, the Mortar PBO presented a behavior similar to Mortar 2 but no interlaminar failure was observed with 15% of contact area. In all the tests performed, no diagonal shear failure was observed. Table 4.6 shows a summary of the limiting values of contact area between interlaminar shear and flexural failure.

<b>Mortar type</b>	<b>Limiting value between IS and FL failure</b>
Mortar 1	5% - 6%
Mortar 2	9% - 10%
Mortar PBO	7% - 8%

**Table 4.6 – Limiting values between IS and FL failure**

Mortar 2, which is characterized by a lower compressive strength compared to the other two mortars, presented the highest limiting value between IS and FL failure, denoting a relationship between the failure mode and the compressive strength of the cementitious matrix.

Figure 4.20, Figure 4.21 and Figure 4.22 show the typical failure modes for the different types of cementitious matrix. For clarity of discussion, only one interlaminar failure and one flexural failure are reported for each kind of mortar.



(a)



(b)

Figure 4.20 – Typical failure modes for Mortar 1: (a) interlaminar failure (b) flexural failure



(a)



(b)

Figure 4.21 – Typical failure modes for Mortar 2: (a) interlaminar failure (b) flexural failure



(a)



(b)

Figure 4.22 – Typical failure modes for Mortar PBO: (a) interlaminar failure (b) flexural failure

As can be observed from the previous pictures, although the interlaminar shear failure can be clearly recognized, it is often combined with flexural cracks. This

phenomenon was something expected because of the cementitious nature of the tested specimens. Moreover, an interesting aspect, highlighted by Figure 4.21b and Figure 4.22b, is the role in tension zone of the polymeric fibers within the Mortar 2 and Mortar PBO. These fibers, less than 5% in volume, increase the flexural capacity of the matrix.

An important observation to note with this test method is the original position of the specimens relative to the cast panel. Indeed, although an external edge of 15 mm was considered in the design phase (Figure 4.18), specimens closer to the edges of the panel demonstrated a higher value of contact area to change from interlaminar to flexural failure. This behavior is due to two main reasons: one is a manufacturing issue, during the casting it is not possible to apply the same pressure in the middle and at the edges of the panel, while the other one is a chemistry issue, during the curing time there is more water evaporating at the edges of the panel compared to the center.

Therefore, it becomes fundamental removing the contribution of the edges to ensure the same conditions for all the tested specimens. To this end, for future studies, during the casting of the panel, it is recommended to consider at least 40 mm as external frame to be removed.

In conclusion, this study on cross-sectional area reduction not only generated interlaminar shear failures, but also explained the reason why the plain specimens with the fabric inside tested in the first study did not show any interlaminar failure. Indeed, the contact area of the mortar at the mid-plane on the specimens with the fabric inside is much larger than the values obtained in this study (maximum 10%), making unlikely the formation of interlaminar failures.

This method represents a matrix characterization and gives the chance of comparing different types of cementitious matrixes related to the fabrics under investigation. Furthermore, the data found with this method could be used in the



design of the fabric with the final purpose of optimizing the geometry and the dimensions of the fabric.

A further modification of the specimen configuration was proposed to enhance the flexural capacity of the FRCM samples and make interlaminar shear the control failure mode. This was done creating a composite sandwich beam made by FRCM and steel. The next section presents the study.

## **4.4 Composite Sandwich Beam: Increasing Flexural Strength**

### *Background*

A sandwich-structured composite is a special class of composite materials that is fabricated by attaching two thin but stiff skins to a lightweight but thick core. The core material is normally low strength material, but its higher thickness provides the sandwich composite with high bending stiffness with overall low density (Zenkert 1995). Sandwich construction is of particular interest and widely used in many structures, because the concept is very suitable to the development of lightweight structures with high in-plane and flexural stiffness.

Commonly used materials for facings are composite laminates and metals, while cores are made of metallic and non-metallic honeycombs, cellular foams, wood or trusses. Sheet metal is also used as skin material in some cases. The face sheets are typically bonded to the core with adhesive. The facings carry most of the bending and in-plane loads and the core defines the flexural stiffness and out-of-plane shear and compressive behavior (Plantema 1966). Some advantages of sandwich construction are (Zenkert 1995):

- Sandwich cross sections are composite. The composite has a considerably higher shear stiffness to weight ratio than an equivalent beam made of only

the core material or the face-sheet material. The composite also has a high tensile strength to weight ratio.

- The high stiffness of the face-sheet leads to a high bending stiffness to weight ratio for the composite.

The structural performance of sandwich beams or panels depends not only on the properties of the skins, but also on those of the core and the adhesive bonding the core to the skins, as well as on the geometrical dimensions of the components (Reddy 1997). In particular, the strength of the composite material depends largely on two factors (Zenkert 1995):

- The outer skins: If the sandwich is supported on both sides and stressed by means of a downward force in the middle of the beam, then the bending moment will introduce shear forces in the material. The shear forces result in the bottom skin in tension and the top skin in compression. The core material spaces these two skins apart. The thicker the core material the stronger the composite. This principle works in much the same way as an I-beam does.
- The interface between the core and the skin: Because the shear stresses in the composite material change rapidly between the core and the skin, the adhesive layer also sees some degree of shear force. If the adhesive bond between the two layers is too weak, the most probable result will be debond.

A great deal of work has been published on the behavior of sandwich structures in the last few decades. The fundamentals of sandwich construction and reviews of analytical and computational methods are described in the works of Zenkert (1995), Noor et al. (1996) and Reddy (1997). Of course, no works have been found on composite sandwich beams with the FRCM system as core material.

An investigation of the FRCM composite sandwich beams was performed in order to increase the flexural strength of the plain samples and generate a high shear

stress concentration in the mid-plane. The FRCM composite sandwich specimen was made by the FRCM system as core material and steel plates as face-sheet material.

The following parameters were studied: the number of reinforcing plies of the FRCM system, the thickness of steel plate facings, and the FRCM core dimensions. Based on a semi-elastic stress analysis, a relationship between the FRCM systems under investigation and the thickness of the steel plates to generate interlaminar failures was calculated. The results of the analysis are presented in Section 4.4.3.

#### **4.4.1 Specimen Preparation**

The FRCM composite sandwich specimen preparation is of particular importance for the effectiveness of the results. The casting and the curing of the FRCM panels were realized as in Section 4.2.1. Therefore, the specimens were cut from FRCM panels considering the final thickness of the coupon, given by FRCM core plus steel face-sheets. The metal face-sheets were bonded to the core with epoxy adhesives 24 hours prior to testing.

#### **4.4.2 Test Results**

First, sandwich specimens with different number of reinforcing plies were tested with a thickness of the steel facings of 2 mm (1/16 of an inch). Then, the dimensions of the FRCM core specimen and the thickness of the steel plates were varied. Table 4.7 shows a summary of the tests performed on sandwich samples and the relative failure modes experienced. The number of specimens and the specimen nominal dimensions are also shown in Table 4.7.

The thickness of the specimen was measured in three different points of the coupon. Then, an average value was computed to determine the span length and width. Although the specimens presented a higher thickness, since the maximum width of the loading knife was 40 mm, the width of the specimen was assumed equal to two times the thickness until a maximum value of 34 mm.

Specimen ID	Repetitions	Thickness of face-sheet (mm)	Average thickness (mm)	Span to thickness ratio	Span length (mm)	Width (mm)	Failure mode*
Carbon1_1P_Sandwich	5	2	16,5	4	66,0	33,0	DF
Carbon1_1P_Sandwich	3	2	15,5	6	92,9	31,0	DF - FL
Carbon1_2P_Sandwich	3	2	15,6	4	62,4	31,2	DF
Carbon1_3P_Sandwich	3	2	18,7	4	74,9	34,0	DF
Carbon1_4P_Sandwich	3	2	21,4	4	85,6	34,0	DF
Carbon1_4P_Sandwich	3	4	24,5	4	98,0	34,0	IS - DF
PBO_2P_Sandwich	3	2	12,1	4	48,5	24,3	DF
PBO_2P_Sandwich	3	2	12,1	3	36,4	24,3	FL
PBO_4P_Sandwich	3	1	16,1	4	64,4	32,2	DF
PBO_4P_Sandwich	4	2	18,4	4	73,6	34,0	IS
PBO_4P_Sandwich	3	4	22,3	4	89,2	34,0	IS

\*FL = flexural failure; DF = matrix diagonal shear failure; IS = interlaminar shear failure

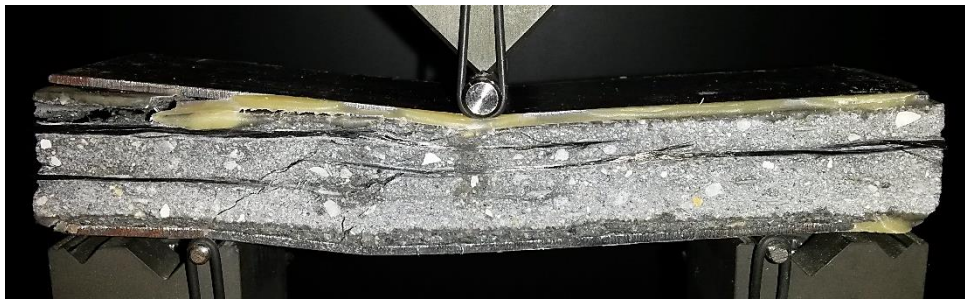
**Table 4.7 – Summary of tests performed on sandwich specimens and relative failure modes**

The FRCM composite sandwich specimens presented quite different results compared to the plain ones. Not only the failure modes for one-ply and two-ply specimens changed from flexural to diagonal shear, but the four-ply sandwich samples presented interlaminar shear failures.

This significant result represented a combination of the cross-sectional area reduction study and the current one. Indeed, the fact that only the four-ply specimens showed the interlaminar shear failure means that the four layers of fabric consistently reduce the cross-sectional contact area, but the interlaminar failures are reached only thanks to the steel facings which increase the flexural strength of the composite and, therefore, the shear stress concentration at the mid-plane. Figure 4.23, Figure 4.24 and Figure 4.25 show the typical failure modes for the different types of FRCM composite sandwich beams. For clarity of discussion, only two-ply and four-ply specimens are reported for each kind of FRCM system.



(a)



(b)

Figure 4.23 – Typical failure modes for two-ply (a) and four-ply (b) Carbon 1-FRCM composite sandwich beams with steel facings of 2.0mm



Figure 4.24 – Typical failure mode for four-ply Carbon 1-FRCM composite sandwich beam with steel facings of 4.0mm



(a)



(b)

**Figure 4.25 – Typical failure modes for two-ply (a) and four-ply (b) PBO-FRCM composite sandwich beams with steel facings of 2.0mm**



**Figure 4.26 – Valid interlaminar shear failure obtained with the four-ply PBO-FRCM**

Figure 4.26 shows the detail of a valid interlaminar shear failure obtained with the four-ply PBO-FRCM. As can be observed from the previous pictures, for the four-ply composite sandwich specimens, the cracks started from the loading nose and flowed diagonally until reaching the fabric which changed the inclination of the cracks from diagonal to horizontal.

*Load-Deflection diagrams*

This Section presents the three-point-bending behavior of some composite sandwich specimens by plotting the load versus deflection results.

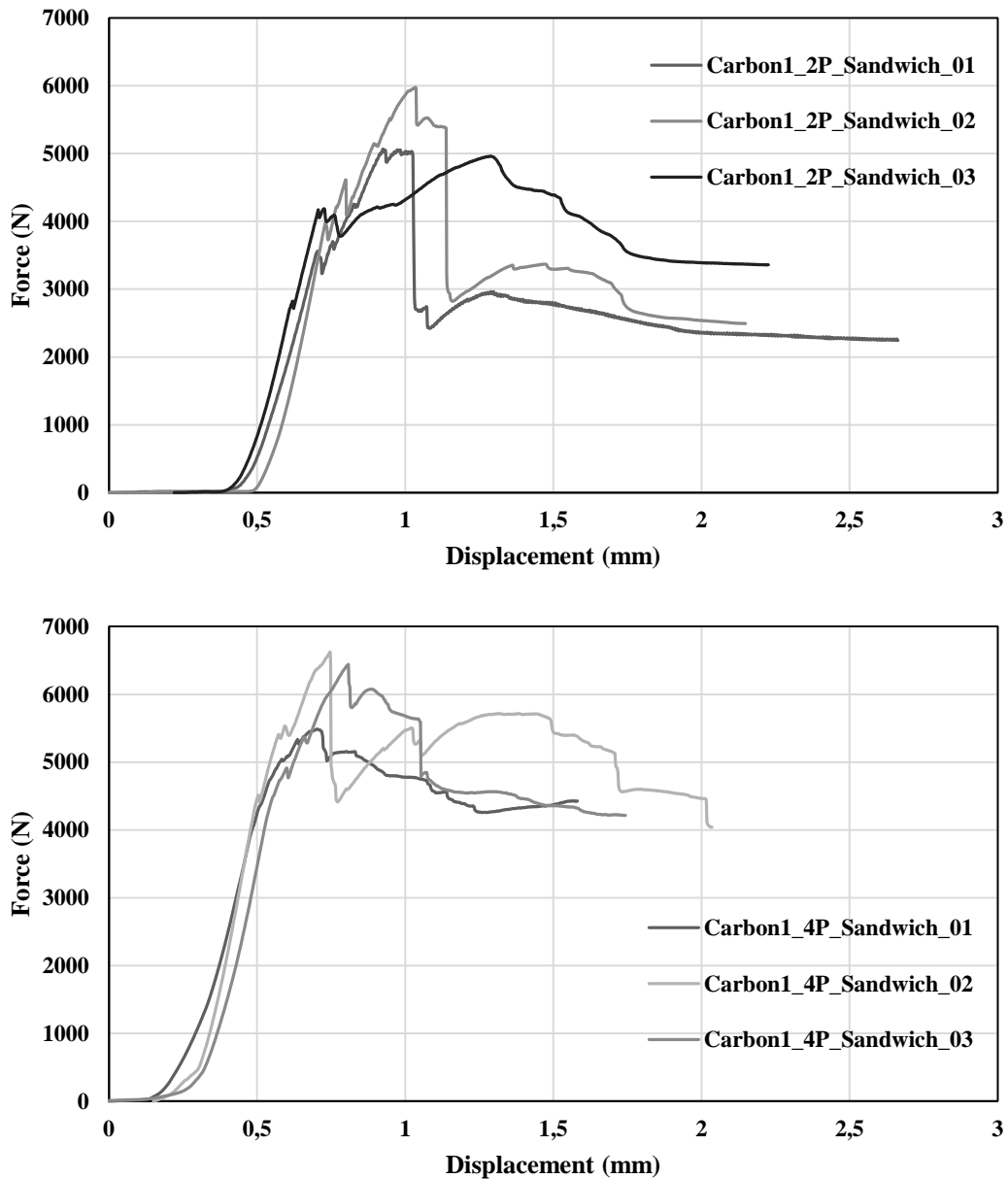


Figure 4.27 – Load-deflection curves of composite sandwich Carbon 1-FRCM with steel plates of 2.0mm, two and four plies respectively

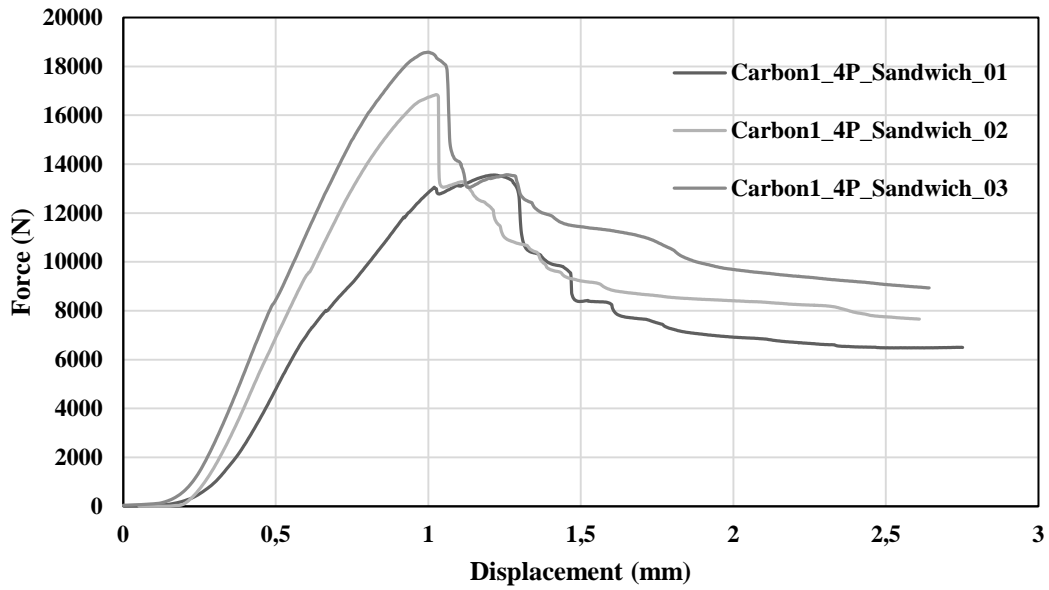
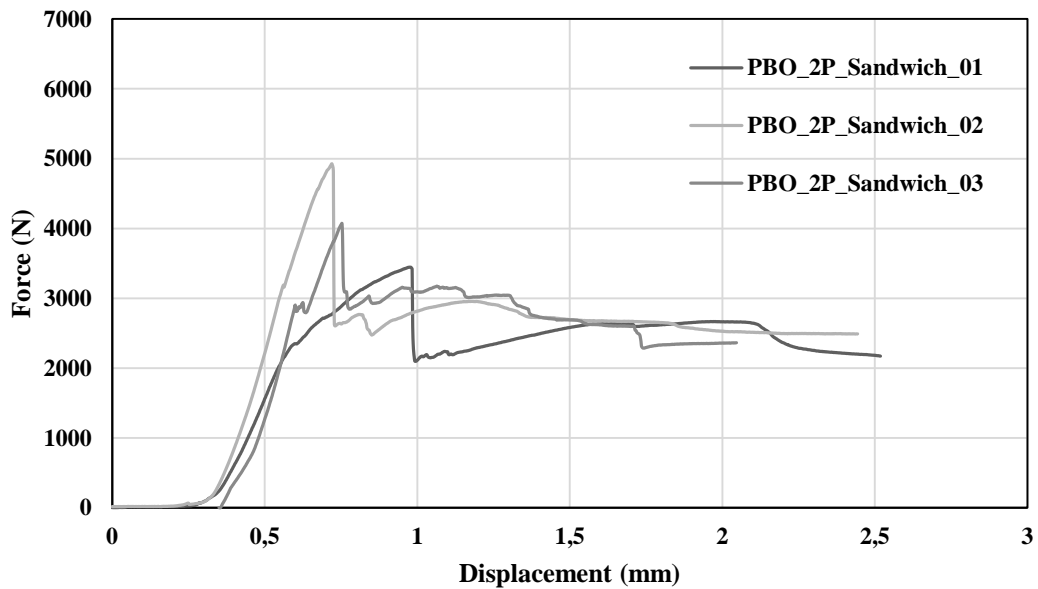
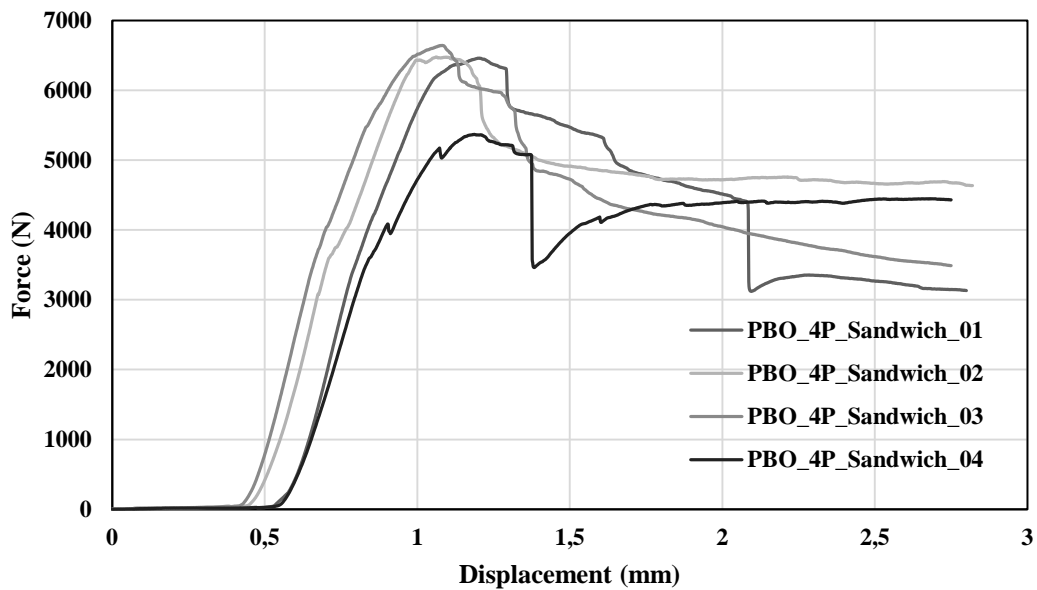


Figure 4.28 – Load-deflection curves of four-ply composite sandwich Carbon 1-FRCM with steel plates of 4.0mm







**Figure 4.29 – Load-deflection curves of composite sandwich PBO-FRCM with steel plates of 2.0mm, two and four plies respectively**

In particular, two-ply and four-ply Carbon 1-FRCM and PBO-FRCM are presented in order to see the behavior of different composite sandwich FRCM systems with varying number of plies and thickness of the steel facings. The short-beam deflection reported in the diagrams is measured from the cross-head displacement, thus it is only qualitative as it includes extraneous items such as settlements.

The two FRCM systems used for this study present a different behavior. The maximum load increases with the amount of reinforcing plies, but with composite sandwich specimens there is no a significant gap between two and four plies. This small difference is due to the steel facings which carry a big amount of the load and change the behavior with respect to plain samples. As expected, a very large difference can be observed between the composite beams with 2 mm thickness steel facings and the ones with 4 mm. The maximum load with 4 mm steel facings was found to be more than two times the one with 2 mm.

However, since the maximum load is related to the dimensions of the specimen and to the cross-section made by FRCM and steel, it becomes important computing and comparing the interlaminar shear stress. To this end, a semi-elastic stress analysis was performed in order to examine the behavior of the composite sandwich specimens. The definition “semi-elastic” is used to address the implication of experimental data performing an elastic analysis.

### 4.4.3 Stress Analysis

Since to compute the interlaminar shear strength a valid interlaminar shear failure has to be obtained, only the specimens which presented an IS failure have been analyzed. These are the four-ply Carbon 1-FRCM and PBO-FRCM composite sandwich systems.

#### *Interlaminar Shear stresses*

In many cases, a three-dimensional state of stress is reduced to a two-dimensional state by the assumption of plane stress. The usual assumption of plane stress for laminated composite materials neglects the stresses,  $\tau_{xy}$ ,  $\tau_{yz}$ , and  $\sigma_y$  (see Figure 4.30), and only the stresses in the plane of the laminate are considered.

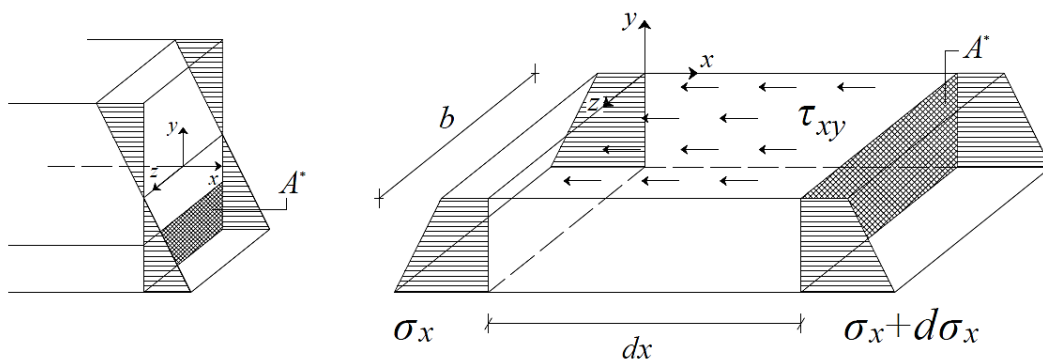


**Figure 4.30 – Interlaminar shear stress**

These neglected stresses are distributed through the specimen thickness and are generally known as the 'interlaminar shear stresses'. Of particular interest are the interlaminar shear stresses which develop at the interfaces of layers of a composite

beam when subjected to a transverse load. An analytical technique was needed to evaluate the shear stress distribution in FRCM composite materials and correlate theoretical with experimental results.

*Cross-section transformation method*

For composite cross sections made from materials with rectangular cross sections a simplified approach is possible in order to determine the characteristics and stresses of the composite sandwich beam. Several mechanics of materials books describe the cross-section transformation method, but fundamentally, the procedure is the same. In the current work, Madhukar-Vable (2012) has been considered.

According to this work, the dimensions of the cross-section in the  $z$  direction are transformed using the equation  $\tilde{z} = z(E_j/E_{ref})$  where  $E_{ref}$  is the modulus of elasticity of any material in the cross-section which is used as the reference material. Figure 4.31 shows a cross-section made from two materials, as in the present work.

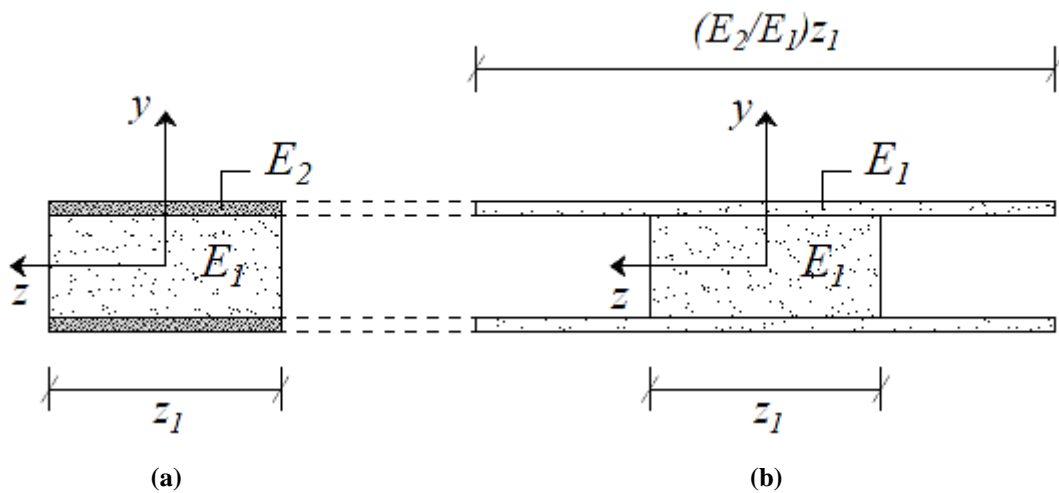


**Figure 4.31 – Transformation of cross-section. (a) Original composite cross-section. (b) Transformed homogenous cross-section.**

The dimensions in the  $z$  direction are transformed using the ratio of the modulus of elasticity of the material to the reference material. The transformed cross-section is considered homogeneous with the modulus of elasticity of the reference material. The centroid, the second area moment of inertia  $\tilde{I}_z$ , and the first area moment  $\tilde{Q}_z$  are

found for the transformed cross-section like for any homogeneous material. The following formulas are then used for finding the bending normal and shear stresses:

$$(\sigma_x)_i = - \left( \frac{E_i}{E_{ref}} \right) \cdot \frac{M_z \cdot y}{\tilde{I}_z} \quad (4.1)$$

$$\tau_{xy} = \tau_{yx} = - \left( \frac{V_y \cdot \tilde{Q}_z}{\tilde{I}_z \cdot b} \right) \quad (4.2)$$

where  $\tilde{I}_z$  and  $\tilde{Q}_z$  are the second area moment of inertia and the first area moment about the axis through the centroid of the transformed homogeneous cross-section, and  $b$  is the thickness perpendicular to the centerline of the original composite cross-section.

#### *Assumptions*

In order to derive a beam theory and using the elastic analysis with the cross-section transformation method presented in the previous section, the following assumptions were made:

- there are no out of-plane bending moments  $M_y = M_{xy} = 0$
- the cross-section remains perfect linear-elastic and it is uncracked
- since the percentage of fabric in term of area in the cross-section is very small, under the 5% of total area, the fabric inside the mortar is neglected in the computation of the stresses and the cross section is considered made by two materials (mortar and steel)
- perfect bond between the core of mortar and the steel facings; therefore, no epoxy deformation is present and the shear stresses are perfectly transmitted between the two materials.

The validity of the various approximations depends on the geometry of the beam, properties of the component materials and loading conditions. Apparently, these assumptions are strong, but they are necessary in order to analyze the composite sandwich specimens. However, considering that the maximum load in the

specimens has been found to be at the end of the elastic phase, the assumption of considering perfect linear-elastic cross-section is reasonable to perform the stress analysis.

### *Stress Analysis*

Under the assumptions previously presented, the elastic stress analysis was performed on the four-ply Carbon 1-FRCM and PBO-FRCM composite sandwich specimens with different thickness of the steel face-sheets. In particular, the cementitious mortar was chosen as reference material for the transformed cross-section. Therefore, for the stress analysis a homogenous cross-section of mortar was considered. To this end, the elastic modulus of the mortar  $E_m$  and the one of the steel  $E_s$  were necessary. For the mortar, the elastic modulus was not provided by the technical specifications of the manufacturer but it was determined in two different ways with consistent results. The first one was the use of Equation 8.5.1 of ACI 318, which is hereby reported:

$$E_m = 33 \cdot w_c^{1.5} \cdot \sqrt{f'_c} \quad (4.3)$$

where  $w_c$  and  $f'_c$  are respectively the density and the compressive strength of the mortar, which can be found in the technical specifications (Section 2.1.1). The result obtained with this equation is in psi. While the second way used to compute the elastic modulus of the mortar was the Ultrasonic Pulse Velocity (UPV) method. The results of the two different methods for the different types of mortar are presented in Table 4.8.

Mortar type	Elastic modulus with ACI formula (GPa)	Elastic modulus with UPV method (GPa)
Mortar 1	26,61	26,88
Mortar 2	12,29	12,52
Mortar PBO	15,19	15,23

**Table 4.8 – Elastic modulus of the different types of mortar**

For the steel, the elastic modulus was assumed equal to 200GPa. Figure 4.32 shows the distribution of the flexural and interlaminar shear stresses with the four-ply PBO-FRCM in the case of plain specimen and composite sandwich one.

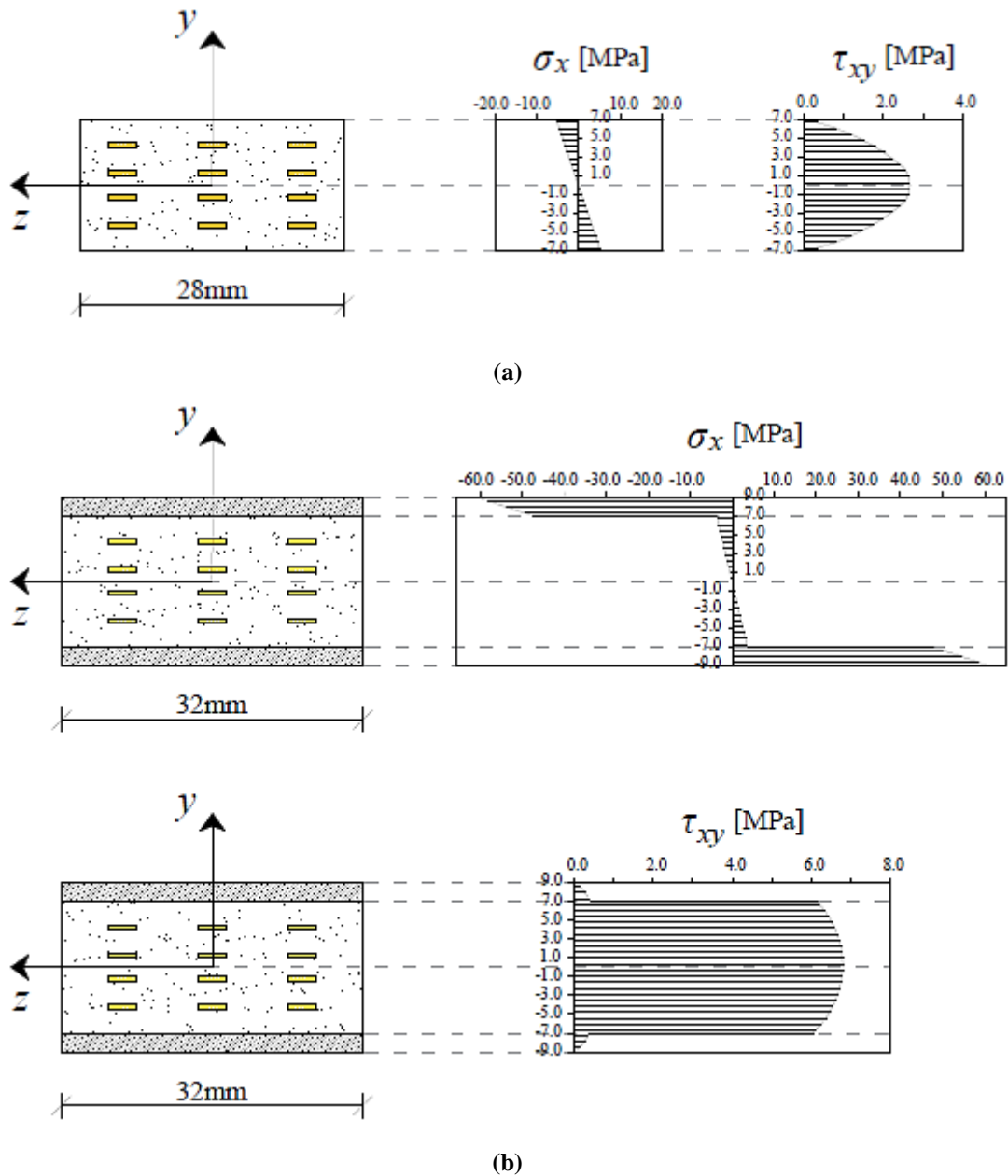


Figure 4.32 – Distribution of the flexural and interlaminar shear stresses with the four-ply PBO-FRCM in the case of plain specimen (a) and composite sandwich one (b)

As can be noted, for the composite sandwich specimens the flexural stress is carried by the steel facings, while the interlaminar shear stress is mostly carried by the core of mortar with the maximum value in the mid-plane where the interlaminar failure was created. Although this behavior justifies the choice of using the composite sandwich specimens, it does not explain the reason why the interlaminar failure was formed. In order to explain the formation of interlaminar failure, a comparison between the principal tensile stress of the analyzed specimen and the tensile strength of the material taken as reference material is necessary.

The principal stresses were computed according to the following expression:

$$\sigma_{1,2} = \frac{\sigma_x + \sigma_y}{2} \pm \sqrt{\left(\frac{\sigma_x - \sigma_y}{2}\right)^2 + \tau_{xy}^2} \quad (4.4)$$

where  $\sigma_x$  and  $\sigma_y$  are the flexural stresses, while  $\tau_{xy}$  is the interlaminar shear stress. In particular, the assumption of no out-of-plane bending leads to  $\sigma_y = 0$ .

Although the principal stresses could be simply computed through Equation 4.10, the determination of the maximum tensile strength of the mortar could be more complex. To this end, two possible approaches were followed; the first was to test specimens made of only mortar under three-point bending and see the tensile strength related to the uncracked beam, while the second one was to perform splitting tensile tests on cylindrical specimens made of only mortar as well. Using the splitting tensile there is the need of relating the tensile strength obtained with this type of test to the flexural one. In particular, there is a very well established relationship between the tensile stresses measured on a splitting test as opposed to a flexural test. Popovics (1998) suggested this relation through an experimental formula, which is hereby reported in MPa:

$$f_{fl} = 1.2 \cdot f_{sp} + 0.69 \text{ [MPa]} \quad (4.5)$$

where  $f_{fl}$  and  $f_{sp}$  are the tensile strength of the mortar under examination related to flexural test and splitting tensile test respectively.

Table 4.9 shows the values of the tensile strength of the different types of mortar derived from the split-tensile test.

<b>Mortar type</b>	<b>Split Tensile stress (MPa)</b>	<b>Flexural stress (MPa)</b>
Mortar 1	6,969	9,053
Mortar PBO	3,545	4,944

**Table 4.9 – Tensile strength of the different types of mortar derived from Splitting Tensile Test**

Once the tensile strength of the material is computed, the comparison between the principal tensile stress of the analyzed specimen and the tensile strength is possible to perform. However, with the composite sandwich specimens a key factor is the thickness of the steel face-sheets. Indeed, as can be noted from Table 4.7, the experimental results demonstrated a different behavior of the FRCM composite sandwich beams with varying thickness of the steel plates and in particular, for the four-ply Carbon 1-FRCM samples the data showed a change in the failure mode due to the different thickness of the steel facings.

To this end, the comparison between the principal tensile stress of the sandwich specimens and the tensile strength of the mortar, considered as reference material for the transformed cross-section, has to be performed with respect to the thickness of the steel plates. In this perspective, this analysis represents an optimization of the steel facings thickness to generate an interlaminar failure, and therefore, to validate a test methodology to measure the interlaminar shear strength of the different FRCM systems. Figure 4.33 and Figure 4.34 show the results of the analysis and explain the experimental behavior of FRCM composite sandwich specimens.



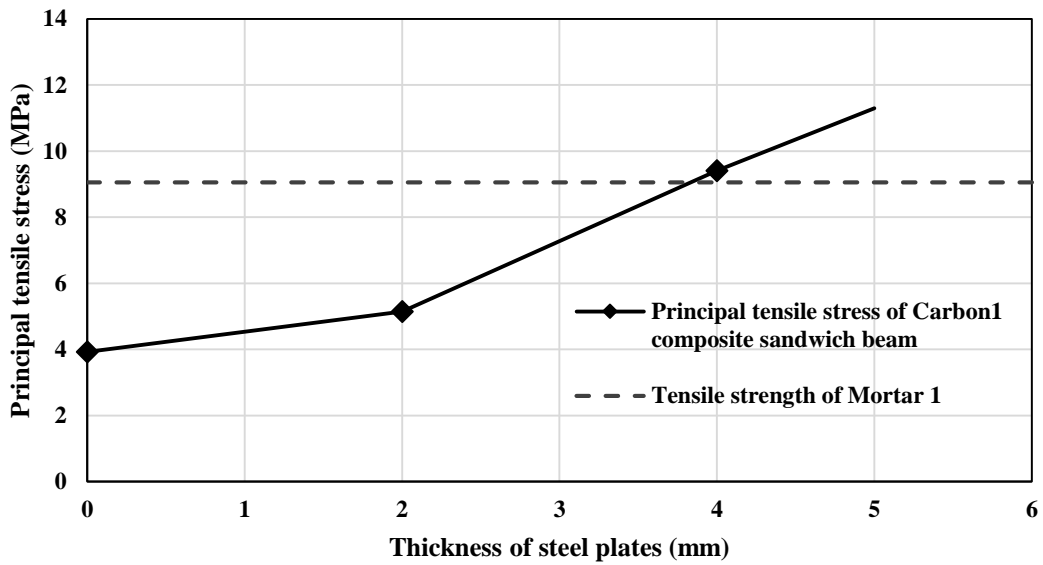


Figure 4.33 – Optimization of the steel facings thickness for Carbon 1-FRCM

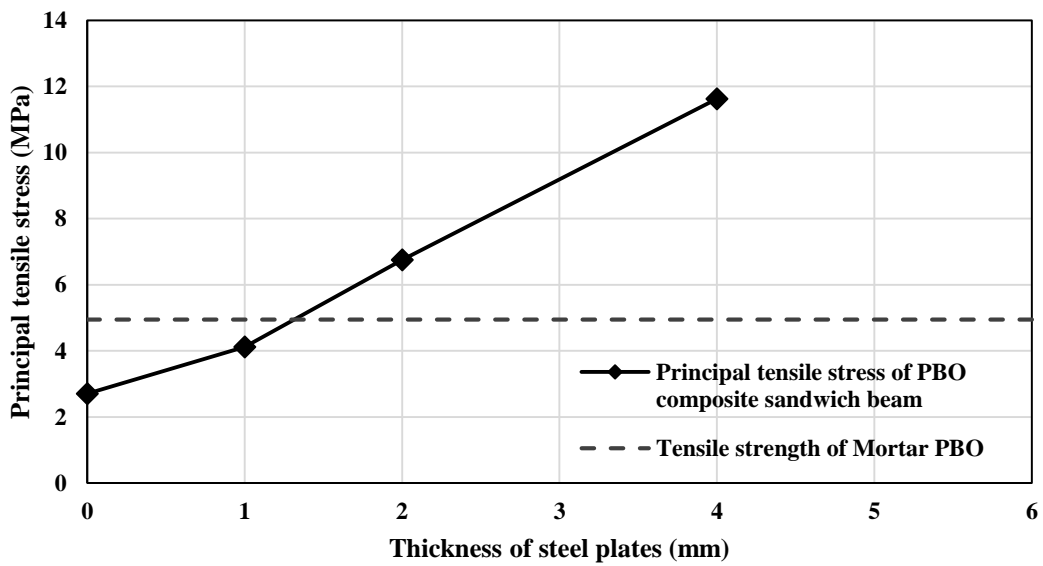


Figure 4.34 – Optimization of the steel facings thickness for PBO-FRCM

The curves derived from the semi-elastic stress analysis confirm the experimental data. For the four-ply Carbon 1-FRCM composite sandwich specimens a 4.0mm thick steel plate represents a limit value between the interlaminar shear failure and matrix diagonal shear failure, and the tested samples reflected this

intermediate situation with some interlaminar failures and some diagonal shear failures (Table 4.7). While for the PBO-FRCM composite sandwich specimens a 2.0mm thick steel plate represents already a sufficient value to ensure the formation of interlaminar shear failures. The tests demonstrated this result with all the specimens which failed interlaminarly (Table 4.7).

*Interlaminar Shear Strength (ISS)*

To close this section, since a valid interlaminar shear failure has been obtained for four-ply Carbon 1 and PBO FRCM composite sandwich beams, it is worthwhile to compute the interlaminar shear strength of these composite systems, which in this case, represents the actual strength of the FRCM systems under investigation in the interlaminar plane. The cross-section transformation method was utilized to consider the composite sandwich structure and Equation 4.4 was used to calculate the Interlaminar Shear Strength (ISS) of the said specimens. The maximum value of the ISS occurs in the mid-plane of the specimen. Table 4.10 shows the results for the different FRCM systems.

Specimen ID	Thickness of face-sheet (mm)	Average thickness (mm)	Span length (mm)	Width (mm)	Average maximum Load (N)	ISS (MPa)
Carbon1_4P_Sandwich	4	24,5	98,0	34,0	16326,2	9,409
PBO_4P_Sandwich	2	18,4	73,6	32,0	6237,7	6,752

**Table 4.10 - Interlaminar Shear Strength (ISS) for different FRCM systems**

Comparing these results with the ones obtained for plain specimens (Table 4.4), it can be noted that the interlaminar shear strength of the FRCM sandwich systems is much higher of the apparent ISS related to flexural or matrix diagonal failures of plain specimens.

## 4.5 Image Analysis of FRCM Composite Systems

In Section 4.4.2, the formation of interlaminar failures was found to be a combination of the cross-sectional area reduction study and the composite sandwich structure. Since for each FRCM system under investigation the results are different depending on the type of fabric and cementitious matrix, it becomes important to characterize each constituent of the composite.

To this end, an image analysis was performed in order to examine the geometric characteristics of the different fabrics, and in particular, to better understand the percentage of coverage of one layer of fabric in the interlaminar plane. The cross-sectional area reduction study showed that by reducing the amount of contact surface this plane becomes the weak part of the composite and generates the formation of interlaminar shear failures.

### *Image analysis method*

Few works have been found in literature for the analysis of composite materials and a growing awareness of the potentiality of this method could bring more accurate results in the study of material properties for characterization and design purposes. Thanks to the use of a free software, different data can be obtained by simply performing an image analysis.

Image analysis was used in this study for:

- determination of contact surface area at interlaminar plane of FRCM composite systems
- determination of net area for stress computation of FRP and FRCM composites subjected to pull-out test
- computation of fabric area within the transverse cross-section for tensile characterization
- determination of epoxy deformation with clevis type grip and of fabric slippage in tensile characterization.

For the current study, the interest is focused on the determination of contact surface area at interlaminar plane of FRCM systems. The other examples of application of the mentioned properties can be found in Appendix B. For clarity of discussion, also the procedure of the analysis performed with the software can be found in Appendix B.

*Analysis results*

Image analysis results are given in an excel file, where it is possible to find different values depending on the purpose of the analysis. Table 4.11 shows the coverage area of the different fabrics under investigation in the interlaminar plane, and therefore, the contact surface of the different FRCM systems. Since the fabrics present irregular geometry (Section 4.1.1), the analysis was performed three times in different regions of the mesh and an average value was computed.

<b>FRCM system</b>	<b>Fabric coverage area (%)</b>	<b>Contact surface at interlaminar plane (%)</b>
Carbon 1	36,59	63,41
Carbon 2	61,20	38,80
PBO	56,99	43,01

**Table 4.11 – Image analysis results for the different FRCM systems**

As can be noted from Table 4.11, the Carbon 1-FRCM presents a higher value of contact surface at interlaminar plane compared with the other FRCM systems, and therefore, for this type of composite there is more continuity in the matrix ensuring a higher interlaminar shear strength. This result is an additional proof of the difficulty of finding an interlaminar failure with that type of FRCM system.

Since this was the first image analysis on FRCM systems, a different investigation was performed on Carbon 1 fabric in order to validate the methodology. In particular, using a CAD software it was possible to determine the same data with a different method. The procedure consists on drawing the fabric for an assigned geometry and the software automatically computes the area covered by the fabric,

and therefore, the contact surface of the matrix. Figure 4.35 shows the fabric drawing while Table 4.12 shows the results of the study.

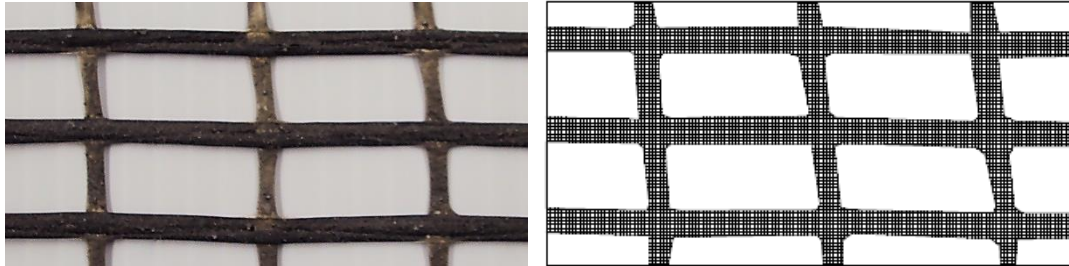


Figure 4.35 – CAD drawing of Carbon 1 fabric

FRCM system	Fabric coverage area (%)	Contact surface at interlaminar plane (%)
Carbon 1	36,90	63,10

Table 4.12 – CAD software analysis results

As can be noted, the results are consistent and confirm the validity of the image analysis method. The results obtained with this method will be used in the following section for the splitting tensile test in order to investigate the behavior of the FRCM specimens in pure tension.

## 4.6 Splitting Tensile Test

Up to now, all the tests have been performed with the short-beam shear (SBS) test method. Because of the complexity of this method and the difficulty of generating interlaminar shear failures, another test methodology was investigated to show that the SBS test is a reasonable choice to investigate the interlaminar shear strength of FRCM systems. This alternative methodology is the Splitting Tensile Test. This test method consists of applying a diametral compressive force along the length of a cylindrical specimen until failure occurs. This loading induces tensile

stresses on the plane containing the applied load and relatively high compressive stresses in the area immediately around the applied load.

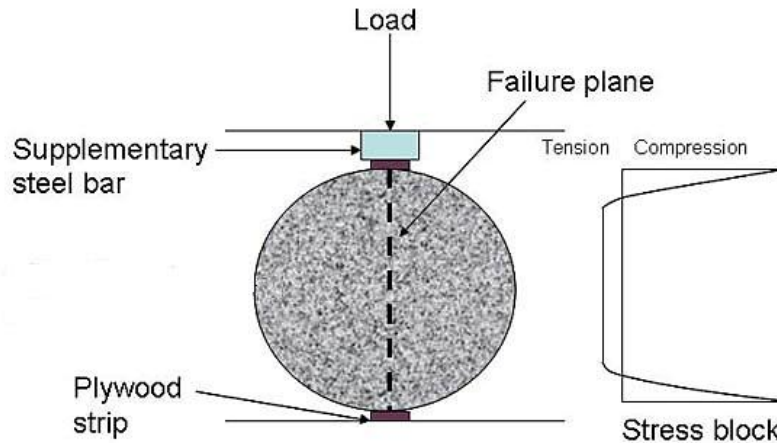


**Figure 4.36 - Splitting tensile test configuration**

In civil engineering, splitting tensile strength is generally used in the design of structural lightweight concrete members to evaluate the shear resistance provided by concrete and to determine the development length of reinforcement. The test method was developed for measuring the tensile strength of cylindrical concrete specimens (ASTM C496) and it has never been applied to FRCM systems before. In the area reduction study, a bond breaker made by a polyethylene sheet was artificially created; the purpose of the current study was to investigate if the polyethylene sheet is actually a bond breaker and which is the behavior of FRCM systems in splitting tension state.

Thanks to the use of the image analysis method (Section 4.5), the percentages of coverage area of the different fabrics under investigation were determined. With the splitting tensile test, it was possible to test different values of coverage area and to examine how the tensile strength of the material varies in function of the covered area of the composite. These varying percentages were created with a polyethylene sheet following a procedure similar to the cross-sectional area reduction method.

In order to validate this methodology, specimens made of only mortar, some with the relative fabric inside and some others with the polyethylene sheet were prepared and tested. A total of 30 cylinders were tested. Table 4.13 shows the test matrix for the splitting tensile test.

Specimen ID	Repetitions	Diameter (mm)	Length (mm)	Reinforcing grid
Carbon1_FRCM	3	50,8	101,6	Carbon1
Carbon2_FRCM	3	50,8	101,6	Carbon2
PBO_FRCM	3	50,8	101,6	PBO
Mortar 1	3	50,8	101,6	No reinforcement
Mortar 2	3	50,8	101,6	No reinforcement
Mortar PBO	3	50,8	101,6	No reinforcement
Mortar1_27%	3	50,8	101,6	Polyethylene sheet
Mortar1_37%	3	50,8	101,6	Polyethylene sheet
Mortar1_47%	3	50,8	101,6	Polyethylene sheet
Mortar1_57%	3	50,8	101,6	Polyethylene sheet

**Table 4.13 – Test matrix for the splitting tensile test**

The different percentages for the polyethylene sheet specimens were chosen with constant intervals depending on the image analysis method. From Table 4.11, the percentage of covering of Carbon 1 fabric is the 37% and the one of the PBO fabric is the 57%. The other percentages were selected to create a linear range of values to be examined.

### 4.6.1 Specimen Preparation

Since this study represents the first investigation on splitting tensile test of FRCM composites, no general procedure is standardized for the specimen preparation. However, some recommendations from the standard ASTM C192 “*Practice for Making and Curing Concrete Test Specimens in the Laboratory*” were considered.

Plastic cylindrical molds with 50.8mm (2 inches) diameter and 101.6mm (4 inches) height were used (Figure 4.37a). For the specimens with the fabric or the polyethylene sheet inside an opening on the bottom of the cylinders were made in order to fix the fabric with the tape to the bottom. This action is fundamental to maintain the alignment of the fabric inside the specimen.

The cylinders were manufactured manually by first adding a layer of cementitious matrix for half of the specimen height (50mm), for compacting the specimen a vibrator can be used, but due to small dimensions of the molds the compaction was performed manually by using a metal stick and perforating the layer of mortar 25 times. The top layer of cementitious matrix was then added and compacted as the previous one. The top of the cylinder was then made as flat as possible with a finishing trowel (Figure 4.37b). The specimens were cured for 28 days at laboratory conditions before testing.

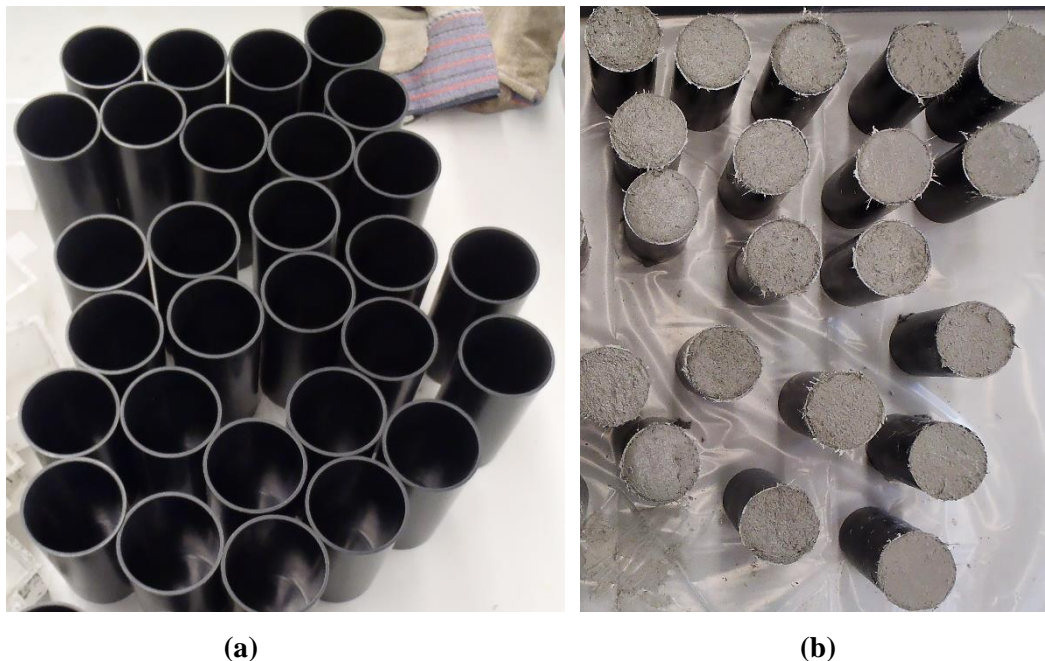


**Figure 4.37 – Specimen preparation for splitting tensile test**

The mid-plane presented an area of 50.8 mm x 101.6 mm (2 in x 4 in). For practical reasons, the percentages of coverage were realized by creating stripes along



the whole length of the specimen. Figure 4.38 shows the layout of the specimens with the different percentages of coverage surface.

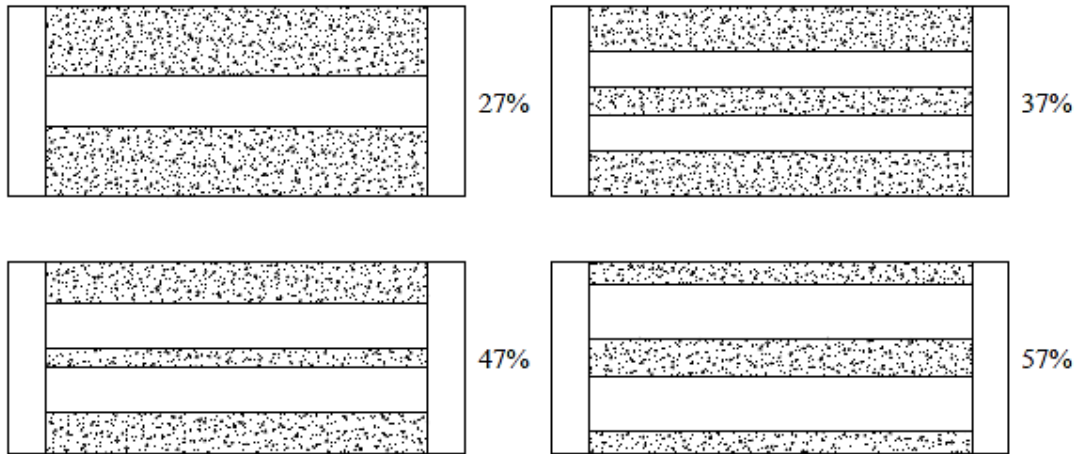


**Figure 4.38 – Layout of polyethylene sheet for the different percentages of coverage surface**

Although an accurate procedure was followed for specimen preparation, it was still challenging to cast the samples with the fabric or the polyethylene sheet inside, and it was hard to ensure the correct alignment of the coating.

For future studies, given the difficulty of truly placing the fabric in the middle, two different methods for specimen preparation are recommended. The first one is casting a panel horizontally of the same thickness of cylinder diameter, placing a layer of fabric or polyethylene sheet in the mid-plane as explained in Section 4.2.1, and then coring the cylindrical specimens from the whole panel. This method not only could result more precise but it is also more representative of what it happens in the field. The second methodology is preparing and testing prismatic specimens. Indeed, none suggests using cylindrical specimens and this method could avoid the problem of alignment and simplify the testing procedure.

## 4.6.2 Test Setup and Procedure

The splitting tensile test was performed using a screw driven Universal Test Frame with a maximum capacity of 130kN. The ASTM C496 recommends applying

the compressive load along the length of the specimen continuously and without shock, at a constant rate within the range 0.7 to 1.4 MPa/min (100 to 200 psi/min) splitting tensile stress until failure of the specimen. However, the testing machine presented some problems working under loading control and a relative displacement control was adopted. In particular, a velocity of 0.25mm/min ensures a constant rate within the range recommended by the ASTM standard.

Thin, particle wood bearing strips were used to distribute the load applied along the length of the cylinder. Specifically, two bearing strips of 3.0 mm thick particle wood, free of imperfections, approximately 25 mm wide, and of a length equal to, or slightly longer than, that of the specimen were provided for each specimen. These bearing strips were placed between the specimen and both the upper and lower bearing blocks of the testing machine. To make the specimen setup easier, the strips were attached to upper and lower blocks of the fixture (Figure 4.39). Bearing strips shall not be reused.



**Figure 4.39 – Arrangement of particle wood bearing strips in the machine fixture**

Diametral lines were drawn on each end of the specimen using a suitable device that ensure that they are in the same axial plane. The specimen was placed on the particle wood strip and aligned so that the lines marked on the ends of the specimen were vertical and centered with the wood strips.

### 4.6.3 Test Results

During the tests, the maximum applied load indicated by the testing machine was recorded. The maximum load sustained by the specimen was divided by appropriate geometrical factors to obtain the splitting tensile strength. Specifically, the splitting tensile strength was computed as follows:

$$T = 2P / \pi \cdot l \cdot d \quad (4.6)$$

where  $T$  is the splitting tensile strength in MPa,  $P$  is the maximum applied load in N,  $l$  and  $d$  are the length and the diameter of the cylinder respectively (mm). Table 4.14 shows the splitting tensile test results; the average maximum load and the tensile strength of the different tested specimens are reported. For clarity of discussion, the comments of the results are presented separately for the different types of specimens.

Specimen ID	Reinforcing grid	Average maximum Load (N)	Splitting tensile strength (MPa)
Mortar 1	No reinforcement	45289,11	5,586
Mortar 2	No reinforcement	29766,67	3,672
Mortar PBO	No reinforcement	33576,66	4,142
Carbon1_FRCM	Carbon1	33208,10	4,096
Carbon2_FRCM	Carbon2	27566,67	3,400
PBO_FRCM	PBO	23427,49	2,890
Mortar1_27%	Polyethylene sheet	31838,59	3,927
Mortar1_37%	Polyethylene sheet	28943,27	3,570
Mortar1_47%	Polyethylene sheet	26603,90	3,281
Mortar1_57%	Polyethylene sheet	24438,53	3,014

**Table 4.14 – Splitting tensile test results**

- *Mortar – No reinforcement inside*

As can be noted from Table 4.14, the splitting tensile strength reflects the different characteristics of the three types of mortar under investigation. As expected,

the tensile strength is related to the compressive strength. In particular, the higher is the compressive strength of the cementitious mortar the higher is the tensile strength.

However, usually the tensile strength of the mortar is assumed as one tenth of its compressive strength, but if this relation is valid for the concrete, it is not possible to state the same for the cementitious matrix of the FRCM systems. Indeed, the experimental results show a tensile strength higher than one tenth of the compressive strength. This additional resistance in tension is due to the presence of the glass short fibers inside the cementitious mortar which enhance the tensile capacity of the material. Figure 4.40 shows a typical failure mode of splitting tensile test and demonstrates the presence of the short fibers in the mortar, simply visible in the opening of the crack failure.



**Figure 4.40 – Typical failure mode of mortar cylinders subjected to splitting tensile test**

The specimens made by cementitious mortar performed very well and the behavior in the load-deflection curves confirms the consistency of the results. Figure 4.41 shows typical load-displacement curves during splitting tensile test.

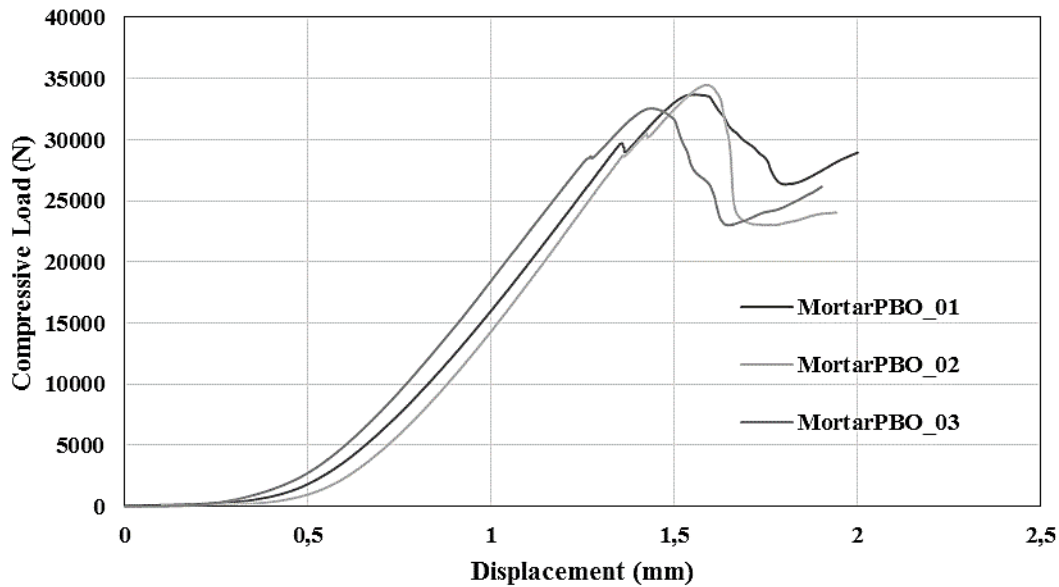


Figure 4.41 – Load-displacement curves for Mortar PBO specimens

These results highlight the relevance of tensile testing, since it is the tensile capacity which controls the behavior of FRCM systems. As an indirect consequence of this work, it was found that the presence of the short fibers in the cementitious mortar really affects not only the ultimate capacity but also the way it fails. Thus, in order to characterize the composite system, a more appropriate quality control should also include tensile testing of the mortar. This test could be performed with the short beam shear test or with the splitting tensile test on cylindrical specimens.

Moreover, tensile testing of the mortar should be implemented in the new version of AC434 as an important parameter to characterize the cementitious matrix of FRCM systems. Indeed, since the experimental results showed it is not possible to find a precise value of tensile capacity from the compressive strength, tensile testing represents a more accurate way to determine this relevant parameter.

- *FRCM composite systems*

Although the specimens composed of only mortar showed consistent results, the samples with the fabric inside demonstrated a much complex behavior. Indeed, the placing of fabric in the failure plane decreases the splitting tensile strength of the

cylinders but only if a correct alignment of the fabric is respected. If it does not, the loading can be carried by the cementitious mortar and values similar to the tensile strength of the mortar are reached. Figure 4.42 shows the problem in casting the cylindrical specimens with the fabric inside; in particular, it is possible to observe the different orientation of fabric at the end sections. To avoid these problems in future investigations, the procedures described in Section 4.6.1 are recommended.

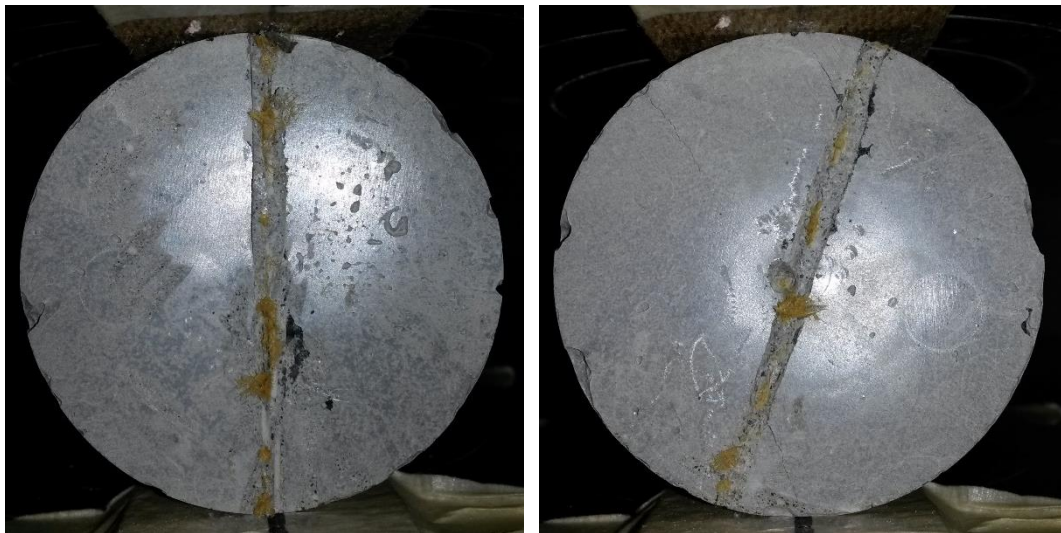


**Figure 4.42 – Problem in casting cylindrical specimens with the PBO fabric inside**

However, the specimens considered for the analysis of results performed quite well, the failure modes were consistent (Figure 4.43) and a reduction of splitting tensile strength compared with the one of cementitious mortar can be observed (Table 4.14).



**Figure 4.43 – Typical failure modes of cylindrical FRCM specimens**

- *Polyethylene sheet – Percentages investigation*

As can be noted from Table 4.14, the experimental results demonstrate that the tensile strength of FRCM composite decreases with the increase of area coverage. Specifically, it was possible to determine the trend of the tensile strength with the varying area coverage (Figure 4.44).

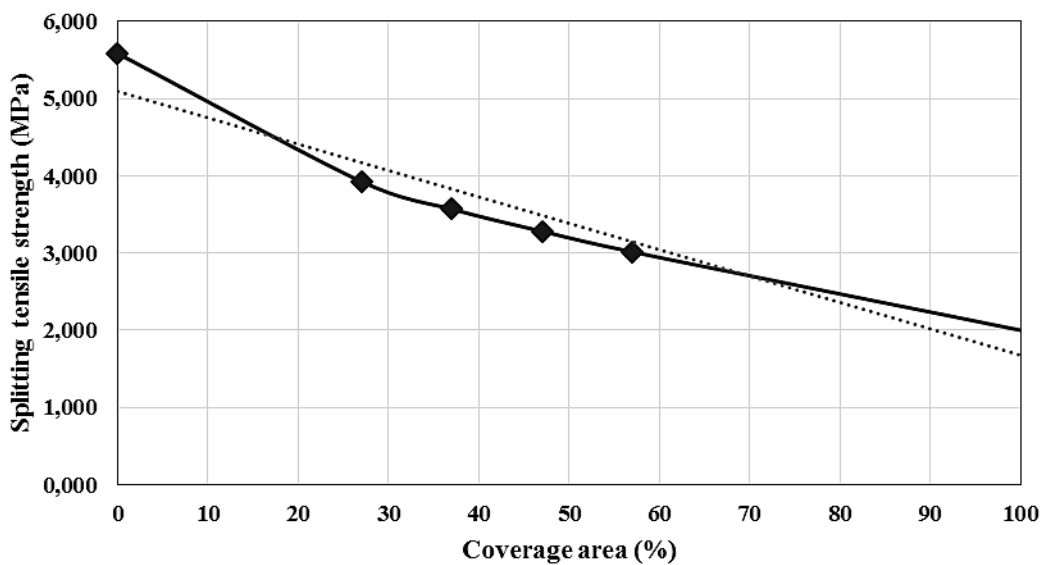


**Figure 4.44 – FRCM tensile strength in function of fabric coverage area**

This result can be related to the short-beam shear test and a comparison between the principal tensile stress obtained with the SBS test and the tensile strength obtained with the current method can be performed. As shown by the stress analysis in Section 4.4.3, in the case of interlaminar shear failure, the principal tensile stress exceeds the tensile strength of the material and allows the formation of that type of failure. However, the complexity in casting proper specimens and the amount of experimental work did not allow drawing a definite conclusion. However, there is potential in further investigation and additional studies are recommended.

Moreover, the test results confirm that the polyethylene sheet is a bond breaker. Comparing the tensile strength obtained for the specimens with the same percentage of coverage area of Carbon 1 (37%), a consistently reduction of the tensile strength

can be observed. Furthermore, compared to the other tests the specimens with the polyethylene sheet in the failure plane failed in a brittle way, with an instantaneous fall of the load, confirming the bond breaker action. Figure 4.45 shows the typical failures obtained with the various percentage of area coverage.

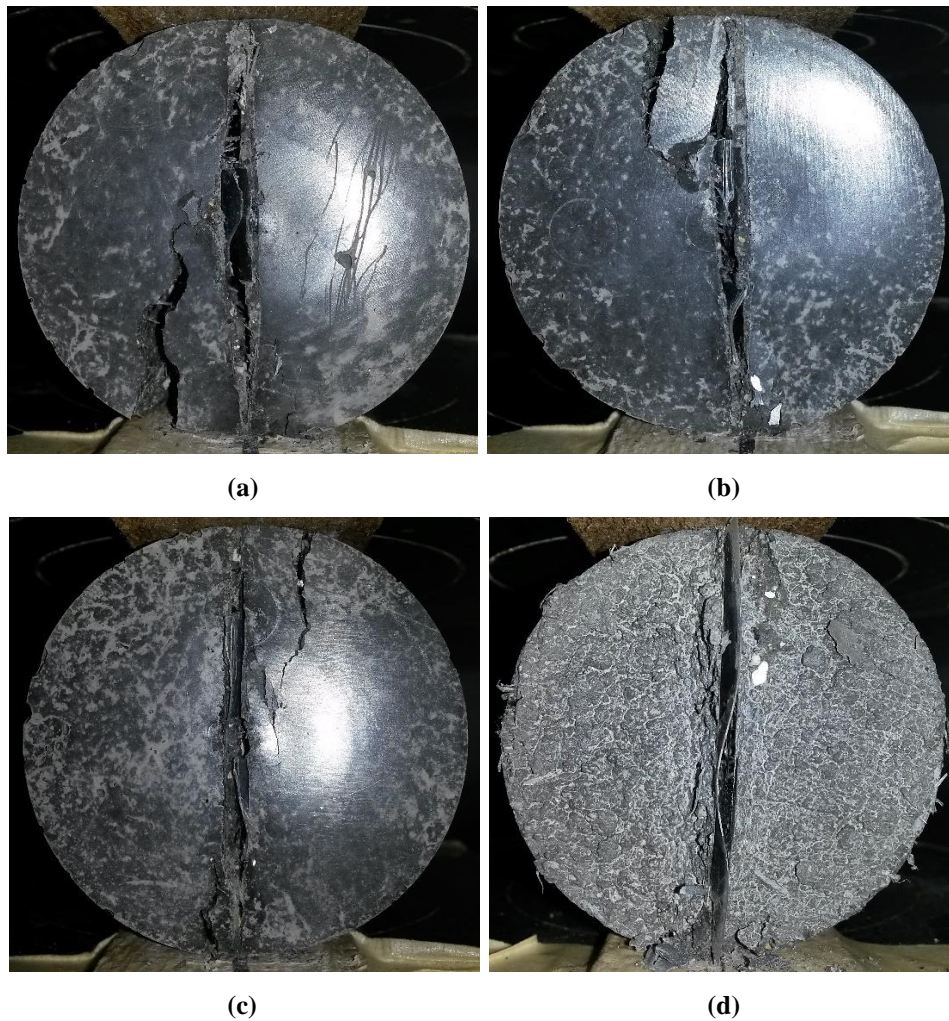


**Figure 4.45 – Typical failures obtained with the various percentage of area coverage:  
(a) 27% (b) 37% (c) 47% (d) 57%**



# 5

## **FRCM PERFORMANCE AFTER ENVIRONMENTAL EXPOSURE**

This chapter explores FRCM behavior under the SBS test after exposure to different aggressive environments. It is divided into three sections: the first gives an overview of the environment characteristics, the second presents the experimental results, and the third draws conclusions and recommendations for FRCM applicability.

### **5.1 Exposure Environments**

Durability is a key factor for safety and sustainability of a structure that must have the capability to maintain required performance over time under the effect of external actions. Structural durability depends on the type and quality of materials, design, manufacturing process, application of such materials, and the service environment.

Factors affecting the durability of FRCM composite systems must consider the environmental performance of each component and their interfaces (Arboleda 2014).

Therefore, the cementitious matrix, the fabric reinforcement, the fabric-matrix interface, and the matrix-substrate interface should be considered. Since this study focuses on interlaminar shear characterization, the interface between the composite and the substrate is outside the purpose of this study.

Degradation mechanisms of the cementitious materials usually involve crumbling or spalling due to chemical reactions that produce compounds that occupy higher volumes such as the alkali-aggregate reaction, sulfate attack, freeze/thaw cycles, and corrosion of steel-based reinforcement (Somayaji 2001). The alkali-aggregate reaction is the reaction between the alkalis, sodium and potassium hydroxide ( $\text{Na}_2\text{O}$  and  $\text{K}_2\text{O}$ ) present in cement, and silica based components present in certain aggregates. Sulfates found in soil (from fertilizers) that react with calcium hydroxide and aluminates in the cementitious paste cause the sulfate attack. Freezing of water in mortar pores produces internal volume expansion that can generate the formation of internal cracks. Corrosion of steel forms rust components which are larger in volume than the initial compounds causing spalling of the concrete and additional exposure of the remaining steel.

For this study, the Carbon 1-FRCM system was used. Since the mortar contains short dispersed fibers in order to improve its toughness and its resistance in tension, the cementitious matrix used in this investigation is a GFRC composite.

Degradation of fabric by chemical agents can occur either by direct attack from the cementitious matrix or by attack from external components that penetrate through the pore structure of the matrix (Bentur and Mindess 2007). Alkaline environments do not affect the carbon fabric of the FRCM composite system used in this study. Moreover, the carbon fabric is chemically stable in the absence of oxidizing agents at very high temperatures (over  $500^\circ\text{C}$ ) (Arboleda 2014).

The fabric-matrix interface represents a crucial element in the mechanical behavior of FRCM. Thus, any factor that can cause degradation of adhesion and frictional bond forces will affect the performance of the composite. One of the

mechanisms of strength loss can occur by densification of the matrix (Brameshuber 2006) which affects the bond characteristics. For GFRC the alkali-glass reaction is the most notable durability concern for the bond performance (Arboleda 2014). However, the cementitious matrix of Carbon 1-FRCM has been designed to optimize the performance and durability of the fabric-matrix interface.

This study aims to investigate the performance of FRCM composites after the exposure to environments known to be harmful to the mechanical properties of construction repair materials. Since FRCM composites have been proposed as an alternative to FRP, it is reasonable to examine their performance under the same conditioning (Arboleda 2014). In the following sub-sections, the environments and their set-up are introduced.

### 5.1.1 Environments Description

The exposure environments proposed for this study and their characteristics are summarized in Table 5.1. In particular, these were selected following the ICC-ES recommendations in AC434 (2013).

Nomenclature	Environment	Temperature (°C)	Relative Humidity (%)	Exposure (hours)
Control	Ambient	22	50	1000
Freeze-Thaw	Freeze/Thaw	-18/37.7	NA/100	(4/12) * 20
AR 1000	Alkaline	22	NA	1000
WR 1000	Water Vapor	37.7	100	1000
SW 1000	Seawater	22	NA	1000

**Table 5.1 – Environment characteristics**

Freeze/thaw cycles are known to be damaging for cementitious materials. Alkalinity, water vapor, and seawater can be detrimental for composites that contain glass fibers and organic material, both present in the FRCM under investigation. The durability study was limited to one-ply and four-ply plain specimens of Carbon 1-FRCM system after an exposure of 1000 hours.

*Aging: Alkaline, Seawater, Water Vapor environments*

Specimens were subjected to three different types of aging processes. The first type consisted of specimens submerged in an alkali solution containing calcium hydroxide ( $\text{Ca}(\text{OH})_2$ ), sodium hydroxide (NaOH), and potassium hydroxide (KOH) mixed to create an environment with  $\text{pH} > 9.5$  and temperature equal to  $22^\circ\text{C}$ . The second type included specimens fully submerged in saltwater at laboratory conditions. Whereas, the third type was a humidity chamber (water vapor) at 100% relative humidity and  $37.7^\circ\text{C}$ .

The water vapor chamber was designed to heat water to  $60^\circ\text{C}$  by inserting a submersible heater at the bottom of a watertight container, which was filled with water at a depth of 150 mm to ensure that the heater was completely submerged. A fixture was used to maintain the specimens above the level of the water. The seawater and alkaline chambers were watertight containers filled with the environmental solution in which the specimens were submerged.

*Freeze/Thaw Environment*

After being conditioned for one week in a chamber at 100% relative humidity at a temperature of  $37.7^\circ\text{C}$ , the specimens were subjected to twenty freeze-thaw cycles. Each cycle consisted of four hours at a temperature of  $-18^\circ\text{C}$ , followed by 12 hours in the humidity chamber (100% RH and  $37.7^\circ\text{C}$ ). The cycles were performed manually.

## **5.1.2 Specimen Preparation**

Since the specimens for all the studies were prepared following the same methodology, refer to the specimen preparation section in Chapter 4. Moreover, the specimens for the current study were prepared at the same time and randomly selected for each exposure environment. The specimens for the different tests were exposed to the same conditions and for the same amount of time.

### **5.1.3 Test Setup and Procedure**

The test setup and procedure is the same of the specimens tested in Chapter 4. A three-point bending test was performed using a screw driven Universal Test Frame with the load applied in displacement control at a rate of 1 mm/min in a quasi-static configuration. The vertical displacement of the specimen was measured according to the cross-head displacement. No device was used to measure the deformations.

Since the test setup remains the same as for control specimens, also the specimens have to be in the same condition at testing. After the environmental exposure to the alkaline, seawater and water vapor environments, the samples have to be dried before testing. Experiments were performed in order to analyze the influence of moisture on the test results.

## 5.2 Test results

This section presents the specimens' behavior and the corresponding failure mode. The study was conducted on one-ply and four-ply plain specimens of Carbon 1-FRCM system after an exposure of 1000 hours. The outcomes are compared with the results of the control condition tests done on the same specimens. Five repetitions were performed for each environmental condition for a total of 50 specimens. Table 5.2 shows a summary of the tests completed and the relative failure modes experienced.

Specimen ID	Average thickness (mm)	Span to thickness ratio	Span Length (mm)	Width (mm)	Failure mode*
Carbon1_1P_Control	12,3	4	49,4	24,7	FL
Carbon1_4P_Control	18,7	4	74,9	34,0	DF
Carbon1_1P_FT	9,5	4	38,1	19,1	FL
Carbon1_4P_FT	18,2	4	72,7	34,0	FL - DF
Carbon1_1P_AR_1000h	9,2	4	36,9	18,4	FL
Carbon1_4P_AR_1000h	18,8	4	75,0	34,0	DF
Carbon1_1P_WR_1000h	10,1	4	40,4	20,2	FL
Carbon1_4P_WR_1000h	18,5	4	74,0	34,0	DF
Carbon1_1P_SW_1000h	9,3	4	37,2	18,6	FL - DF
Carbon1_4P_SW_1000h	19,0	4	75,9	34,0	DF

\*FL = flexural failure; DF = matrix diagonal shear failure

**Table 5.2 – Tests performed and relative failure modes for durability study**

In reference to the failure mode, the only two environmental conditions that denoted a deleterious effect on the FRCM system under investigation are the freeze-thaw cycles and the seawater exposure. For the seawater specimens, the reason for a different behavior is due to the moisture content of the samples. The seawater specimens were left intentionally wet in order to examine if there was any difference in the failure mode and resistance of the composite versus the dry condition. Comments on these experiments can be found in Section 5.2.5.

### 5.2.1 Control Condition

The following figures show the experimental behavior of FRCM control specimens and the corresponding failure modes experienced.

#### Load-Deflection diagrams

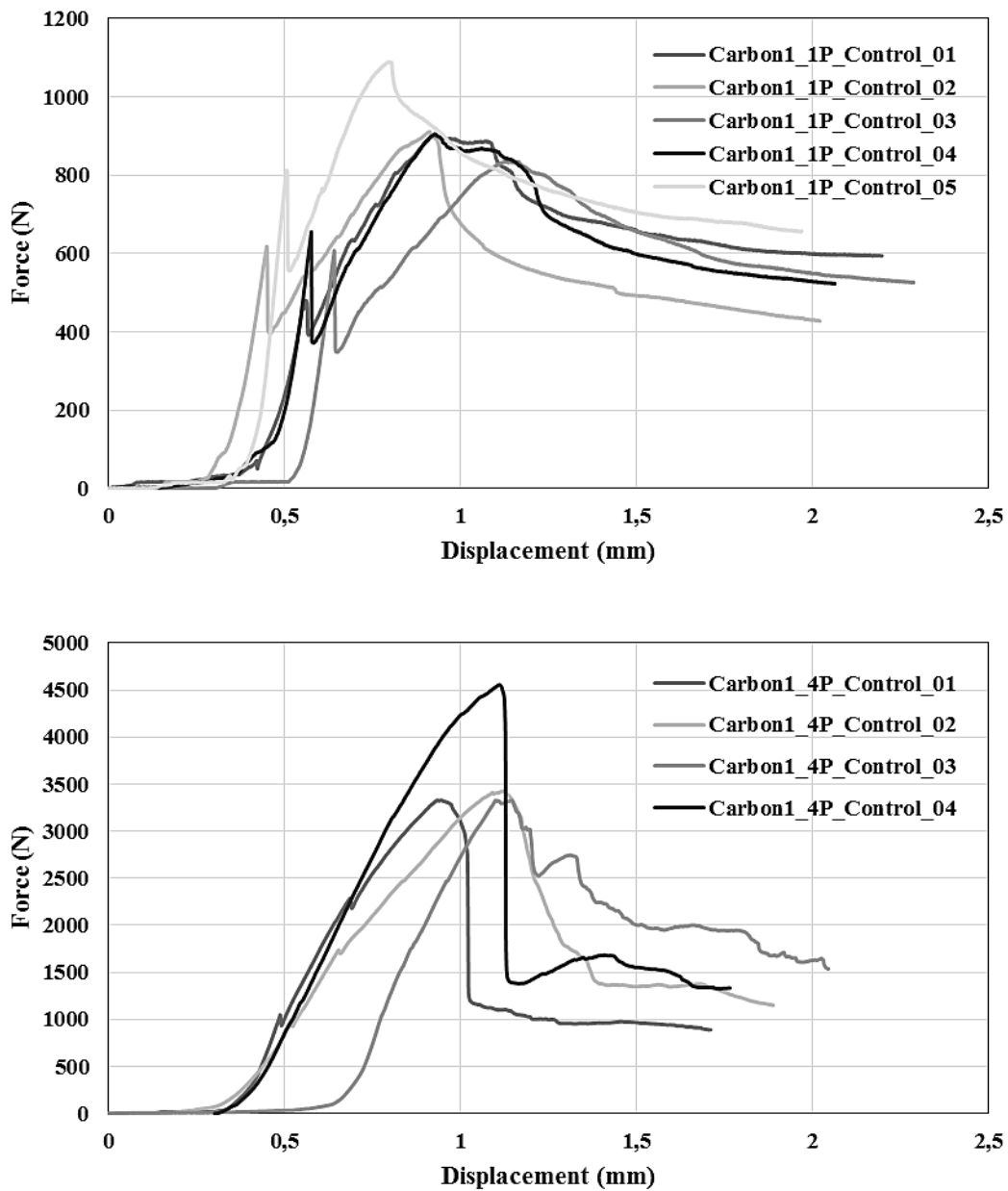


Figure 5.1 – Control specimens: one-ply and four-ply

*Failure modes*



(a)



(b)

**Figure 5.2 – Typical failure modes of control specimens: (a) one-ply (b) four-ply**



## 5.2.2 Freezing and Thawing Resistance

The following figures show the experimental behavior of FRCM specimens and the corresponding failure modes experienced after freeze-thaw cycles.

### *Load-Deflection diagrams*

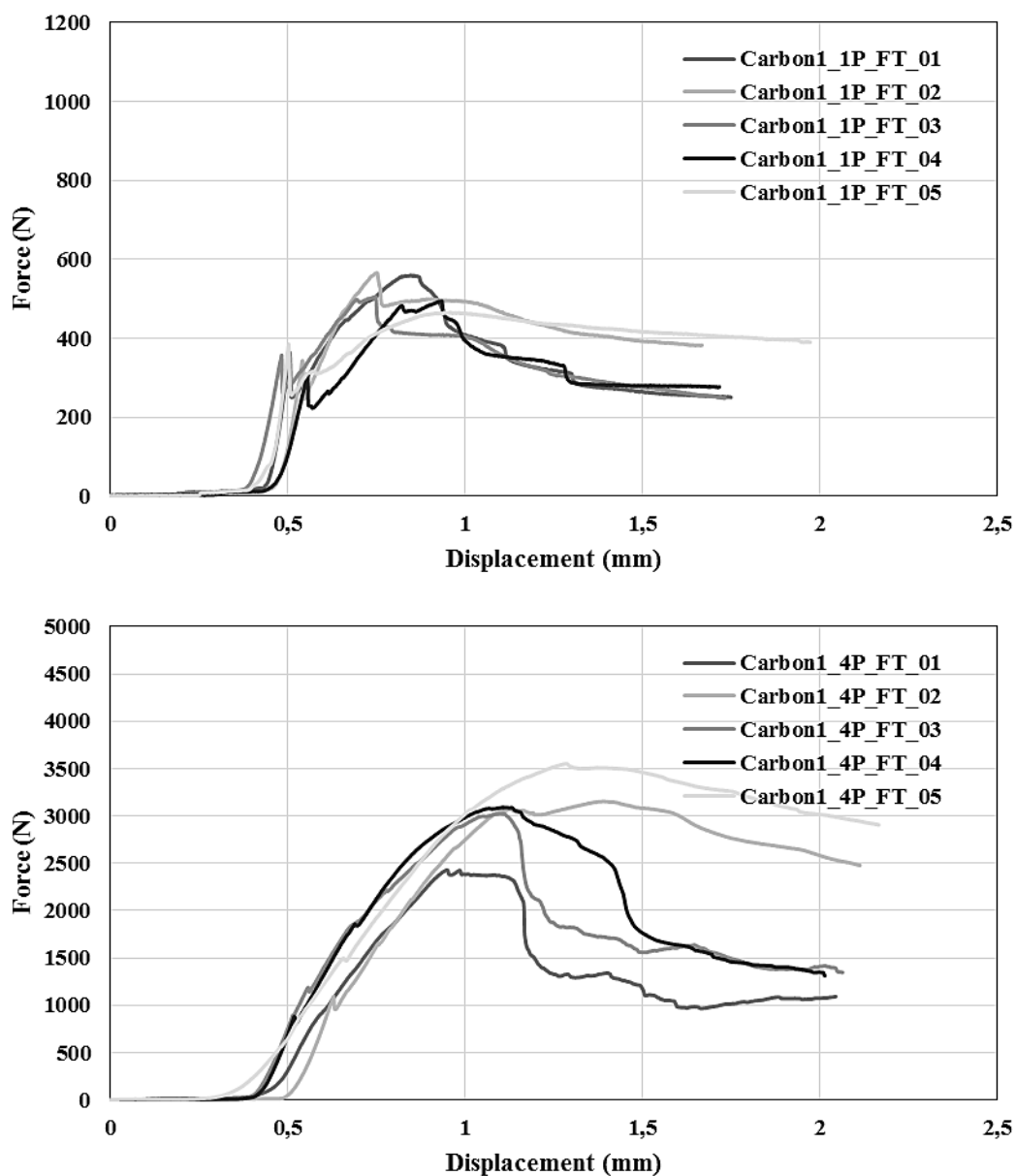


Figure 5.3 – Freeze-Thaw specimens: one-ply and four-ply

*Failure modes*



(a)



(b)

**Figure 5.4 - Typical failure modes of freeze-thaw specimens: (a) one-ply (b) four-ply**

The variability on the outcomes is moderate except for the failure mode of the four-ply specimens, which presented a combination of diagonal shear and flexural failures with some cracks that have a horizontal path (Figure 5.4b). For all the one-ply specimens the failure mode was flexural and therefore consistent with the control samples. Although some degradation in the cementitious matrix was observed, the behavior of the specimens after freeze-thaw cycles was quite similar to the one observed with the control specimens. The comparison of the apparent interlaminar shear strength (ISS) is presented in Section 5.3.

### 5.2.3 Alkaline Resistance

The following figures show the experimental behavior of FRCM specimens and the corresponding failure modes experienced after alkaline conditioning.

#### Load-Deflection diagrams

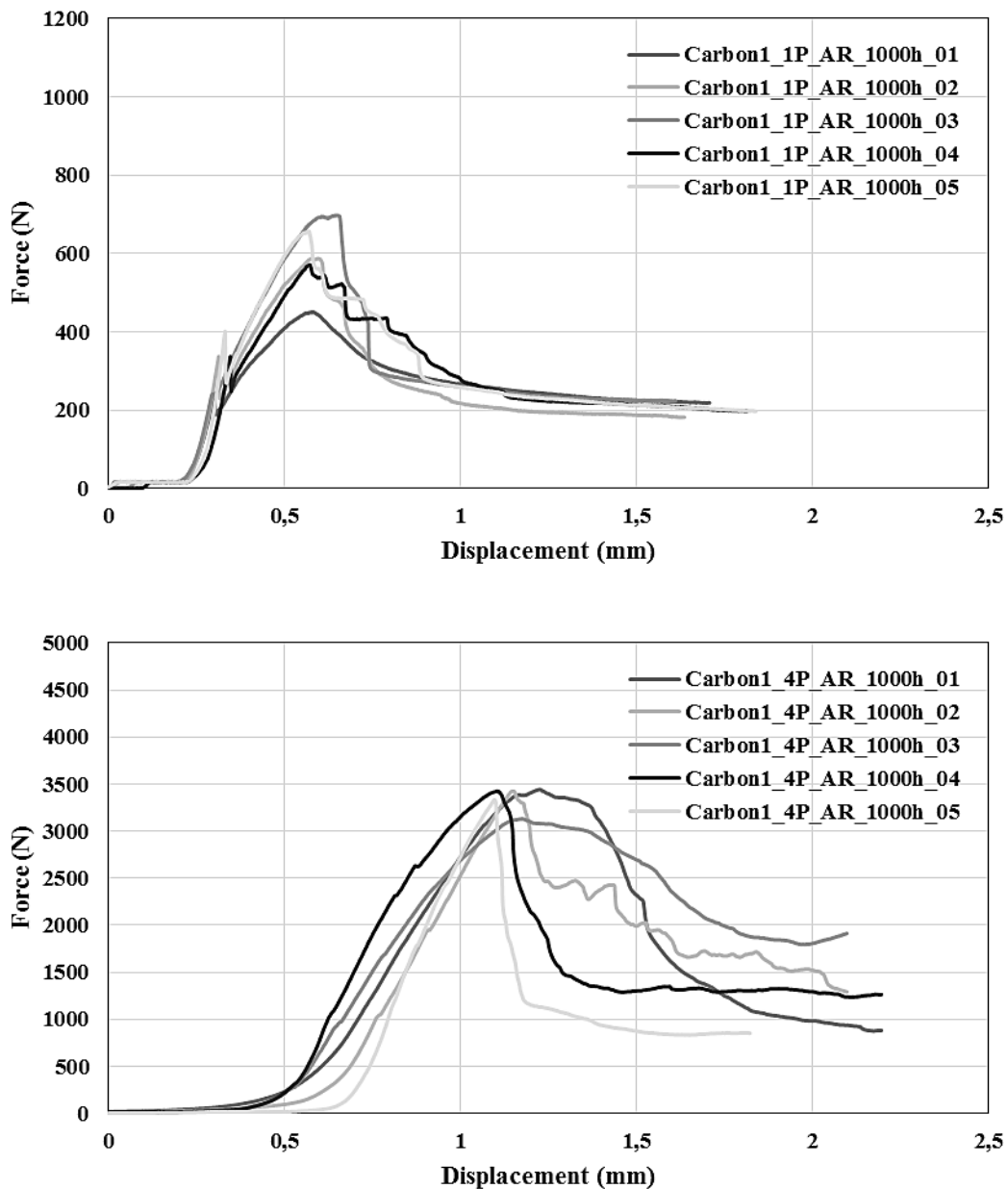


Figure 5.5 – Alkaline specimens: one-ply and four-ply

*Failure modes*



(a)



(b)

**Figure 5.6 – Typical failure modes of alkaline specimens: (a) one-ply (b) four-ply**

The FRCM system used for this study does not contain reactive silica, and the glass fibers are made of alkali resistant glass such as zirconium glass or zirconium oxide coated glass. The tests performed after immersion in a high alkalinity environment show that there are no adverse effects on the mechanical performance.

For all the tested specimens the failure mode was flexural for one-ply samples and matrix diagonal shear for the four-ply ones. The behavior of the specimens after the exposure to alkaline environment was the same observed with the control specimens, and the parameters computed are similar. Therefore, the alkaline environment does not affect the durability of the FRCM system under examination. The only difference with the control specimens was the white residual from the solution, deposited on the specimen surface. The comparison of the apparent interlaminar shear strength (ISS) is presented in Section 5.3.

## 5.2.4 Water Vapor Resistance

The following figures show the experimental behavior of FRCM specimens and the corresponding failure modes experienced after water-vapor conditioning.

*Load-Deflection diagrams*

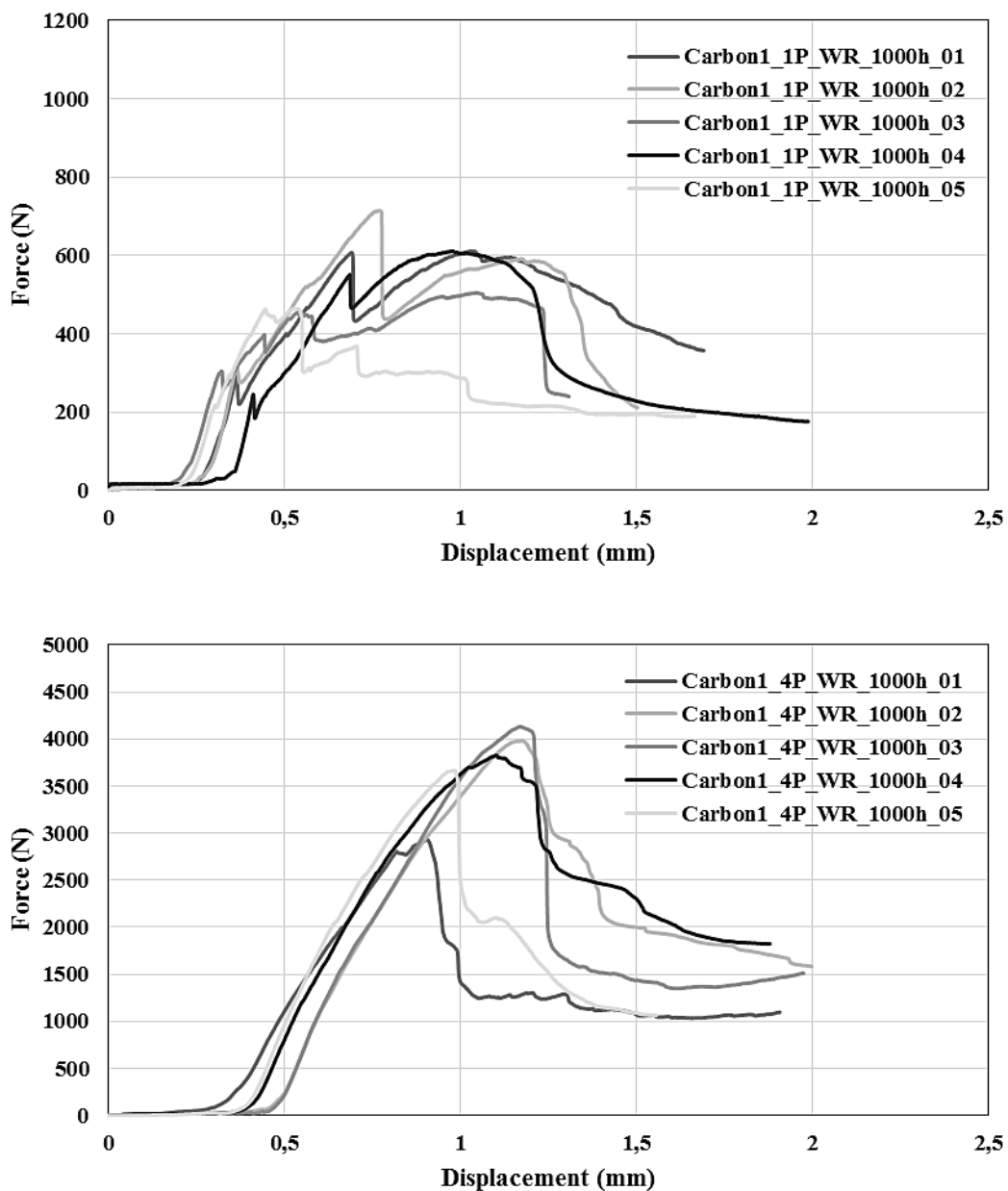


Figure 5.7 – Water vapor specimens: one-ply and four-ply

*Failure modes*



(a)



(b)

**Figure 5.8 – Typical failure modes of water vapor specimens: (a) one-ply (b) four-ply**

For all the tested specimens the failure mode was flexural for one-ply samples and matrix diagonal shear for the four-ply ones. The behavior of the specimens after the exposure to water vapor environment was the same observed with the control specimens, and the parameters computed are similar. Therefore, the water vapor environment does not affect the durability of the FRCM system under investigation. The comparison of the apparent interlaminar shear strength (ISS) is presented in Section 5.3.

## 5.2.5 Seawater Resistance

The following figures show the experimental behavior of FRCM specimens and the corresponding failure modes experienced after seawater conditioning.

### Load-Deflection diagrams

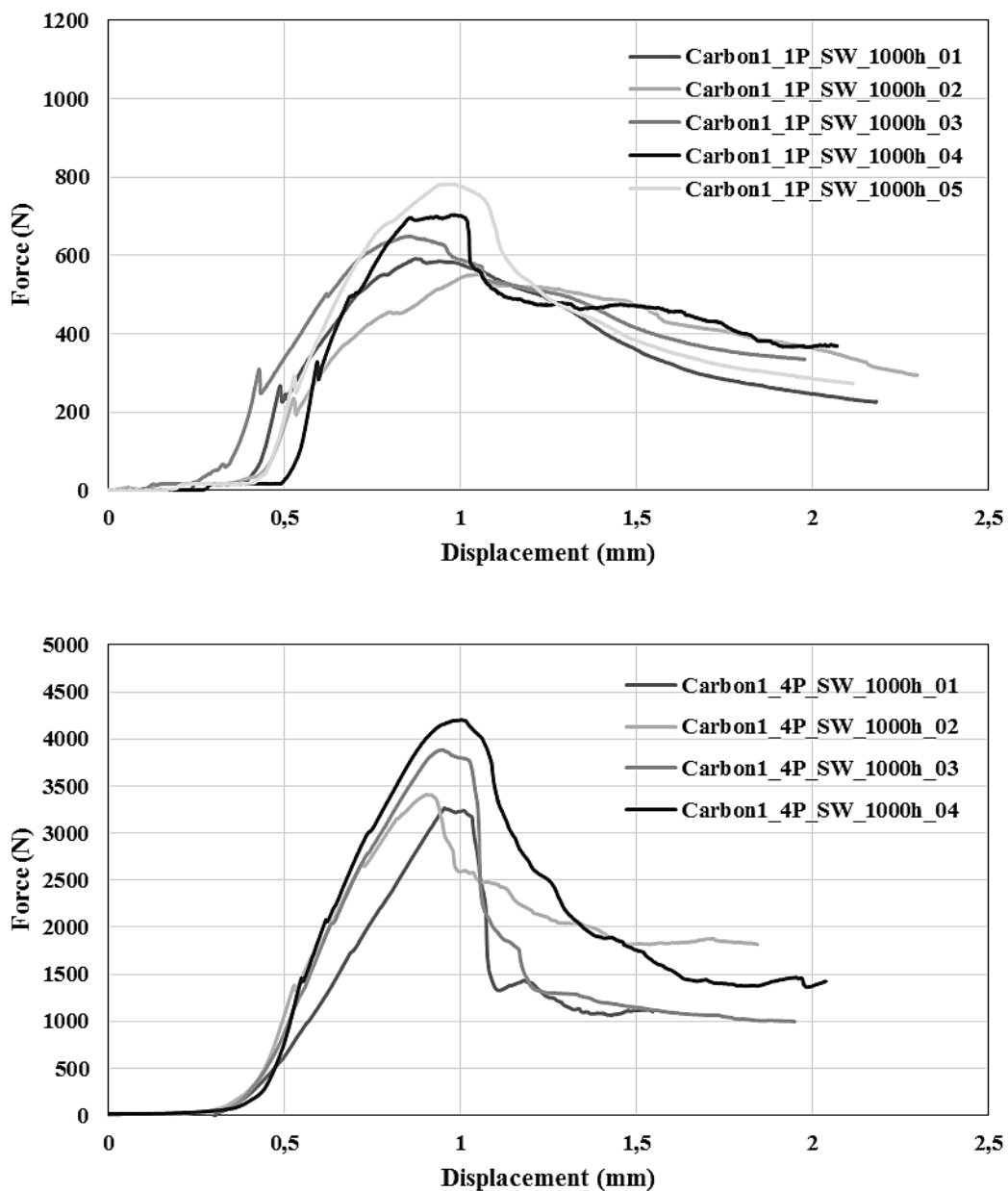
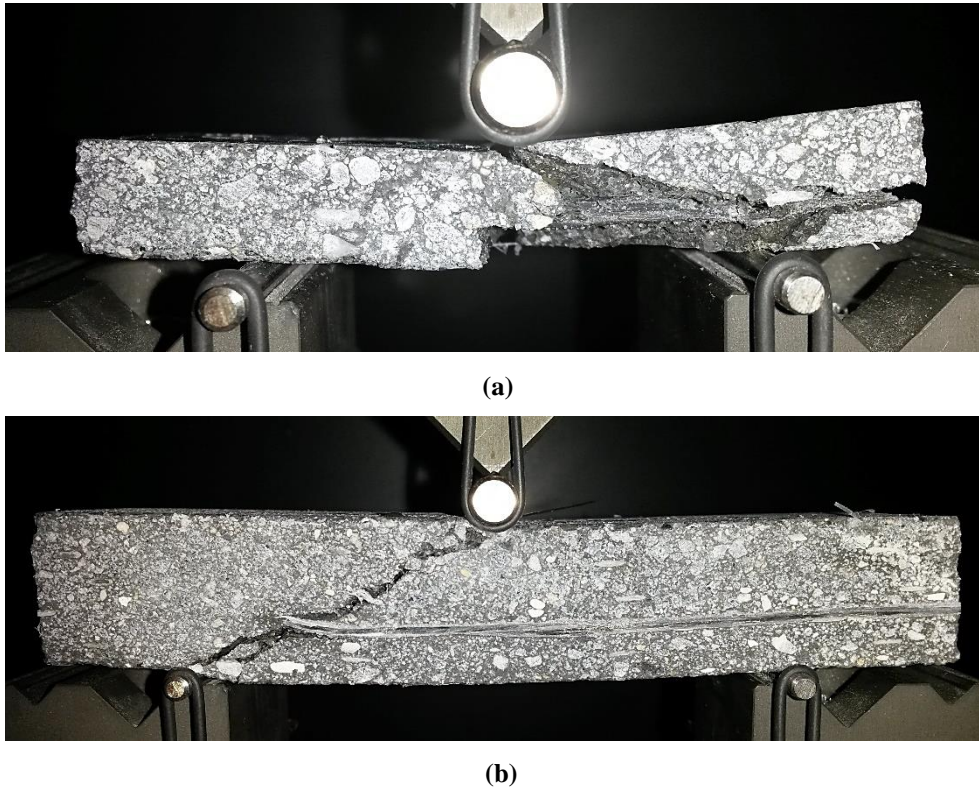


Figure 5.9 – Seawater specimens: one-ply and four-ply

*Failure modes*



**Figure 5.10 – Typical failure modes of seawater specimens: (a) one-ply (b) four-ply**

Although for the alkaline and water vapor exposure the experimental results showed a behavior quite similar to the control condition, durability testing after the seawater exposure demonstrated some differences in the specimen behavior and in its failure mode. As mentioned before, the main reason of this different behavior is the moisture content inside the samples.

Since the experimental results after the exposure to the previous environmental conditions highlighted a small degradation of the FRCM system, intentionally the seawater specimens were left wet in order to examine if there was any difference in the failure mode and resistance of the composite system. Therefore, after seawater conditioning, the situation of the specimens was not identical to the benchmark. The tested specimens were surface dry but saturated by water, while the control specimens were completely dry. As can be observed from Figure 5.10a, this choice



led to delamination of the specimen with the loss of a part of it and the formation of an interlaminar shear failure. Moreover, the strong degradation of the one-ply specimen uncovered the fabric inside the cementitious matrix and this is something never noticed before during this research. Based on these findings, it appears evident the importance of the test conditions for the consistency of the results. To this end, it becomes necessary after environmental exposure to bring the specimens back to the benchmark conditions.

### 5.3 Comparison of the Results

Since in this study only plain specimens were tested, the primary failure mode of the short-beam shear tests was a flexural crack on the tension zone for one-ply specimens and a matrix diagonal shear crack for the four-ply samples, thus only the durability performance of the tensile capacity of the mortar can be evaluated with this test. The apparent interlaminar shear strength (ISS) was computed according to ASTM D2344 (2006) section 12. Table 5.3 shows the average maximum load and the apparent ISS for the specimens exposed to the different environments.

Specimen ID	Average thickness (mm)	Span Length (mm)	Width (mm)	Average maximum Load (N)	Apparent ISS (MPa)
Carbon1_1P_Control	12,3	49,4	24,7	928,8	2,285
Carbon1_4P_Control	18,7	74,9	34,0	3659,7	4,309
Carbon1_1P_FT	9,5	38,1	19,1	517,9	2,140
Carbon1_4P_FT	18,2	72,7	34,0	3050,2	3,704
Carbon1_1P_AR_1000h	9,2	36,9	18,4	592,8	2,619
Carbon1_4P_AR_1000h	18,8	75,0	34,0	3351,4	3,942
Carbon1_1P_WR_1000h	10,1	40,4	20,2	581,1	2,136
Carbon1_4P_WR_1000h	18,5	74,0	34,0	3706,5	4,421
Carbon1_1P_SW_1000h	9,3	37,2	18,6	656,2	2,849
Carbon1_4P_SW_1000h	19,0	75,9	34,0	3691,6	4,293

**Table 5.3 – Average maximum load and apparent Interlaminar Shear Strength (ISS) for the different environmental conditions**

The first observation that can be made is the progressive in curing after 1000 hours of the specimens which led to a higher strength of the composite compared to the plain samples tested after 28 days of curing at laboratory conditions. Table 5.4 reports the maximum load and the apparent ISS of the said specimens.

Specimen ID	Average thickness (mm)	Span length (mm)	Width (mm)	Average maximum Load (N)	Apparent ISS (MPa)
Carbon1_1P_Plain	11,7	46,7	23,3	625,9	1,722
Carbon1_4P_Plain	19,8	79,3	34,0	3424,5	3,809

**Table 5.4 – Average maximum load and apparent Interlaminar Shear Strength (ISS) of plain specimens tested after 28 days of curing**

For clarity of discussion, the durability results are summarized in bar graphs representing the average values of apparent ISS together with their standard deviations for each environment for one-ply and four-ply specimens independently. The control (unexposed) samples are reported as a reference. Figure 5.11 and 5.12 show the said diagrams.

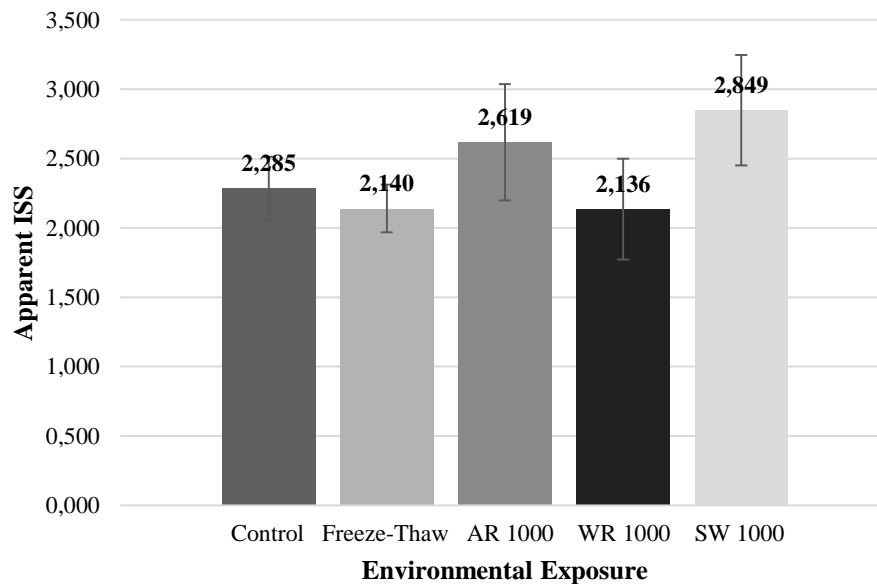


**Figure 5.11 – Apparent ISS for one-ply Carbon1-FRCM after environmental exposure**

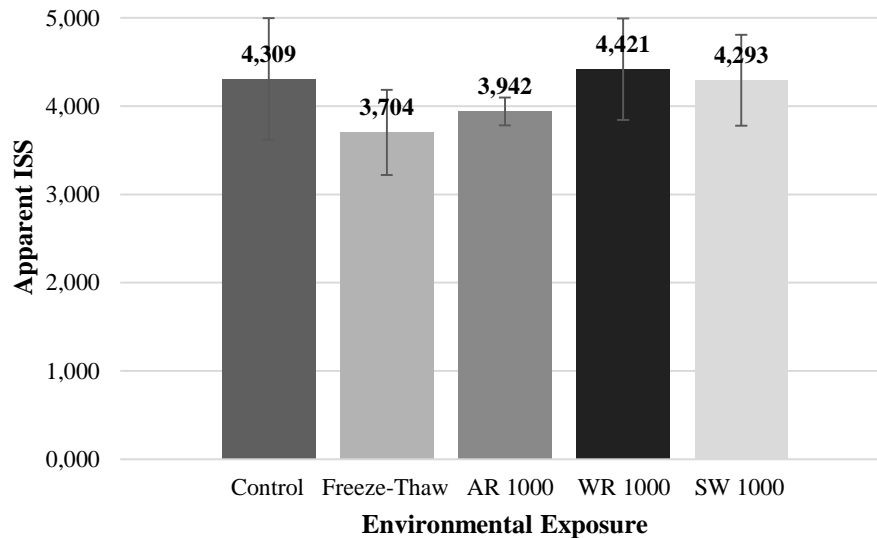


**Figure 5.12 – Apparent ISS for four-ply Carbon1-FRCM after environmental exposure**

However, the average values of ISS are not enough to compare the results, especially for a material which is characterized by high variability like the FRCM. For this reason, a statistical evidence of the effect of the environmental exposure is needed. In particular, it is necessary to understand if the difference between the means is significant in order to conclude if a certain environment affects the specimen behavior. To this end, a statistical analysis has been performed.

In order to determine if two sets of data are significantly different from each other, the first step is to choose the appropriate statistic test. The ANOVA test (Analysis of Variance) allows to verify whether or not the means of several groups are equal, under the hypothesis that the different groups must have the same number of elements, which is exactly the case of this study. Therefore, this methodology was chosen in order to compare each environment to the control condition. The significance level for the analysis is  $\alpha = 0,05$  (5%), indicative of the probability of a false rejection of the null hypothesis in the statistical test. The null hypothesis is that the means of the considered populations are equal and if the p-value is below the threshold chosen of 0,05, then the null hypothesis is rejected in favor of the alternative hypothesis of having two populations with different means.

The ANOVA analysis was performed using the software Minitab, which provided the p-value for all the groups compared to the control condition. Table 5.5 shows the results of the analysis for the different environments.

Group ID	p-value
Carbon1_1P_FT	0,08
Carbon1_1P_AR_1000h	0,16
Carbon1_1P_WR_1000h	0,17
Carbon1_1P_SW_1000h	0,14

Group ID	p-value
Carbon1_4P_FT	0,13
Carbon1_4P_AR_1000h	0,09
Carbon1_4P_WR_1000h	0,13
Carbon1_4P_SW_1000h	0,12

**Table 5.5 – ANOVA analysis results: one-ply and four-ply**

As can be noted, the results of the analysis detected a difference among the means between the control specimens and those that were exposed to the conditioning for 1000 hours (p-value) significantly higher than 0,05. Therefore, for Carbon 1-FRCM composite system there were no significant differences among the values of apparent ISS after environmental exposure.

## 5.4 Conclusions

An experimental study was conducted on Carbon 1-FRCM in order to assess the implications of conditioning on the performance of the short-beam shear test and to evaluate the applicability of FRCM after environmental exposure. One-ply and four-ply plain specimens were tested, denoting flexural and diagonal shear failures respectively. As expected, no interlaminar shear failure was observed. Therefore, only the durability performance of the flexural capacity of the mortar can be evaluated with this test method.

The FRCM specimens were subjected to environmental attacks with the exposure to freeze/thaw cycles, high temperature water vapor, immersion in seawater, and in an alkaline solution. The apparent interlaminar shear strength was determined after exposure and compared for the different conditions (Section 5.3). The results of the analysis indicate there are no significant degradations for the proposed environments.

However, some saturated specimens were tested after seawater exposure in order to evaluate the implications of the moisture content on the consistency of the results. These samples showed a different behavior and an important degradation of the FRCM system compared to the control condition. The fundamental reason of this difference appears to be the presence of water in the pores. A specimen that is dry and a specimen that is surface dry but saturated present a difference in compressive strength between 15 and 20% (Popovics 1998).

For FRCM systems, this is not an issue related to the fabric but to the cementitious matrix. What really affects the FRCM behavior is not the degradation after seawater exposure, but the difference in the moisture content. Therefore, it is fundamental that the specimens are tested in the same moisture condition. After taking the specimens outside their conditioning environment, it is necessary to over dry them until the moisture content drops under a certain value (same of control specimens), and at that point, it is possible to perform the tests because one potential parameter that can alter the test results has been eliminated.

To validate this theory, other specimens subjected to seawater exposure were tested after being placed for 24 hours in the oven at the temperature of 60°C and the results were consistent with the control samples (Figure 5.11 and Figure 5.12). Therefore, for future investigations on FRCM durability characteristics, before testing, for conditioning purposes, it is recommended to place the specimens for 24 hours in the oven at the temperature of 60°C.

# 6

## CONCLUSIONS

In Civil Engineering, the advancement of alternative materials and methods for structural rehabilitation is of critical importance to the safety and preservation of the world's heritage. Fabric Reinforced Cementitious Matrix (FRCM) composite systems represent an advance in repair methodology for structural rehabilitation. To this end, a research project was established with the aim to investigate the interlaminar shear behavior of cement-based matrix composites in order to better understand the actual interlaminar shear strength capacity.

Chapter 3 presented a critical analysis of the test methodologies encountered during literature search in order to understand the available methods for investigation of interlaminar shear behavior. Since most of the available material in literature is for FRP systems, the applicability of FRP test methodologies to FRCM composites was analyzed. In particular, four shear test methods were selected for review and studied in detail: short beam (three-point) shear, four-point shear, Iosipescu shear, and axial tension of a laminate. After the analysis of pros and cons of each test method, thanks to its simplicity of use and small specimen size, which allows testing many replicates permitting also the generation of a statistically meaningful data set, the short beam

shear test (ASTM D2344) was recognized as the most suitable way to examine the interlaminar shear behavior of FRCM composites. Although the present work did not focus on this methodology, the Iosipescu shear test method could represent an available alternative to the SBS test and further studies are recommended.

Chapter 4 dealt with the determination of the parameters to investigate the interlaminar shear behavior of FRCM composites. An extensive experimental campaign was conducted followed by the analysis of the results. The focus was mainly placed on the failure mode experienced during the test in order to have a better understanding of the behavior of the FRCM specimens. The failure mode has a significant effect on the measured interlaminar shear strength, since in order to measure the interlaminar shear strength correctly, a valid shear failure mode must be obtained.

The first study represented a critical analysis of the chosen test method (ASTM D2344). Dimensions of the specimens, number of reinforcing plies, span length, thickness, position of the fabric, diameter of loading nose and supports cylinders were varied and tested in order to choose the best parameters to generate an interlaminar shear failure. However, all the tested specimens presented a flexural or matrix diagonal tension failure. In particular, failure modes were found to be related to the amount of plies. Flexural failure mode occurred for one-ply specimens while diagonal shear failure characterized the ones with four plies. This result demonstrates a higher resistance of the material in the interlaminar plane compared to its flexural capacity.

Based on these findings, the second study presented an investigation of mid-plane in order to find a limit value of contact surface to generate an interlaminar shear failure. Since the continuity and the bond of the cementitious matrix ensure the strength of the FRCM samples, the proposed method was to consistently reduce the contact surface area at the shear plane until obtaining an interlaminar failure. Different percentages of contact surface for three types of mortar were analyzed and the limiting value between interlaminar shear and flexural failure for each kind of

matrix was determined. This study clarified the reason why the specimens tested in the first study did not show any interlaminar failure. Indeed, the contact area on specimens with the fabric inside is much larger than the values obtained in this study (maximum 10%), making unlikely the formation of interlaminar failures. This method represents a matrix characterization and allows comparing different types of cementitious matrixes. Moreover, the data found with this method can be used in design phase in order to optimize the geometry and dimensions of the fabric.

The third part of the work proposed a further modification of the specimen configuration to make interlaminar shear the control failure mode. This was done creating a composite sandwich beam made by FRCM and steel. This choice increases the flexural strength of the plain samples and generates a high shear stress concentration in the mid-plane allowing the formation of interlaminar failures. However, only four-ply specimens showed interlaminar shear failure because the four layers of fabric consistently reduce the contact surface area. Through a semi-elastic stress analysis based on cross-section transformation method, not only it was possible to compute the actual interlaminar shear strength of FRCM composites but thanks to a parametric study a relationship between the FRCM systems under investigation and the thickness of the steel plates to generate interlaminar failures was calculated.

This procedure represents a reliable way to obtain a valid interlaminar failure and compute the actual interlaminar shear strength of FRCM composite systems. However, it is reasonable to observe that in situ the FRCM is applied without the steel plates and that this methodology can be used only for research purposes. Furthermore, since the lack of interlaminar failures for FRCM material is representative of a good reinforcing system, the short-beam shear test (ASTM D2344) is recommended as quality control test and represents a screening tool for the reliability of the composite under investigation.

Digital image analysis represents a powerful means to compute geometric characteristics of composite materials like the contact surface area at interlaminar



plane of FRCM systems or the net area for stress computation of FRP and FRCM composites subjected to pull-out test. Interesting results have been reached and presented in Section 4.5 and a growing awareness of the potentiality of this method could bring more accurate results in the study of material properties for characterization and design purposes.

In addition, split tensile tests were performed in order to show that the test method developed in the previous studies is actually the most appropriate way to investigate the interlaminar shear behavior of FRCM systems. The experimental results showed that assuming the tensile strength of the mortar as one tenth of its compressive strength is not a reliable evaluation being this one higher than one tenth of the compressive strength. This additional resistance is due to the presence of the glass short fibers inside the cementitious mortar which increase the tensile capacity of the material. These results highlight the relevance of tensile testing and demonstrate that the presence of the short fibers in the cementitious mortar affects not only the ultimate capacity but also the way it fails. Thus, in order to characterize the composite system, a more appropriate quality control should also include tensile testing of the mortar. This test could be performed with the short beam shear test or with the splitting tensile test on cylindrical specimens. Tensile testing of the mortar should be also implemented in the new version of AC434 as an important parameter to characterize the cementitious matrix of FRCM systems.

Chapter 5 examined FRCM behavior under the SBS test after exposure to different aggressive environments. In particular, the specimens were exposed for 1000-hours to alkaline, seawater, water vapor environments and 20 freeze/thaw cycles. A statistical analysis by means of the ANOVA test demonstrated that there were no significant differences among the values of apparent ISS after environmental exposure. The proposed environments do not affect the performance of FRCM composite and other durability environments are recommended for future studies.

---

## REFERENCES

### ASTM and International standards

ASTM C1583/C1583M, (2013). “Standard Test Method for Tensile Strength of Concrete Surfaces and the Bond Strength or Tensile Strength of Concrete Repair and Overlay Materials by Direct Tension (Pull-off Method)”. ASTM International, West Conshohocken, PA.

ASTM C192, (2012). “Standard Practice for Making and Curing Concrete Test Specimens in the Laboratory”. ASTM International, West Conshohocken, PA.

ASTM C496/C496M, (2011). “Standard Test Method for Splitting Tensile Strength of Cylindrical Concrete Specimens”. ASTM International, West Conshohocken, PA.

ASTM C947, (2009). “Standard Test Method for Flexural Properties of Thin-Section Glass-Fiber-Reinforced Concrete (Using Simple Beam with Third-Point Loading). ASTM International, West Conshohocken, PA.

ASTM D2344/D2344M, (2006). “Standard test method for short-beam strength of polymer matrix composite materials and their laminates”. ASTM International, West Conshohocken, PA.

ASTM D3518/D3518M, (2013). “Standard Test Method for In-Plane Shear Response of Polymer Matrix Composite Materials by Tensile Test of a  $\pm 45^\circ$  Laminate”. ASTM International, West Conshohocken, PA.

ASTM D5379/D5379M, (2012). “Standard Test Method for Shear Properties of Composite Materials by the V-Notched Beam Method”. ASTM International, West Conshohocken, PA.

---

ISO 14130, (1997). “Fibre-reinforced plastic composites - Determination of apparent interlaminar shear strength by short-beam method”. CEN - European Committee for Standardization.

### **Building codes and technical reports**

ACI Committee 318. (2011). “Building code requirements for reinforced concrete”. ACI 318-11, Farmington Hills, MI.

ACI Committee 549. (2013). “Guide to design and construction of externally bonded FRCM systems for repair and strengthening concrete and masonry structures”. Farmington Hills, MI: American Concrete Institute.

AC218. (2003). “Acceptance Criteria for Cement-Based Matrix Fabric Composite Systems for reinforced and Unreinforced Masonry”. ICC-Evaluation Service, Whittier, CA.

AC434. (October 2011). “Acceptance criteria for masonry and concrete strengthening using Fiber-Reinforced Cementitious Matrix (FRCM) composite systems”. ICC-Evaluation Service, Whittier, CA.

AC434. (December 2012). “Proposed acceptance criteria for masonry and concrete strengthening using Fabric-Reinforced Cementitious Matrix (FRCM) composite systems”. ICC-Evaluation Service, Whittier, CA.

AC434. (February 2013). “Acceptance criteria for masonry and concrete strengthening using Fabric-Reinforced Cementitious Matrix (FRCM) composite systems”. ICC-Evaluation Service, Whittier, CA.

CNR-DT 200/2004. (2004). “Guide for the design and construction of externally bonded FRP systems for strengthening existing structures”. Rome: National Research Council.

---

Fib bulletin 14. (2001). "Externally bonded FRP reinforcement for RC structures"  
Technical Rep., Int. Federation for Structural Concrete, Lausanne, Switzerland.

RILEM TC 201-TRC, (2006), "Textile Reinforced Concrete - State-of-the-Art  
Report", Edited by W. Brameshuber, ISBN: 2-912143-99-3.

### **Publications**

Abegaz, A.; Suaris, W.; De Luca, A.; and Nanni, A., 2012, "Fiber Reinforced  
Cementitious Matrix (FRCM) Composites as Confining Systems for Reinforced  
Concrete Columns," X International Symposium on Ferrocement and Thin  
Reinforced Cement Composites (FERRO 10), Havana, Cuba.

Adams, D. F. and Lewis, E. Q., (1994). "Current Status of Composite Material Shear  
Test Methods," SAMPE, Vol 31, No. 6, pp. 32-41.

Adams, D. F., and Walrath, D. E., "Further Development of the Iosipescu Test  
Method," Experimental Mechanics, Vol 27, No. 2, June 1987, pp. 113-119.

Adams D.F. and Walrath D.E., (1987). Journal of Composite Materials, 21(6) 494.

Adams D.F. (2004). "The Short Beam Shear test method for composite materials".  
Salt Lake City, Utah.

Al-Jamous, A., Ortlepp, R., Ortlepp, S., & Churbach, M. (2006). "Experimental  
investigations about construction members strengthened with textile  
reinforcement". Proc., 1st Int. RILEM Symposium on Textile Reinforced  
Concrete (ICTRC), RILEM, Aachen, Germany, 170.

Al-Salloum, Y. A., Elsanadedy, H. M., Alsayed, S. H., & Iqbal, R. A. (2012).  
"Experimental and numerical study for the shear strengthening of reinforced  
concrete beams using textile-reinforced mortar". Journal of Composites for  
Construction, 16(1), 74-90.

- 
- Aldea, C.-M., ed., (2007), "Thin Fiber and Textile Reinforced Cementitious Systems", SP-244, American Concrete Institute, Farmington Hills, MI.
- Arboleda, D., (2014). "Fabric Reinforced Cementitious Matrix (FRCM) Composites for Infrastructure Strengthening and Rehabilitation: Characterization Methods". Open Access Dissertations, University of Miami. Paper 1282.
- Arboleda, D., Montesi, M., Carlsson, L., Nanni, A., (2015) "Interlaminar Shear Characterization for FRCM composites", Submitted 2015.
- Augenti, N.; Parisi, F.; Prota, A.; and Manfredi, G., (2011), "In-Plane Lateral Response of a Full-Scale Masonry Sub-Assemblage with and without an Inorganic Matrix-Grid Strengthening System," *Journal of Composites for Construction*, V. 15, No. 4, pp. 578-590.
- Badanoiu, A., and Holmgren, J. (2003). "Cementitious composites reinforced with continuous carbon fibers for strengthening of concrete structures." *Cement Concr. Compos.*, 25(3), 387–394.
- Banholzer, B. (2004). "Bond behavior of a multi-filament yarn embedded in a cementitious matrix." PhD dissertation, RWTH Aachen Univ., Aachen, Germany.
- Barnes J.A., Kumosa M., and Hull D., (1987). *Composites Science and Technology*, 28 (4) 251 (1987).
- Bentur, A., & Mindess, S. (2007). "Fibre reinforced cementitious composites" (2nd ed.). London; New York: Taylor & Francis.
- Berg, C. A., Tirosh, J., and Israeli, M., (1972). "Analysis of Short Beam Bending of Fiber Reinforced Composites," in *Composite Materials: Testing and Design (Second Conference)*, ASTM STP 497, ASTM, pp. 206-218.

- 
- Bianchi, G., Arboleda, D., Carozzi, F. G., Nanni, A., & Poggi, C. (2013). "Fabric Reinforced Cementitious Matrix (FRCM) materials for structural rehabilitation". Proceedings of the 39th IAHS World Congress.
- Bianchi, G., (2013). "Mechanical characterization of fabric reinforced cementitious matrix (FRCM) materials for structural strengthening." Master thesis, Politecnico di Milano, Milano, Italia.
- Bisby, L. A., Roy, E. C., Ward, M., & Stratford, T. J. (2009). "Fibre reinforced cementitious matrix systems for fire-safe flexural strengthening of concrete: Pilot testing at ambient temperature". Proc. Advanced Composites in Construction, Network Group for Composites in Construction, Chesterfield, U.K.
- Blanksvärd, T., Täljsten, B., & Carolin, A. (2009). "Shear strengthening of concrete structures with the use of mineral-based composites". Journal of Composites for Construction, 13(1), 25-34.
- Bournas, D. A., Triantafillou, T. C., Zygouris, K., & Stavropoulos, F. (2009). "Textile-reinforced mortar versus FRP jacketing in seismic retrofitting of RC columns with continuous or lap-spliced deformed bars". Journal of Composites for Construction, 13(5), 360-371.
- Brameshuber, W. (2006). "Report 36: Textile reinforced concrete-state-of-the-art report of RILEM TC 201-TRC". RILEM publications.
- Browning C.E., Abrams F.L., and Whitney J.M., (1983). "A Four-Point Shear Test for Graphite/Epoxy Composites," Composite Materials: Quality Assurance and Processing, ASTM STP 797, Browning, C.E., Ed., American Society for Testing and Materials, pp. 54-74.
- Brückner, A., Ortlepp, R., & Curbach, M. (2006). "Textile reinforced concrete for strengthening in bending and shear". Materials and structures, 39(8), 741-748.

- 
- Brückner, A., Ortlepp, R., & Curbach, M. (2008). "Anchoring of shear strengthening for T-beams made of textile reinforced concrete (TRC)". *Materials and Structures*, 41(2), 407-418.
- Buttner, T., Raupach, M., & Maintz, H. (2011). "Retrofitting Aachen Cathedral with an Innovative Flexible Textile Reinforced Mortar Bandage". *Restoration of Buildings and Monuments*, 17(3-4), 191-202.
- Callister, W. D., & Rethwisch, D. G. (2012). "Fundamentals of materials science and engineering: An integrated approach". John Wiley & Sons.
- Carozzi, F. G., Milani, G., & Poggi, C. (2014). "Mechanical properties and numerical modeling of Fabric Reinforced Cementitious Matrix (FRCM) systems for strengthening of masonry structures". *Composite Structures*, 107, 711-725.
- Cui, W., Wisnom, M. R., and Jones, M., (1994). "Effect of Specimen Size on Interlaminar Shear Strength of Unidirectional Carbon Fibre-Epoxy," *Composites Engineering*, Vol 4, No. 3, pp. 299-307.
- Curbach, M., Ortlepp, R., and Triantafillou, T. C. (2006). "TRC for rehabilitation." Rep. TC 201-TRC, RILEM, Aachen, Germany.
- D'Ambrisi, A., & Focacci, F. (2011). "Flexural strengthening of RC beams with cement-based composites". *Journal of Composites for Construction*, 15(5), 707-720.
- D'Ambrisi, A., Feo, L., & Focacci, F. (2012). "Bond-slip relations for PBO-FRCM materials externally bonded to concrete". *Composites Part B: Engineering*, 43(8), 2938-2949.
- Daniel, I. M., & Ishai, O. (1994). "Engineering mechanics of composite materials". Oxford University press New York.
- De Caso y Basalo, F.; Matta, F.; and Nanni, A., (2009), "Fiber Reinforced Cementitious Matrix Composites for Infrastructure Rehabilitation," Ninth

- 
- International Symposium on Fiber Reinforced Polymer Reinforcement for Concrete Structures (FRPRCS-9), D. Oehlers, D.; M. Griffith, and R. Seracino, eds., Sydney, Australia.
- De Caso y Basalo, F.; Matta, F.; and Nanni, A., (2012), "Fiber Reinforced Cement-Based Composite System for Concrete Confinement," *Construction & Building Materials*, V. 32, pp. 55-65.
- Ditcher, A. K., Rhodes, F. E. and Webber, J. P. H. (1981). "Non-linear stress-strain behavior of carbon fibre reinforced plastic laminates". *J. Strain Anal.* 16, 43-51.
- Donaldson, S., & Miracle, D. (2001). "Introduction to composites". *ASM Handbook*, 21.
- Faella, C.; Martinelli, E.; Nigro, E.; and Paciello, S., 2004, "Experimental Tests on Masonry Walls Strengthened with an Innovative C-FRP Sheet," *Proceedings of the First International Conference on Innovative Materials and Technologies for Construction and Restoration*, Lecce, V. 2, pp. 458-474.
- Fallis, G. J. (2009). "Innovation for Renovation". *Concrete international*, 31(04), 62-64.
- Hartig, J., Häubler-Combe, U., and Schicktanz, K. (2008). "Influence of bond properties on the tensile behavior of textile reinforced concrete." *Cement Concr. Compos.*, 30(10), 898–906.
- Hegger, J., Will, N., Curbach, M., & Jesse, F. (2004). "Tragverhalten von textilbewehrtem Beton". *Beton und Stahlbetonbau*, 99(6), 452-455.
- Hegger, J., Will, N., Bruckermann, O., and Voss, S. (2006). "Load-bearing behavior and simulation of textile reinforced concrete." *Materials Struct.*, 39(8), 765–776.
- Herakovich C.T. and Tarnopol'skii Y.M., (1989). Ed., *Structures and Design, Handbook of Composites, Volume 2*, Elsevier' Science Publishers, New York.



- 
- Hollaway L.C., & Teng, J.G. (2008). "Strengthening and rehabilitation of civil infrastructures using fibre-reinforced polymer (FRP) composites". Woodhead Publishing and Maney Publishing on behalf of The Institute of Materials, Minerals & Mining. CRC Press Boca Raton Boston New York Washington, DC.
- Langone, I.; Venuti, F.; Eusebio, M.; Bergamo, G.; and Manfredi, G., (2006), "Behavior of Masonry Buildings Strengthened with G-FRP Grid Bonded with Cementitious Matrix," Proceedings of First European Conference on Earthquake Engineering and Seismology, Geneva, Switzerland.
- Leardini, L., (2013). "Performance of RC beam elements reinforced with fabric-reinforced cementitious matrix (FRCM) for bending and shear." Master thesis, Politecnico di Milano, Milano, Italia.
- Lewis E.Q. and Adams D.F., (1991). "An Evaluation of Composite Material Shear Test Methods," Report UW-CMRG-R-91-103, University of Wyoming, Laramie.
- Loreto, G., Leardini, L., Arboleda, D., & Nanni, A. (2013). "Performance of RC Slab-Type Elements Strengthened with Fabric-Reinforced Cementitious-Matrix Composites". *Journal of Composites for Construction*, 18(3).
- Loreto, G., Babaeidarabad, S., Leardini, L., & Nanni, A. (2014). "RC beams shear-strengthened with Fabric-Reinforced-Cementitious-Matrix (FRCM)". *Materials and Structures*, under review.
- Marshall, O., (2002), "Test Report on CMU Wall Strengthening Technology," Internal Report, U.S. Army Construction Engineering Research Laboratory (CERL), Urbana, IL.
- Mobasher, B.; Jain, N.; Aldea, C.-M.; and Soranakom, C., (2007), "Development of Fabric Reinforced Cement Composites for Repair and Retrofit Applications," *Textile Reinforced Concrete (TRC)—German/International Experience*

---

Symposium Sponsored by ACI Committee 549, SP-244, American Concrete Institute, Farmington Hills, MI, pp. 125-139.

Nanni, A. (1999). "Composites: coming on strong". *Concrete Construction*, 44(1), 120-124.

Nanni, A. (2012). "A new tool in the concrete and masonry repair". *Concr. Int. Des. Constr.*, 34, 43-49.

Noor, A. K., Burton, W. S. and Bert, C. W. (1996). "Computational Models for Sandwich Panels and Shells", *Applied Mechanics Reviews*, Vol. 49, pp. 15-199.

Ombres, L. (2007). "Confinement effectiveness in concrete strengthened with fiber reinforced cement based composite jackets". *Proc., 8th Int. Symposium on Fiber Reinforced Polymer Reinforcement for Concrete Structures, FRPRCS-8*, American Concrete Institute (ACI), Detroit.

Ombres, L. (2009). "Failure modes in reinforced concrete beams strengthened with PBO fiber reinforced mortars." *Proc., 9th Int. Symposium on Fiber Reinforced Polymer Reinforcement for Concrete Structures (FRPRCS-9)*, American Concrete Institute (ACI), Detroit.

Ombres, L., Trimboli, A., Mantegazza, G., & Gatti, A. (2009). "Strengthening of old reinforced concrete structures using fiber reinforced cementitious mortars (FRCM): A case study." *Proc., 9th Int. Symposium on Fiber Reinforced Polymer Reinforcement for Concrete Structures (FRPRCS-9)*, American Concrete Institute (ACI), Detroit.

Ombres, L. (2011). "Flexural analysis of reinforced concrete beams strengthened with a cement based high strength composite material." *Composite Structures*, 94(1), 143–155.

- 
- Ombres, L. (2012), "Debonding analysis of reinforced concrete beams strengthened with fibre reinforced cementitious mortar." *Engineering Fracture Mechanics* 81 (2012) 94–109.
- Ortlepp, R., Ortlepp, S., and Curbach, M. (2004). "Stress transfer in the bond joint of subsequently applied textile reinforced concrete strengthening." *Proc., 6th Int. RILEM Symp. on Fiber-Reinforced Concretes (FRC)*, M. Di Prisco, R. Felicetti and G. A. Plizzari, eds., Sept. 20–22, Varenna, Italy, 1483–1494.
- Ortlepp, R., Hampel, U., Curbach, M. (2006) "A new approach for evaluating bond capacity of TRC strengthening." *Cement & Concrete Composites* 28, 589–597.
- Papanicolaou, C. G., Triantafillou, T. C., Karlos, K., & Papathanasiou, M. (2007). "Textile-reinforced mortar (TRM) versus FRP as strengthening material of URM walls: in-plane cyclic loading". *Materials and structures*, 40(10), 1081-1097.
- Papanicolaou, C. G.; Triantafillou, T. C.; Papathanasiou, M.; and Karlos, K., (2008), "Textile Reinforced Mortar (TRM) Versus FRP as Strengthening Material of URM Walls: Outof- Plane Cyclic Loading," *Materials and Structures*, V. 41, No. 1, pp. 143-157.
- Papanicolaou, C. G.; Triantafillou, T. C.; and Lekka, M., (2011), "Externally Bonded Grids as Strengthening and Seismic Retrofitting Materials of Masonry Panels," *Construction & Building Materials*, V. 25, No. 2, pp. 504-514.
- Pareek, S., Suzuki, Y., & Kobayashi, A. (2007). "Flexural and shear strengthening of RC beams using newly developed CFRP and polymer-cement pastes as bonding agents." *Proc., 8th Int. Symposium on Fiber Reinforced Polymer Reinforcement for Concrete Structures, FRPRCS-8*, American Concrete Institute (ACI), Detroit.
- Parisi, F.; Lignola, G. P.; Augenti, N.; Prota, A.; and Manfredi, G., (2011), "Nonlinear Behavior of a Masonry Sub-Assemblage Before and After Strengthening with Inorganic Matrix-Grid Composites," *Journal of Composites for Construction*, V. 15, No. 5, pp. 821-832.

- 
- Peled, A. (2007). "Confinement of damaged and non-damaged structural concrete with FRP and TRC sleeves". *Journal of Composites for Construction*, 11(5), 514-522.
- Peled A., Zaguri E., Marom G. (2008) "Bonding characteristics of multifilament polymer yarns and cement matrices". *Composite Structures*, 39: 930-939.
- Pindera M.J., Ifju P., and Post D., (1990). *Experimental Mechanics*, 30 (3) 101 (1990).
- Pipes R.B. and Pagano N.J., (1970). *Journal of Composite Materials*, 4, 538 (1970).
- Plantema, F. J., (1966), "Sandwich Construction: The Bending and Buckling of Sandwich Beams, Plates, and Shells", Jon Wiley and Sons, New York.
- Popovics, S., (1998). "Strength and related properties of concrete", John Wiley & Sons.
- Prota, A.; Marcari, G.; Fabbrocino, G.; Manfredi, G.; and Aldea, C.-M., (2006), "Experimental In-Plane Behavior of Masonry Strengthened with Cementitious Matrix-Grid System," *Journal of Composites for Construction*, V. 10, No. 3, pp. 223-233.
- Reddy, J. N., (1997). "Mechanics of Laminated Composite Plates: Theory and Analysis", CRC Press, Boca Raton, FL.
- Soranakom, C., and Mobasher, B. (2009). "Geometrical and mechanical aspects of fabric bonding and pullout in cement composites." *Materials Struct.*, 42(6), 765–777.
- Shivakumar K., Abali F. and Pora A., (2002). "Modified Short Beam Shear Test for Measuring Interlaminar Shear Strength of Composites". North Carolina A&T State University, Greensboro, North Carolina.

- 
- Somayaji, S. (2001). "Civil engineering materials". Upper Saddle River, NJ: Prentice Hall.
- Sullivan J.L., (1988). *Experimental Mechanics*, 28 (3) 326 (1988).
- Täljsten, B., & Blanksvärd, T. (2007). "Mineral-based bonding of carbon FRP to strengthen concrete structures". *Journal of Composites for Construction*, 11(2), 120-128.
- Triantafillou, T. C., & Papanicolaou, C. G. (2006). "Shear strengthening of reinforced concrete members with textile reinforced mortar (TRM) jackets". *Materials and structures*, 39(1), 93-103.
- Triantafillou, T. C., Papanicolaou, C. G., Zissimopoulos, P., & Laourdekis, T. (2006). "Concrete confinement with textile-reinforced mortar jackets". *ACI Structural Journal*, 103(1).
- Triantafillou, T. C., (2007). "Textile-Reinforced Mortars (TRM) versus Fibre-Reinforced Polymers (FRP) as Strength- ening and Seismic Retrofitting Materials for Reinforced Concrete and Masonry Structures," *International Conference on Advanced Composites in Construction (ACIC07)*, University of Bath.
- Triantafillou, T. C., & Bournas, D. A. (2008). "Seismic upgrading of RC columns in flexure with NSM reinforcement and textile-based jacketing." *Proc., 4th Int. Conference on FRP Composites in Civil Engineering, CICE, Zurich, Switzerland.*
- Verbovszky, S., Loreto, G., De Luca, A., Nanni, A., Focacci, F. (2012) "Experimental analysis of twist-off and pull-off testing methodologies to measure the bond strength between GFRP and concrete."
- Whitney, J. M., and Browning, C. E., (1985). "On Short-Beam Shear Tests for Composite Materials," *Experimental Mechanics*, Vol 25, pp. 294-300.

- 
- Whitney J.M., (1985). *Composites Science and Technology*, 22, 167 (1985).
- Whitney J.M., Daniel J.M., and Pipes R.B., (1985). "Experimental Characterization of Fiber Reinforced Composite Materials", Society for Experimental Stress Analysis, Prentice-Hall, Englewood Cliffs, NJ.
- Wiberg, A. (2003). "Strengthening of concrete beams using cementitious carbon fibre composites". Ph.D. thesis, Royal Institute of Technology, Stockholm, Sweden.
- Wu, H. C., & Sun, P. (2005). Fiber reinforced cement based composite sheets for structural retrofit. Proc., Int. Symposium on Bond Behaviour of FRP in Structures (BBFS 2005), International Institute for FRP in Construction, Manitoba, Canada.
- Yadama, V., M.P. Wolcott and D.G. Pollock. (2007). "Out-of-plane strand deviation in oriented strand composites". *Wood and Fiber Science*. 39(4):603-613.
- Zastrau, B., Lepenies, I., and Richter, M. (2008). "On the multi scale modeling of textile reinforced concrete." *Technische Mechanik*, 28(1), 53-63.
- Zenkert, D., (1995). "An Introduction to Sandwich Construction," Engineering Materials Advisory Services, London.

## APPENDIX A: Complete test matrix

An extensive experimental campaign has been conducted by the author at University of Miami for a total of 231 tested specimens. The following tables show the complete test matrix of the research work.

ANALYSIS OF TEST METHOD (ASTM D2344)					
Specimen ID	Repetitions	Average thickness (mm)	Span to thickness ratio	Span Length (mm)	Width (mm)
Carbon1_1P_Plain	5	11,7	4	46,7	23,3
Carbon1_2P_Plain	3	12,1	4	48,4	24,2
Carbon1_3P_Plain	3	15,0	4	60,1	30,1
Carbon1_4P_Plain	3	19,8	4	79,3	34,0
Carbon2_1P_Plain	3	9,1	4	36,6	18,3
PBO_2P_Plain	5	8,56	4	34,2	17,1
PBO_4P_Plain	3	14,5	4	58,0	29,0
<b>TOTAL</b>	25				

CONTACT AREA REDUCTION STUDY					
Specimen ID	Repetitions	Average thickness (mm)	Span to thickness ratio	Span length (mm)	Width (mm)
Mortar 1_0%	5				
Mortar 1_5%	5				
Mortar 1_10%	5	10,0	4	40,0	20,0
Mortar 1_15%	5				
Mortar 1_20%	5				
Mortar 1_25%	5				
Mortar 2_0%	5				
Mortar 2_5%	5				
Mortar 2_10%	5	10,0	4	40,0	20,0
Mortar 2_15%	5				
Mortar 2_20%	5				
Mortar 2_25%	5				

Mortar PBO_0%	5				
Mortar PBO_5%	5				
Mortar PBO_10%	5	10,0	4	40,0	20,0
Mortar PBO_15%	5				
Mortar PBO_20%	5				
Mortar PBO_25%	5				
<b>TOTAL</b>	90				

<b>COMPOSITE SANDWICH SPECIMENS</b>					
<b>Specimen ID</b>	<b>Repetitions</b>	<b>Average thickness (mm)</b>	<b>Span to thickness ratio</b>	<b>Span length (mm)</b>	<b>Width (mm)</b>
Carbon1_1P_Sandwich	5	16,5	4	66,0	33,0
Carbon1_1P_Sandwich	3	15,5	6	92,9	31,0
Carbon1_2P_Sandwich	3	15,6	4	62,4	31,2
Carbon1_3P_Sandwich	3	18,7	4	74,9	34,0
Carbon1_4P_Sandwich	3	21,4	4	85,6	34,0
Carbon1_4P_Sandwich	3	24,5	4	98,0	34,0
PBO_2P_Sandwich	3	12,1	4	48,5	24,3
PBO_2P_Sandwich	3	12,1	3	36,4	24,3
PBO_4P_Sandwich	3	16,1	4	64,4	32,2
PBO_4P_Sandwich	4	18,4	4	73,6	34,0
PBO_4P_Sandwich	3	22,3	4	89,2	34,0
<b>TOTAL</b>	36				

<b>DURABILITY STUDY</b>					
<b>Specimen ID</b>	<b>Repetitions</b>	<b>Average thickness (mm)</b>	<b>Span to thickness ratio</b>	<b>Span Length (mm)</b>	<b>Width (mm)</b>
Carbon1_1P_Control	5	12,3	4	49,4	24,7
Carbon1_4P_Control	5	18,7	4	74,9	34,0
Carbon1_1P_FT	5	9,5	4	38,1	19,1
Carbon1_4P_FT	5	18,2	4	72,7	34,0
Carbon1_1P_AR_1000h	5	9,2	4	36,9	18,4
Carbon1_4P_AR_1000h	5	18,8	4	75,0	34,0
Carbon1_1P_WR_1000h	5	10,1	4	40,4	20,2
Carbon1_4P_WR_1000h	5	18,5	4	74,0	34,0
Carbon1_1P_SW_1000h	5	9,3	4	37,2	18,6
Carbon1_4P_SW_1000h	5	19,0	4	75,9	34,0
<b>TOTAL</b>	50				



---

<b>SPLITTING TENSILE TEST</b>				
<b>Specimen ID</b>	<b>Repetitions</b>	<b>Diameter (mm)</b>	<b>Length (mm)</b>	<b>Reinforcing grid</b>
Carbon1_FRCM	3	50,8	101,6	Carbon1
Carbon2_FRCM	3	50,8	101,6	Carbon2
PBO_FRCM	3	50,8	101,6	PBO
Mortar 1	3	50,8	101,6	No reinforcement
Mortar 2	3	50,8	101,6	No reinforcement
Mortar PBO	3	50,8	101,6	No reinforcement
Mortar1_27%	3	50,8	101,6	Polyethylene sheet
Mortar1_37%	3	50,8	101,6	Polyethylene sheet
Mortar1_47%	3	50,8	101,6	Polyethylene sheet
Mortar1_57%	3	50,8	101,6	Polyethylene sheet
<b>TOTAL</b>	30			

---

## APPENDIX B: Image analysis procedure

As explained in Section 4.5, the image analysis is a powerful means to reach more accurate results in the study of material properties for characterization and design purposes. Different data can be obtained by using a free software. This software is called ImageJ and the next steps describe the general procedure of the analysis. In particular, the method for the determination of the percentage of an image area is presented.

- First of all open the image with the software ImageJ (File – Open – select the image to analyze);
- Crop the area of the image that has to be examined (Image – Crop);
- Since the higher is the contrast between the quantity to analyze and the background of the picture the more precise is the result of the analysis, if the contrast is not good, it is recommended to adjust the quality of the image (Image – Adjust – then use the available options to modify the picture);
- Once the picture is ready for the analysis, it is necessary to make it a binary system in order to transform the neutral colors in black or white (Process – Binary – Make Binary);
- Before performing the analysis select the quantities to be measured (Analyze – Set Measurements). In this example it is enough to check Area, Min & max gray value, Area fraction; but a variety of measurements can be selected depending on the final purpose of the analysis;
- Now the analysis of the image can be performed (Analyze – Measure);
- Image analysis results are given in an excel file where it is possible to find the different values required.